# AN EVALUATION OF THE USE OF MODERATE RESOLUTION IMAGING SPECTRORADIOMETER (MODIS)-DERIVED AEROSOL OPTICAL DEPTH TO ESTIMATE GROUND LEVEL PM2.5 IN ALASKA

By

Alyson Marie McPhetres Mathers, B.S., B.A.

A Thesis Submitted in Partial Fulfillment for the Degree of

Master of Science

in

Civil Engineering

December 2018

APPROVED:

Srijan Aggarwal, Ph.D., Committee Chair
Nathan Belz, Ph.D., Committee Member
Robert Perkins, Ph.D., Committee Member
Leroy Hulsey, Ph.D., Chair
*Department of Civil Engineering*
Douglas Goering, Ph.D., Dean
*College of Engineering and Mines*
Michael Castellini, PhD, *Dean of the Graduate School*

Abstract

The air quality monitoring (AQM) network in Alaska is limited to major urban areas and national parks thus leaving a large proportion of the state unmonitored. To evaluate the use of Moderate Resolution Imaging Spectroradiometer (MODIS)-derived aerosol optical depth (AOD) to predict ground-level PM2.5 concentrations and thereby increase the spatial coverage of the AQM network in Alaska, MODIS AOD was first validated against ground-based measurements of AOD in Utqiagvik and Bonanza Creek Alaska.

MODIS AOD from 2000 to 2014 was obtained from MODIS collection 6 using the dark target land and ocean algorithms between the months of April and October. Based on validation results, individual Aqua and Terra products are valid for both locations at 10-kilometer and 3-kilometer resolution. In addition, combined Aqua and Terra MODIS AOD products are valid for both locations at 3-kilometer resolution and 10-kilometer resolution for Utqiagvik.

The available PM2.5 data was then compared for satellite retrieval and all retrieval days to determine if there was sufficient data and the amount of bias introduced by possible low retrieval rates. Overall, Juneau had the lowest retrieval rates while Fairbanks and North Pole had the highest retrieval rates. In addition, Juneau appeared to have relatively high bias while stations located in Anchorage, Palmer, Fairbanks and North Pole had relatively low bias. Based on these findings, no models were developed for Juneau (southeast Alaska).

Multilinear regression models were then developed for southcentral (Anchorage and Palmer) and interior (Fairbanks and North Pole) Alaska where the log-transform of PM2.5 was the response and meteorological data and the log-transform of MODIS AOD were the predictors. MODIS AOD appeared to be most highly correlated with PM2.5 in interior Alaska, while there was little to no correlation between MODIS AOD and PM2.5 in southcentral Alaska. All models underestimate surface PM2.5 concentrations which may be due to the high percentage of low PM2.5 values used to develop the models and the limited retrieval rates. Alternative modeling methods such as mixed-effects modeling may be necessary to develop adequate models for predicting surface PM2.5 concentrations. The MLR models did not perform well and should not be used to predict ground-based PM2.5 concentrations. Further research using alternative modeling methods should be performed. Model performance may also be improved by only using higher concentrations of PM2.5 to develop models.

Overall, the limited spatial coverage of Alaska's air quality monitoring network and the low temporal resolution of MODIS-derived AOD make modeling the relationship between MODIS AOD and PM2.5 difficult in Alaska.

Table of Contents

List of Figures

Page

List of Tables

List of Abbreviations

| | |
|---|---|
| ADEC | Alaska Department of Environmental Conservation |
| AERONET | Aerosol Robotic Network |
| ALA | American Lung Association |
| AllPM | All ground-based PM2.5 retrievals |
| ANOVA | Analysis of Variance |
| AOD | Aerosol Optical Depth |
| AP | Air pressure |
| AQM | Air quality monitor/monitoring |
| AQS | Air Quality System |
| AquaPM | PM2.5 data retrieved on Aqua MODIS AOD retrieval days |
| AquaTerraPM | PM2.5 data retrieved on Aqua and/or Terra MODIS AOD retrieval days |
| ATV | All-terrain vehicle |
| BAM | Beta Attenuation Monitor |
| b | y-intercept |
| CALIPSO | Cloud-Aerosol Lidar and Infrared Pathfinder Satellite Observation |
| CF | cloud fraction |
| CMB | Chemical mass balance |
| CV-$R^2$ | Cross-validated r-squared |
| CV-R | Cross-validated Pearson correlation coefficient |
| DAAC | Distributed Active Archive Center |
| DB | Deep blue |
| DT | Dark target |
| EE | Error envelope |
| EPA | Environmental Protection Agency |
| FEM | Federal equivalent method |
| FNSB | Fairbanks North Star Borough |
| FRM | Federal reference method |
| HC3 | Type 3 heteroscedasticity consistent |
| HCCM | Heteroscedasticity consistent covariance matrix |
| IMPROVE | Interagency Monitoring of Protected Visual Environments |
| K | Kelvin |
| km | kilometer |
| kPA | kilopascal |

| | |
|---|---|
| LAADS | Level-1 Atmosphere Archive & Distribution System |
| m/s | meters per second |
| MAPSS | Multi-sensor Aerosol Products Sampling System |
| MISR | Multi-Angle Imaging Spectroradiometer |
| MLR | Multilinear regression |
| MODIS | Moderate Resolution Imaging Spectroradiometer |
| MSE-CV | Cross-validated mean square error |
| MSE | Mean square error |
| m | slope |
| NAAQS | National Ambient Air Quality Standard |
| NA | Not available |
| NCORE | National Core |
| ND | Non-detect |
| nm | nanometer |
| NPFS3 | North Pole Fire Station #3 |
| OLS | Ordinary least squares |
| OMI | Ozone Monitoring Instrument |
| PM10 | Particulate matter with aerodynamic diameter less than 10 microns |
| PM2.5 | Particulate matter with aerodynamic diameter less than 2.5 microns |
| PMF | Positive matrix factorization |
| PM | Particulate Matter |
| QA | Quality assurance |
| QR | Quantile regression |
| RH | Relative humidity |
| RMSE | Root mean square error |
| R | Pearson correlation coefficient |
| SD | Standard deviation |
| se | Standard error |
| Temp | Temperature |
| TerraPM | PM2.5 data retrieved on Terra MODIS AOD retrieval days |
| VIIRS | Visible Infrared Imaging Radiometer Suite |
| WRF-Chem | Weather research and forecasting with inline chemistry |
| WS | Wind speed |
| $\tau_A$ | AERONET-derived aerosol optical depth |

| | |
|---|---|
| $\tau_M$ | MODIS-derived aerosol optical depth |
| $\mu g/m^3$ | micrograms per cubic meter |
| $\mu m$ | micron |

Acknowledgements

I would like to thank the staff of the Civil and Environmental Engineering department at the University of Alaska Fairbanks for their support and assistance. I am also grateful to Dr. Pawan Gupta for his guidance in the early stages of this research. I would also like to acknowledge that part of this research was funded by the Alaska National Aeronautics and Space Administration (NASA) Established Program to Stimulate Competitive Research (EPSCoR) Program (N NNX15AK31A). Finally, I would like to thank my family and friends for their encouragement, support and insight while completing this thesis.

# Introduction

Fine particulate matter pollution negatively impacts cardiopulmonary health [1]–[4]. Poor air quality in the United States is more commonly associated with places like Los Angeles, California or Salt Lake City, Utah because of their higher population densities. Unbeknownst to many, the American Lung Association (ALA) ranks Anchorage and Fairbanks, Alaska as the fourteenth and fourth of U.S. cities with the worst short-term particulate (24-hour PM2.5) pollution [4]. In fact, Los Angeles, California and Salt Lake City, UT are ranked below Fairbanks with respect to short-term particulate pollution at seventh and eighth, respectively [4]. In addition, in 2018, Fairbanks was moved up to the worst U.S. city with long-term particulate pollution from seventeenth [4]. A portion of the Fairbanks North Star Borough was first classified as a non-attainment area in 2009 and then reclassified as a serious nonattainment area in 2017 by the Environmental Protection Agency (EPA) for the 24-hour (short-term) PM2.5 National Ambient Air Quality Standard (NAAQS) [5]. According to ALA, it is likely that the air quality in the Fairbanks North Star Borough has not gotten worse with respect to long-term (year-round) particulate pollution but improvements in air quality monitoring in the area and changes in the NAAQS has drawn attention to the issue [4].

As indicated by the recent classification of Fairbanks as the U.S. city with the worst long-term particulate pollution based on results from the improved air quality monitoring system in Fairbanks, air quality monitoring is essential for identifying possible risks to human health. In fact, many rural communities in Alaska report concerns with poor air quality yet year-round air quality monitors (AQM) are only located in Alaska's major urban areas (Anchorage, Juneau, Fairbanks) and national parks due to the high cost of installation and maintenance [6]. Currently, a weather research and forecasting model with inline chemistry (WRF-Chem) is used to forecast surface concentrations of PM2.5 due to wildfires in Alaska; however, it does not evaluate possible concentrations due to sources outside wildfires [7], [8]. A relatively low cost, high spatial coverage option, such as satellite remote sensing, would be invaluable to air quality monitoring efforts in Alaska [9].

Moderate Resolution Imaging Spectroradiometer (MODIS) derived aerosol optical depth (AOD) has been used successfully to monitor air quality trends, identify hot spots and estimate ground-level PM2.5 concentrations globally in areas such as the continental U.S., Australia, Beijing, and India [9]–[11]. The MODIS instrument is located onboard both the Terra and Aqua satellites and has been obtaining data since 1999 and 2002, respectively. The MODIS collection 6 Dark Target ocean and land algorithms are used to retrieve AOD from MODIS-observed spectral reflectance at 10-kilometer and 3-kilometer resolution [12], [13]. The addition of the use of satellite remote sensing to monitor long-term and short-term trends in PM2.5 throughout Alaska may enable regulators to identify areas in need of more stringent monitoring or regulations.

The objective of this research is to evaluate the current status and sources of particulate matter in Alaska and to determine if MODIS AOD may be used to predict ground-level PM2.5 concentrations in southcentral, interior, and southeast Alaska. This will be accomplished by first determining the extent to which there is agreement between ground-based and satellite-based measurements of AOD. Available data and retrieval rates will also be evaluated to determine possible bias and to determine if the data is appropriate for use in model development. If retrieval rates and bias are satisfactory, then models of the relationship between MODIS AOD and PM2.5 will be developed using multilinear regression and meteorological parameters.

## Chapter 1 Particulate Matter Impacts in Air Quality and Exposure in Alaska: Current Status and Future Directions[1]


### Abstract

Alaska is the largest state in the US by land area, yet it has one of the smallest populations. The small population is distributed mainly in three major cities (Fairbanks, Anchorage, Juneau), and about 130 village communities with a population ranging from 50 to 1000 people. Given the wide population spread over a large geographical area, the air quality monitoring network in Alaska is currently limited primarily to major cities and national parks. This paper provides a comprehensive review of air quality issues and studies undertaken in Alaska in the last two decades, with a specific focus on particulate matter. Source apportionment studies using Alaska's ground-based air quality monitoring network show that wood smoke, residential home heating, gas and diesel vehicle emissions, and dust are the primary sources of PM10 and PM2.5 in Alaska. Wintertime exceedances of the 24-hour PM2.5 national ambient air quality standards (NAAQS) in Fairbanks and Juneau typically occur when low temperatures increase the demand for heating and surface inversions trap pollutants in the lower levels of the atmosphere. Throughout Alaska, summertime exceedances of the 24-hour PM2.5 NAAQS are typically caused by smoke from wildfires. Mainly in rural villages and the Matanuska-Susitna Valley, summertime exceedances of the 24-hour PM10 NAAQS typically occur due to fugitive road dust and major dust events caused by high winds. Due to the limited spatial coverage of Alaska's air quality network, human exposure to particulate pollution cannot be monitored consistently in rural areas which constitute nearly one-third of the population of Alaska. In the future, satellite remote sensing could be a viable option for monitoring particulate pollution and human exposure in Alaska in the summertime. A better understanding of hotspots and regions of critical need in the state could help in prioritizing monitoring and mitigation efforts.


### 1.1 Introduction

Issues with particulate pollution are typically associated with large population densities (e.g. Beijing, Los Angeles), but Alaska has the smallest population density in the United States (www.census.gov) and is home to many communities that report issues with particulate pollution [1]–[3]. In fact, the American Lung Association ranked Fairbanks and Anchorage as the fourth and fourteenth U.S. cities most polluted by short-term particulate pollution (24-hour PM2.5) [4]. Bakersfield, CA was ranked first followed by two other California cities; and Salt Lake City, UT and Los Angeles, CA were ranked seventh and eighth most

[1]McPhetres, A., Aggarwal, S. Particulate Matter Impacts in Air Quality and Exposure in Alaska: Current Status and Future Directions. Unpublished Manuscript. 2018.

polluted by short-term particulate pollution in the U.S [4]. Also, Fairbanks is ranked as the U.S. city with the worst long-term particulate pollution; the Fairbanks North Star Borough was also ranked first as the U.S. county with the worst long-term air quality with an annual mean of 23.0 μg/m$^3$ between the years of 2014 and 2016, nearly two times the National Ambient Air Quality Standard (NAAQS) of 12.0 μg/m$^3$ [4]. In addition, while national annual mean PM2.5 concentrations have decreased between the years of 2000 and 2015, average annual concentrations appear have increased (Figure 1.1) (www.epa.gov). Portions of the Fairbanks North Star Borough (FNSB) were designated as nonattainment for 24-hour PM2.5 concentrations by the Environmental Protection Agency (EPA) in 2009 (www.epa.gov) and continue to struggle with poor air quality.

Exceedances of the 24-hour PM2.5 NAAQS are typically a function of meteorological conditions and volume and source of emissions. In the FNSB, an exceedance of the 24-hour PM2.5 NAAQS will occur if the air temperature is less than -20 °C, the air is drier than 1 hPa, and there is a surface inversion [5]. The main sources of PM10 and PM2.5 in Alaska are smoke from residential wood burning, wildfires, residential heating, fugitive road dust, windblown dust, diesel and gas emissions, and arctic haze. Table 1.1 lists the current EPA-designated maintenance and non-attainment areas in Alaska.

Despite the poor air quality reported by many of Alaska's rural communities, year-round air quality monitors (AQMs) are located only in Alaska's urban areas and national parks due to the high cost of site installation and maintenance [6]. The limited spatial coverage of air quality monitors poses a problem for monitoring air quality and thereby human exposure to pollutants in rural areas. Satellite remote sensing may prove to be a useful tool for monitoring air quality in Alaska due to the increased spatial coverage and relatively low cost of acquiring data from satellite remote sensing [7].

The purpose of this article is to review the current status of particulate matter (PM) research in Alaska and to assess the need for further research. Currently, there is little to no research regarding ambient PM concentrations in rural areas except past air quality monitoring projects by the Alaska Department of Environmental Conservation (ADEC). Most of the published research focuses on Anchorage, Fairbanks, and Juneau, the three largest cities in Alaska. The three most recent published source apportionment studies were for Fairbanks and Anchorage. Therefore, aside from Anchorage and Fairbanks, most particulate sources are based on ADEC observations such as the color of the filters removed from the air quality monitors and the environment. Table 1.2 lists past studies regarding particulate pollution in Alaska. The following topics will be addressed in this review: sources of particulate matter, current monitoring methods and potential monitoring methods in Alaska.

### 1.2 Sources of Particulate Matter

Sources of PM2.5 and PM10 in Alaska include wood smoke, vehicle emissions, residential heating, ship emissions, dust, arctic haze, salt, and volcanic eruptions. Table 1.3 summarizes the results of two different source apportionment studies for PM2.5 in Fairbanks, Alaska. In comparison, major sources of PM2.5 identified in the U.S. are the metals industry, crustal/soil particles, motor vehicle traffic, the steel industry, coal combustion, salt particles, and biomass burning [8]. In the U.S., the top three contributors to PM2.5 listed in order of contribution are motor vehicles, sulfates, and biomass burning[8]. The main PM2.5 contributors in Alaska are biomass burning, secondary aerosols, and vehicle emissions.

### 1.2.1 Wood Smoke

Wood smoke is one of the primary contributors to PM2.5 concentrations in Alaska. The two main sources of wood smoke in Alaska are residential wood burning and wildfires [1], [9]. Residential wood burning is the primary source of wood smoke in winter as the cold temperatures cause an increase in the demand for heating. Wildfires are the primary source of wood smoke in the summer as warmer temperatures reduce the demand for residential heating and warm, dry weather increases the probability of wildfires. Increased PM2.5 concentrations from wood smoke is a problem throughout Alaska. Residents in Seward, Juneau, Skagway, Fairbanks, villages in northwest Alaska, and Palmer have all expressed concern over exposure to wood smoke from both wildfires and residential wood burning [2], [10]–[13].

#### *1.2.1.1 Residential Wood Burning*

In both Fairbanks and Juneau, the second and third largest cities in Alaska respectively, extreme temperature inversions and low wind speeds cause poor dispersion of pollutants as pollutants become trapped in the lowest layer of the atmosphere, while cold temperatures increase the demand for heating [9], [10], [14]. Wood smoke from residential wood burning is considered to be the primary source of wintertime PM2.5 in both cities [9], [10]. Wood smoke is the main contributor to PM2.5 concentrations in Fairbanks based on two separate studies using different source apportionment methodologies [1], [9]. In the study by Ward et al. (2012), the chemical mass balance (CMB) method was used to analyze air quality data obtained from four sites in Fairbanks and North Pole. Wood smoke contributed between 63 and 80 percent of the total wintertime PM2.5 levels in Fairbanks and North Pole and 63.1 to 72.4 percent at the Fairbanks State Office Building (FSOB) from 2008 to 2011. In a study by Wang and Hopke, the positive matrix factorization method was used to perform source apportionment analysis using year-round air quality data from FSOB. Per the study results, wood smoke contributed between 39.6 and 41.1 percent of the total wintertime PM2.5 levels from 2005 to 2012 [1]. Wood smoke contributions from residential home heating are typically higher on weekends and doubled on exceedance days due to increased demand for heating on the colder days and lower mixing heights due to inversions [1]. Heating demands and thereby home heating contributions tend to be higher on the weekends due to the fact that most people are home from work on weekends and are away from home on weekdays.

Due to the large contribution of wood smoke to PM2.5 levels in FNSB region, Tran and Mölders conducted a simulation study on the potential effectiveness of a wood stove change-out program in the

FNSB in which non-certified wood burning devices would be exchanged for EPA certified ones [15]. Simulations for October through March 2009 were run using the Weather Research and Forecasting model inline coupled with a chemistry package (WRF/CHEM) [15]. The average decrease in 24-hour PM2.5 levels was 0.6 μg/$m^3$ with the exchange of 90 outdoor wood boilers and 2390 uncertified wood stoves[15]. The effectiveness of the program was dependent on the type and number of devices exchanged [15]. While the change-out program did decrease the PM2.5 levels and decreased the number of exceedances, the decrease would only be significant for PM2.5 levels close to the NAAQS of 35 μg/$m^3$ [15]. Overall, the study concluded that change in PM2.5 levels as a result of the change-out program alone would not be sufficient for the FNSB to comply with the 24-hour PM2.5 NAAQS [15].

Between 1993 and 2009, the current federal 24-hour PM2.5 NAAQS of 35 μg/$m^3$, was exceeded 11 times in Juneau [10]. One of the main contributors to high wintertime PM2.5 concentrations in Juneau is wood smoke [10], [16]. Wintertime inversions and cold temperatures in the Mendenhall Valley trap pollutants near the surface causing elevated PM2.5 concentrations and increased demand for heating [10]. To minimize PM2.5 concentrations, burn bans are implemented when inversions are predicted [10]. Since the implementation of the burn bans in Juneau in 2007, Juneau has been successful in meeting the PM2.5 NAAQS [10]. Based on the success of the burn bans in Juneau, strict implementation of burn bans and a wood stove change-out program may improve air quality in Fairbanks as it did in Juneau.

#### *1.2.1.2 Wildfires-PM2.5*

Smoke from wildfires is the main cause of summertime PM2.5 exceedances in Alaska. In the FNSB, smoke from wildfires contributed approximately 50% of total summertime PM2.5 concentrations between 2005 and 2012 [1]. Similarly, wildfires contribute up to 40% of the total PM2.5 concentrations in the western U.S. [17] Wildfires are also the main source of summertime PM2.5 in many of Alaska's national parks, particularly in the interior and the north, such as Denali National Park and Gates of the Arctic National Park [18]. The smoke from wildfires can also be transported long distances from locations such as interior Alaska and Canada throughout the rest of Alaska and thereby cause exceedances and hazardous levels of PM2.5 throughout Alaska [11], [19].

Due to their proximity to Canada, many of the cities in southeast Alaska experience increased PM2.5 levels due to smoke from wildfires in Canada. Through 2004 and part of 2005, the ADEC monitored PM2.5 concentrations in Skagway [11]. Residents of Skagway were concerned with smoke from wildfires, road dust, railroad emissions and cruise ship emissions[11]. Overall, the air quality in Skagway was good, and only one exceedance of the 24-hour PM2.5 NAAQS was recorded. The exceedance was caused by smoke from wildfires in Canada [11]. Further studies on the impact of smoke from wildfires in Canada on air quality in southeast Alaska would be beneficial as elevated PM2.5 levels negatively impact health and AQM stations are limited. Exceedances of the PM2.5 24-hour NAAQS in the summer in Alaska tend to occur when smoke is transported throughout Alaska from wildfires in both Alaska and Canada [1], [11], [19].

### *1.2.1.3 Slash Burning*

Wood smoke from slash burning of trees has not been found to be a significant contributor to PM2.5 concentrations in Alaska as compared to that from residential wood burning and wildfires [20]. PM10 concentrations were monitored in Homer, AK from 2000 to 2001. The main concern in Homer was wood smoke from slash burning of trees. If fires occurred at the time of measurement, the PM10 concentration was considered to be indicative of PM2.5 concentration and mostly due to smoke. If no fires occurred, then the PM10 measurement was considered to be indicative of PM10 concentration and mostly due to dust. The study in Homer was conducted prior to when the 24-hour PM2.5 NAAQS of 65 $\mu g/m^3$was decreased to 35 $\mu g/m^3$, and thus it was evaluated using the old standard [20]. The PM10 values in Homer that exceeded the old NAAQS for PM2.5 were considered to be due to dust, which is assumed to be PM10 and not PM2.5, thus no exceedances of the 24-hour PM2.5 NAAQS were considered to occur [20].

## 1.2.2 Vehicular Emissions

Vehicle emissions are the are main contributors to PM2.5 in Anchorage [21], the largest city in Alaska; and they are the third biggest contributors in Fairbanks behind wood smoke and secondary aerosols [1]. The two main contributors to vehicle emissions are diesel and gasoline vehicles. The contributions from gasoline and diesel vehicles are analyzed separately. Increased emissions from cold starts and idling in the winter-time are the biggest concern regarding PM2.5 contributions from vehicles in Fairbanks, Anchorage, and Juneau.

### *1.2.2.1 Gasoline*

Southcentral Alaska is the most populated region of Alaska. Anchorage is the largest city in Alaska with a population of 298,908 people. Anchorage is currently designated as a maintenance area for carbon monoxide and is an attainment area for both yearly and 24-hour PM2.5. Based on one source characterization study for Anchorage, the main source of PM2.5 is gasoline vehicle emissions. Gasoline vehicles contributed 44% to the average total PM2.5 concentrations; however, the air quality monitor used in the study was located in a parking lot, which may have impacted the results [21].

In Juneau, cold-start idling of vehicles is considered the other main source of PM2.5. The emissions from gasoline automobiles include nitrates, hydrocarbons, carbon monoxide and carbon dioxide. In Fairbanks, the contribution of emissions from gasoline vehicles is higher in the summer than in the winter [1]. This may be due to increased traffic and activity from tourists during the tourist season, June through August. The emissions from gasoline vehicles contribute significantly more than diesel vehicles to total PM2.5 concentrations from June through August as shown in Table 1.3.

#### *1.2.2.2 Diesel*

Heavy duty diesel trucks are the main contributors of diesel vehicle emissions. Fall and winter contributions from diesel vehicles in the FNSB (4.244 $\mu g/m^3$) are significantly greater than those in summer (0.123 $\mu g/m^3$) [1]. The large difference in seasonal diesel emission contribution is most likely due to the increase in the number of heavy duty trucks travelling to the North Slope from 160 trucks in the summer to 250 trucks in the winter with the opening of the ice road [1]. On exceedance days, the contributions from diesel emissions are double those on non-exceedance days [1]. The increased concentrations on exceedance days are most likely due to lower mixing heights from inversions. Other potential sources of diesel emissions are diesel power electric generators and ships. Diesel vehicle emissions typically contain sulfates, ammonium, nitrates, and elemental carbon [1]. Diesel emissions from vehicles are the third largest contributor to wintertime PM2.5 concentrations in the FNSB with highs in the winter and lows in the summer [1]. On average, in Anchorage, diesel vehicle emissions contribute only 0.33 $\mu g/m^3$ (5%) to total PM2.5 concentrations as compared to the 2.61 $\mu g/m^3$ (44%) contributed by gas vehicles [21]. The greater measured contributions of diesel emissions to PM2.5 concentrations in the FNSB as compared to Anchorage is most likely due to temperature inversions which decrease the overall mixing height in FNSB and that the FNSB receives a large amount of traffic from heavy duty trucks because it is located on the route to the North Slope [1].

### 1.2.3 Residential Heating: Distillate Fuel Oil

Many residences in Alaska use distillate fuel oil for heating. For example, approximately half the population of the FNSB uses distillate fuel oil for residential heating [1]. Distillate fuel oil has a higher sulfur content than the diesel used in vehicles. In the FNSB, sulfate is the second highest contributor to wintertime PM2.5 concentrations, contributing high concentrations of PM2.5 in the winter (5.8 $\mu g/m^3$) and low concentrations in the summer (0.31 $\mu g/m^3$) [1], [9]. Due to the sulfur content of the distillate fuel oil used for home heating, it is most likely the primary source of secondary sulfate in the FNSB and thereby one of the main sources of wintertime PM2.5 concentrations. Other sources of secondary sulfate include arctic haze, volcanic eruptions, industrial operations, and oil production [1], [9], [22], [23].

### 1.2.4 Ship Emissions

The Gulf of Alaska receives a significant amount of traffic from ships such as tankers, cargo ships, and cruise ships. Most ships have diesel turbines with gas turbines. Emissions from ships include sulfates, nitrates and black carbon [22]. Increased sulfate concentrations in Alaska are partially due to increased ship emissions along sea lanes [22]. To determine the impact of ship emissions on air quality and visibility, Mölders et al. used WRF/CHEM to perform simulations for the length of the 2006 tourist season in the Gulf of Alaska [24]. In Valdez, ship emissions contributed about 60% of the total PM2.5 concentration [24]. In Prince William Sound, ship emissions can decrease visibility by 30% which affects tourists' ability to sightsee [24]. They found that in the Gulf of Alaska, ship emissions contribute 30-40% to the total PM2.5 concentrations during the tourist season; but the concentration levels were low enough to not cause any exceedances of the NAAQS during the period of the study [24].

In the summer, cruise ships bring nearly one million tourists to Alaska[25]. Emissions from cruise ships are highest in ports of call (i.e., intermediate stops) and by glaciers where cruise ships operate at low engine load to either stop or enable viewing of sights such as glaciers[25]. Ports of call in southern Alaska are located in Anchorage, Sitka, Haines, Juneau, Ketchikan, and Skagway. Based on simulations conducted by Mölders et al.(year) using WRF-Chem for the 2008 cruise season, pollutants from ship emissions were often trapped between steep mountains by nighttime inversions causing maximum pollutant concentrations to occur during the night times. The same study also found that particulate matter counts remained below the NAAQS despite ship emissions in Glacier Bay; however, on days when no cruise ships entered glacier bay, PM2.5 and PM10 values were 15% and 18% lower, respectively [25]. Ship emissions only marginally affected visibility in Glacier Bay, and weather had a significantly greater impact on visibility than the ship emissions [25].

### 1.2.5 Dust

Dust particles are typically considered to be PM10 but can also be measured as PM2.5 [1], [9], [21]. Dust has both anthropogenic and natural sources. Dust issues are of significant concern in Alaska in areas with unpaved roads, and activity along those roads increases total PM10 concentrations, such as in many rural areas in Alaska [3], [16]. Increased dust can also be due to land-clearing, construction, and mining [2], [10]. Natural sources of dust are glaciers, glacial valleys, and exposed riverbeds [2], [10]. Major dust events are typically a result of high winds that transport soils, such as glacial silt and sand, from exposed riverbeds, glaciers, and beaches into the surrounding areas. Dust is mainly a problem during the spring and summer. In the spring, water levels tend to be low leaving riverbeds more exposed. As the snow melts in the spring, vehicles and wind kick up the sand and gravel that was applied on icy roads to improve traffic safety. Limited precipitation in the summer decreases the cohesiveness of soil particles causing an increase in dust events.

#### *1.2.5.1 Fugitive Road Dust*

Fugitive road dust tends to be a problem in areas with unpaved roads. Rural villages and cities in northern and western Alaska are primarily concerned with fugitive road dust and wood smoke from both wildfires and home heating. The dirt roads in Northwestern Alaska are mainly composed of a mixture of gravel, sand, and silt [3]. The roads are used by pedestrians, cyclists, cars, trucks, all-terrain vehicles (ATVs), and playing children[3]. The ADEC measured PM10 concentrations in eight villages in the Northwest Arctic Borough in the summers from 2003 to 2005: Selawik, Ambler, Kiana, Buckland, Kotzebue, Kivalina, Noatak, and Noorvik [3]. Many of the villages complained of road dust from ATVs and other vehicles [13]. At the time of the monitoring, most of the villages were not paved [3]. They measured a total of 29 exceedances of the PM10 NAAQS. No exceedances were measured in Kotzebue, and Selawik with maximum measured PM10 concentrations of 125 $\mu g/m^3$ and 13 $\mu g/m^3$ (no data was obtained from Kivalina)[3]. The low PM10 concentrations in Selawik can be attributed to the fact that the village uses boardwalks instead of dirt roads[3].

The ADEC conducted fugitive road dust mitigation studies in Kotzebue, Buckland, and Noorvik (along the upper western coast of Alaska). Between 2002 and 2005, 31 exceedances of the 24-hour PM10 NAAQS were measured prior to paving Second Avenue in Kotzebue [26]. To determine the effectiveness of paving, PM10 concentrations were measured 2006 to 2008 [26]. In 2008, six exceedances were measured, indicating the need to pave more roads or treat them with dust palliatives (suppressants). In that time, paving resulted in a 64% reduction in dust concentrations on the upwind side of the street and 71% reduction on the downwind side[26]. Overall, paving is an effective dust mitigation strategy when the roads are regularly maintained.

The effectiveness of dust palliatives as a dust mitigation strategy was tested in the communities of Buckland and Noorvik. In 2003 and 2004, one exceedance was measured per year in Buckland, and a total of nine exceedances were measured in Noorvik prior to the application of dust palliatives [27], [28]. Multiple roads in Buckland were treated with dust palliatives (EK-35, Soil Sement) in July of 2012, and with only one exceedance measured after the treatment and an overall improvement in PM10 concentrations[28]. In 2010, three types of dust palliatives (Alastac, FB400, Earth Armour) were used to treat a few of the roads in Noorvik [27]. Post-treatment, one exceedance was measured in 2011, and six exceedances were measured in 2012. The increase in exceedances with time indicates that the effectiveness of dust palliatives decreases with time and that roads must regularly be treated [27]. Both paving and dust palliatives are effective dust mitigation strategies with proper maintenance and regular treatment.

#### *1.2.5.2 Windblown dust*

Glaciers and dried riverbeds are other major sources of dust. It is typically a problem in glacial valleys such as the Mendenhall Valley (Southeast Alaska) and the Matanuska-Susitna Valley (Southcentral Alaska). It can also be a problem along coastal areas in Southcentral Alaska, such as Seward and Homer, but no exceedances of the NAAQS PM10 have been reported in those areas. In the Mendenhall Valley, winds blow glacial dust off the Mendenhall Glacier into the valley below causing an increase in PM10 concentrations. The Matanuska-Susitna Valley is prone to large dust events when water levels are low, typically in spring and fall, and katabatic (downslope) winds stir up glacial silt from the exposed gravel bars and tidal flats [2]. Between 1999 and 2010, a total of 9 exceedances of the PM10 NAAQS were measured with a maximum PM10 concentration of 605 $\mu g/m^3$ in the Butte near Palmer. In the Butte, all exceedances occurred during high wind events [2].

### 1.2.6 Arctic Haze-PM2.5

Arctic haze is mainly of Eurasian origin and consists primarily of secondary sulfate and particulate organic matter from industrial processes, wildfires, and dust storms [23]. Due to its proximity to Russia and the Arctic, northern and western Alaska are prone to pollution from Arctic haze [19], [23], [29]. Arctic haze has a seasonal cycle with lows in the summer and highs at least two times greater than the summer concentrations in the winter [23], [29]. Source apportionment studies show that arctic haze impacts PM2.5 concentrations as far south as Anchorage [21]. In Anchorage, an unknown source "likely included sources from incinerators or metal processors with high impacts from the northwest" and highs in the spring, which is consistent with Arctic haze [21]. In Denali National Park, secondary sulfates are the dominant aerosol species from November through May [19]. The diurnal variability in Denali National Park is consistent with that of arctic haze, indicating that the secondary sulfate is most likely from the Arctic haze. Source apportionment studies using the IMPROVE (Interagency Monitoring of Protected Visual Environments) network showed a gradient of sulfate content from northwestern to southeastern Alaska, indicating that pollutants from arctic haze are being transported from the north/northwest of Alaska [19].

### 1.2.7 Salt

Both road salt and seas salt are sources of PM2.5 in Alaska. Road salt is used in the wintertime to melt snow and prevent it from freezing. Therefore, road salt PM2.5 concentrations are relatively higher in the winter and nearly non-existent in the summer [1]. On average in the FNSB, road salt contributes 0.4% (0.021 $\mu g/m^3$) to total PM2.5 concentrations in the summer and 1.9% (0.426 $\mu g/m^3$) to total PM2.5 concentrations on average in the winter [1]. The overall contributions of road salt are negligent when compared to PM2.5 contributions by wood smoke, secondary aerosols, and vehicle emissions.

While road salt is used on road systems throughout Alaska, sea salt typically only contributes to PM2.5 concentrations in coastal areas [18], [19], [21]. In Anchorage, aged sea salt contributes on average approximately 0.33 $\mu g/m^3$ (5%) of the total PM2.5 concentrations [21]. In contrast, aged seas salt contributes nearly 3 $\mu g/m^3$ in Los Angeles, CA and is the third major contributor to PM2.5 concentrations behind vehicle emissions and secondary aerosols. Overall, road salt and sea salt are minor contributors of PM2.5 concentrations in Alaska, and thereby not a major concern with regard to PM2.5 levels.

### 1.2.8 Volcanic Eruptions

Most of the active volcanoes in Alaska are located along the Aleutian Islands and in southcentral Alaska, such as Mt. Redoubt and Mt. Spur. Volcanic emissions include volcanic ash mixed with volcanic gases and aerosols. Elevated concentrations of PM10 and PM2.5 were measured in both Anchorage and Soldotna during the 2009 eruption of Mt. Redoubt, but it was not sufficient to cause any exceedances of the 24-hour PM2.5 NAAQS [30]. The impact of volcanic emissions on measured PM10 and PM2.5

concentrations is dependent on the fraction of volcanic emissions that are PM10 and PM2.5 and meteorological conditions.

### 1.3 Current Methods of Air Quality Analysis

Alaska's air quality monitoring network currently consists of year-round ground air quality monitors that are monitored by the ADEC and the IMPROVE network. The ADEC air quality monitors are a part of the EPA air quality monitoring system and located in Fairbanks, North Pole, Anchorage, Eagle River, Palmer, Bethel, and Juneau. The IMPROVE network is used to monitor air quality and visibility in many of Alaska's National Parks. Currently, PM2.5 monitors are located in Petersburg, Denali National Park, Simeonof, Gates of the Arctic National Park, Trapper Creek, and Tuxedni. Figure 1.2 shows the locations of past and present air quality monitors.

The two main types of air quality monitors used by the ADEC are the Thermo Scientific Inc. Partisol 2000 with a BGI Inc. very sharp cut cyclone (R&P Partisol 2000) and the PM2.5 Met One Beta Attenuation Monitor (BAM 1020) [31]. The R&P Partisol 2000 is designated as the Federal Reference Method (FRM) and takes measurements once every three days. Because the FRM was used to develop the NAAQS, all other monitors must obtain measurements that correlate strongly with those obtained with the FRM to be designated as the Federal Equivalent Method (FEM). The BAM 1020 is designated as the FEM, and it can be used instead of the FRM in Anchorage, Juneau, and the Matanuska-Susitna Valley. The disparity in the measurements using the FRM and the BAM 1020 in North Pole and Fairbanks at present is too high, therefore, the BAM1020 is not designated as an FEM in North Pole and Fairbanks. Due to the extreme temperatures and PM2.5 concentrations in Fairbanks, further calibration of the BAM 1020 is necessary. All of the BAM 1020s used in Alaska are designated as Class III monitors because they are continuous monitors; they take hourly and daily measurements.

The Weather Research Forecasting model coupled with chemistry (WRF-Chem) "simulates the emission, transport, mixing, and chemical transformation of trace gases and aerosols simultaneously with the meteorology" (UCAR, 2016). Mölders et al. evaluated the WRF-Chem model at higher latitudes and found that it would work well for examining emission reduction scenarios [32]. The WRF-Chem model best predicted PM2.5 values at concentrations between 15 and 50 $\mu g/m^3$ [32]. It also underestimated the inversion strength and overestimated wind speed, which caused errors in the data [32]. Other errors in the model could be attributed to errors in emissions data[32]. At lower temperatures, the error between ground air quality monitors also increases, which makes it more difficult to evaluate the accuracy of the WRF-Chem model [32]. To improve the WRF-Chem model for Alaska, the ground air quality network would need to be extended and the emissions inventory would need to be updated. The WRF-Chem model has successfully been used in Alaska to evaluate the impact of ship activity on air quality, the effectiveness of a wood-burning device change-out program, and the effects of urbanization on precipitation [24], [25], [32], [33].

### 1.4 Future Directions

Alaska's current air quality network is limited. Satellite remote sensing has been used successfully to estimate ground-level PM2.5 concentrations in the various locations such as the continental United States, Australia, Beijing, and India [7], [34], [35]. In Alaska, satellite remote sensing is used to map wildfires and estimate volcanic emissions. No studies have been published on the use of satellite remote sensing for the prediction of ground-level PM2.5 concentrations in Alaska. The benefit of the use of satellite remote sensing is that it can be used on a larger spatial scale and to identify hot spots of pollution in Alaska.

Aerosol optical depth (AOD) is defined as the total columnar loading of aerosols. It is typically used in a model to estimate ground-level PM2.5 in locations where the AOD data has been validated. The following instruments are used to derive AOD: Moderate Resolution Imaging Spectroradiometer (MODIS), Multi-Angle Imaging Spectroradiometer (MISR), and Visible Infrared Imaging Radiometer Suite (VIIRS). MISR can also be used to determine the amount and types of aerosols (www.nasa.gov). Both the MODIS and MISR instruments are situated on the Terra satellite and MODIS is located on the Aqua satellite. The Ozone Monitoring Instrument (OMI) is located on the Aura satellite and is used to distinguish and measure aerosol types, trace gases and ozone. Data from the Cloud-Aerosol Lidar and Infrared Pathfinder Satellite Observation (CALIPSO) can be used to determine the vertical distribution of aerosols. MODIS, MISR, and VIIRS are used as primary aerosol sensors. One of the limitations of using satellite remote sensing data is that there is limited temporal coverage. For example, MODIS has a temporal resolution of 1 to 2 days. Another limitation is that because AOD is a measure of reflectance, measurements cannot be obtained in snow-covered or cloudy areas due to the high reflectivity of snow and clouds. Also, the total columnar loading of aerosols is measured which includes all particulate sizes and may not reflect ground level conditions.

While satellite remote sensing may not be a viable option for estimating wintertime ground-level PM2.5 concentrations in Alaska; it could be a useful tool for monitoring summertime air quality in Alaska, particularly rural Alaska, and other unmonitored areas affected by smoke from wildfires and dust. AOD measurements from MODIS, MISR, and VIIRS should be validated, and a model should be developed to estimate ground-level PM2.5 concentrations throughout Alaska.

### 1.5 Conclusion

The main sources of PM10 and PM2.5 in Alaska are dust, wood smoke, vehicle emissions, and residential home heating. Exceedances of the 24-hour PM2.5 and PM10 NAAQS due to anthropogenic sources typically occur at low temperatures during surface inversions and fugitive road dust, respectively. Exceedances of the PM10 and PM2.5 NAAQS due to natural sources may occur during high wind events and wildfires, respectively. Alaska's air quality network is currently limited to urban areas, and national parks, with nearly one-third of Alaskans, live in rural areas that remain unmonitored. The limited spatial resolution of air quality monitors poses a problem for monitoring air quality and thereby human exposure to pollutants in rural Alaska. A larger air quality monitoring network is necessary for Alaska. Remote sensing has been used successfully to monitor ground-level PM2.5 concentrations in various regions throughout the world. While remote sensing may not be used in wintertime, it would provide a useful tool for monitoring exposure and air quality as both wildfires and dust can cause unhealthy levels of both PM10 and PM2.5 throughout Alaska.

### 1.6 References


[1] Y. Wang and P. K. Hopke, "Is alaska truly the great escape from air pollution???? Long term source apportionment of fine particulate matter in Fairbanks, Alaska," *Aerosol Air Qual. Res.*, vol. 14, no. 7, pp. 1875–1882, 2014.

[2] ADEC, "Air Quality Monitoring at Harrison Court, Butte, Alaska," *Alaska Department of Environmental Conservation: Air Quality Division Air Monitoring and Quality Assurance Program*, 2011. [Online]. Available: http://dec.alaska.gov/air/am/projects&Reports/Butte_rpt_2feb12.pdf. [Accessed: 24-Jan-2017].

[3] ADEC, "A preliminary assessment of fugitive dust from roads in eight Alaskan villages in the Northwest Arctic Borough," *Alaska Department of Environmental Conservation: Air Quality Division Air Monitoring and Quality Assurance Program*, 2011. [Online]. Available: http://dec.alaska.gov/air/am/projects&Reports/dust_NWAB_03-05.pdf. [Accessed: 24-Jan-2017].

[4] ALA, "American Lung Association State of the Air 2018," *American Lung Association,* 2018. [Online]. Available: https://www.lung.org/assets/documents/healthy-air/state-of-the-air/sota-2018-full.pdf. [Accessed: 11-Oct-2018].

[5] H. N. Q. Tran and N. Mölders, "Investigations on meteorological conditions for elevated PM 2.5 in Fairbanks, Alaska Multiday inversions Alaska Air quality in high latitudes," 2010.

[6] ADEC, "Assessment of the continuous PM 2.5 Met One BAM 1020 sampler performance in the State of Alaska Air monitoring Network," *Alaska Department of Environmental Conservation: Air Quality Division Air Monitoring and Quality Assurance Program*, 2014. [Online]. Available: http://dec.alaska.gov/air/anpms/projects-reports/DOCS/Alaska-PM2.5-FRM-FEM-Correlations-Report.pdf. [Accessed: 24-Jan-2017].

[7] P. Gupta, S. a. Christopher, M. A. Box, and G. P. Box, "Multi year satellite remote sensing of particulate matter air quality over Sydney, Australia," *Int. J. Remote Sens.*, vol. 28, no. November 2014, pp. 4483–4498, 2007.

[8] G. D. Thurston, K. Ito, and R. Lall, "A source apportionment of U.S. fine particulate matter air pollution," *Atmos. Environ.*, vol. 45, no. 24, pp. 3924–3936, Aug. 2011.

[9] T. Ward, B. Trost, J. Conner, J. Flanagan, and R. K. M. Jayanty, "Source Apportionment of PM2.5 in a Subarctic Airshed - Fairbanks, Alaska," *Aerosol Air Qual. Res.*, vol. 12, no. 4, pp. 536–543, 2012.

[10] ADEC, "Juneau Air Quality Monitoring Report," *Alaska Department of Environmental Conservation: Air Quality Division Air Monitoring and Quality Assurance Program*, 2010. [Online]. Available: http://dec.alaska.gov/air/am/FDMS_rpt_93-09.pdf. [Accessed: 24-Jan-2017].

[11] ADEC, "Skagway Air Monitoring Study of Airborne Fine Particulate Matter During 2004-5," *Alaska Department of Environmental Conservation: Air Quality Division Air Monitoring and Quality Assurance Program*, 2007. [Online]. Available: http://dec.alaska.gov/air/am/Skagway_AQ_rpt_6apr07.pdf. [Accessed: 24-Jan-2017].

[12] ADEC, "Seward PM 10 Air Monitoring Program January 2011 to May 2012 Final Report," *Alaska Department of Environmental Conservation: Air Quality Division Air Monitoring and Quality Assurance Program*, 2013. [Online]. Available: http://dec.alaska.gov/air/am/projects&Reports/Seward PM10 Air Monitoring Program Jan 2011-May 2012 Final Report.pdf. [Accessed: 24-Jan-2017].

[13] D. Ware, J. Lewis, S. Hopkins, B. Boyer, C. Noonan, and T. Ward, "Sources and perceptions of indoor and ambient air pollution in rural Alaska," *J. Community Health*, vol. 38, no. 4, pp. 773–780, 2013.

[14] S. M. Bourne, U. S. Bhatt, J. Zhang, and R. Thoman, "Surface-based temperature inversions in Alaska from a climate perspective," *Atmos. Res.*, vol. 95, no. 2–3, pp. 353–366, 2010.

[15] H. N. Q. Tran and N. Mölders, "Wood-burning device changeout: Modeling the impact on PM concentrations in a remote subarctic urban nonattainment area," *Adv. Meteorol.*, vol. 2012, p. 12 pages, 2012.

[16] ADEC, "Juneau Air Quality Monitoring Project Lemon Creek Valley 1984-1994.pdf," *Alaska Department of Environmental Conservation*, 1994. [Online]. Available: http://dec.alaska.gov/air/am/FDMS_rpt_93-09.pdf. [Accessed: 24-Jan-2017].

[17] S. P. Urbanski, W. M. Hao, and B. Nordgren, "The wildland fire emission inventory: western United States emission estimates and an evaluation of uncertainty," *Atmos. Chem. Phys.*, vol. 11, no. 24, pp. 12973–13000, Dec. 2011.

[18] A. V. Polissar, P. K. Hopke, P. Paatero, W. C. Malm, and J. F. Sisler, "Atmospheric aerosol over Alaska: 2. Elemental composition and sources," *J. Geophys. Res.*, vol. 103, no. D15, p. 19045, 1998.

[19] V. Polissar, P. K. Hopke, and P. Service, "Atmospheric aerosol over Alaska 1 . Spatial and seasonal variability processes," *New York*, vol. 103, pp. 35–44, 1998.

[20] ADEC, "Air Quality Monitoring at Homer, AK," *Alaska Department of Environmental Conservation: Air Quality Division Air Monitoring and Quality Assurance Program*, 2013. [Online]. Available: http://dec.alaska.gov/air/am/Homer air monitoring rpt 26JUL13.pdf. [Accessed: 02-Oct-2017].

[21] E. Kim and P. Hopke, "Characterization of Ambient Fine Particles in the Northwestern Area and Anchorage, Alaska," *J. Air Waste Manage. Assoc.*, vol. 58, no. 10, pp. 1328–1340, 2008.

[22] T. T. Tran, G. Newby, and N. Moelders, "Impacts of emission changes on sulfate aerosols in Alaska," *Atmos. Environ.*, vol. 45, no. 18, pp. 3078–3090, 2011.

[23] K. S. Law and A. Stohl, "Arctic Air Pollution: Origins and Impacts," *Science (80-. ).*, vol. 315, no. 5818, pp. 1537–1540, 2007.

[24] N. Mölders, S. E. Porter, C. F. Cahill, and G. A. Grell, "Influence of ship emissions on air quality and input of contaminants in southern Alaska National Parks and Wilderness Areas during the 2006 tourist season," *Atmos. Environ.*, vol. 44, no. 11, pp. 1400–1413, 2010.

[25] N. Mölders, S. Gende, and M. Pirhalla, "Assessment of cruise–ship activity influences on emissions, air quality, and visibility in Glacier Bay National Park," *Atmos. Pollut. Res.*, vol. 4, no. 4, pp. 435–445, 2013.

[26] ADEC, "Effectiveness of Paving on Airborne Particulate Matter: A Preliminary Assessment of Fugitive Dust from Roads in Kotzebue, Alaska," *Alaska Department of Environmental Conservation: Air Quality Division Air Monitoring and Quality Assurance Program*, 2011. [Online]. Available: http://dec.alaska.gov/air/am/projects&Reports/Kotzebue Road Dust Report Final 8-11.pdf. [Accessed: 24-Jan-2017].

[27] ADEC, "Air Quality Monitoring in Noorvik, AK 2003-2012," *Alaska Department of Environmental Conservation: Air Quality Division Air Monitoring and Quality Assurance Program*, 2013. [Online]. Available: http://dec.alaska.gov/air/am/Noorvik_Rd_Dust_2003-2012.pdf. [Accessed: 24-Jan-2017].

[28] ADEC, "Air Quality Monitoring in Buckland, AK," *Alaska Department of Environmental Conservation: Air Quality Division Air Monitoring and Quality Assurance Program*, 2013. [Online]. Available: http://dec.alaska.gov/air/am/Buckland_Rd_Dust_2003-2012.pdf. [Accessed: 24-Jan-2017].

[29] G. E. Shaw, "Aerosol Chemical-Components in Alaska Air Masses .1. Aged Pollution," *J. Geophys. Res.*, vol. 96, no. D12, pp. 22357–22368, 1991.

[30] J. R. Schaefer, "The 2009 Eruption of Redoubt Volcano, Alaska," 2012.

[31] ADEC, “Alaska Department of Environmental Conservation Annual Air Quality Monitoring Network Plan,” *Alaska Department of Environmental Conservation: Air Quality Division Air Monitoring and Quality Assurance Program*, 2015. [Online]. Available: http://dec.alaska.gov/air/am/2015_Air_Monitoring_plan.pdf. [Accessed: 24-Jan-2017].

[32] N. Mölders, H. N. Q. Tran, C. F. Cahill, K. Leelasakultum, and T. T. Tran, “Assessment of WRF/Chem PM 2.5 forecasts using mobile and fixed location data from the Fairbanks, Alaska winter 2008/09 field campaign,” *Atmos. Pollut. Res.*, vol. 3, no. 2, pp. 108–191, 2012.

[33] N. Mölders and M. A. Olson, “Impact of Urban Effects on Precipitation in High Latitudes,” *J. Hydrometeorol.*, vol. 5, no. 1980, pp. 409–429, 2004.

[34] Y. Xie, Y. Wang, K. Zhang, W. Dong, B. Lv, and Y. Bai, “Daily Estimation of Ground-Level PM2.5 Concentrations over Beijing Using 3 km Resolution MODIS AOD,” *Environ. Sci. Technol.*, vol. 49, no. 20, pp. 12280–12288, 2015.

[35] H. Zhang, R. M. Hoff, and J. A. Engel-Cox, “The Relation between Moderate Resolution Imaging Spectroradiometer (MODIS) Aerosol Optical Depth and PM2.5 over the United States: A Geographical Comparison by U.S. Environmental Protection Agency Regions,” *J. Air Waste Manag. Assoc.*

[36] C. A. Pope and D. W. Dockery, “Health Effects of Fine Particulate Air Pollution: Lines that Connect,” *J. Air Waste Manage. Assoc.*, vol. 56, no. 6, pp. 709–742, 2006.

[37] N. Fann, A. D. Lamson, S. C. Anenberg, K. Wesson, D. Risley, and B. J. Hubbell, “Estimating the National Public Health Burden Associated with Exposure to Ambient PM2.5 and Ozone,” *Risk Anal.*, vol. 32, no. 1, pp. 81–95, Jan. 2012.

[38] S. Dey and L. Di Girolamo, “A decade of change in aerosol properties over the Indian subcontinent,” *Geophys. Res. Lett.*, vol. 38, no. 14, pp. 1–5, 2011.

[39] R. C. Levy *et al.*, “The Collection 6 MODIS aerosol products over land and ocean,” *Atmos. Meas. Tech.*, vol. 6, pp. 2989–3034, 2013.

[40] A. M. Sayer, N. C. Hsu, C. Bettenhausen, and M. J. Jeong, “Validation and uncertainty estimates for MODIS Collection 6 ‘deep Blue’ aerosol data,” *J. Geophys. Res. Atmos.*, vol. 118, no. 14, pp. 7864–7872, 2013.

[41] N. C. Hsu *et al.*, “Enhanced Deep Blue aerosol retrieval algorithm: The second generation,” *J. Geophys. Res. Atmos.*, vol. 118, no. 16, pp. 9296–9315, Aug. 2013.

[42] M. Petrenko, C. Ichoku, and G. Leptoukh, “Multi-sensor Aerosol Products Sampling System (MAPSS),” *Atmos. Meas. Tech*, vol. 5, pp. 913–926, 2012.

[43] J. P. Sherman, P. Gupta, R. C. Levy, and P. J. Sherman, "An Evaluation of MODIS-Retrieved Aerosol Optical Depth over a Mountainous AERONET Site in the Southeastern US," *Aerosol Air Qual. Res.*, vol. 16, pp. 3243–3255, 2016.

[44] C. Ichoku *et al.*, "A spatio-temporal approach for global validation and analysis of MODIS aerosol products," *Geophys. Res. Lett.*, vol. 29, no. 12, pp. 1–4, 2002.

[45] L. A. Remer *et al.*, "Validation of MODIS aerosol retrieval over ocean," *Geophys. Res. Lett.*, vol. 29, no. 12, pp. 2–5, 2002.

[46] T. F. Eck *et al.*, "Wavelength dependence of the optical depth of biomass burning, urban, and desert dust aerosols," *J. Geophys. Res.*, vol. 104, no. D24, pp. 31333–31349, 1999.

[47] B. N. Holben *et al.*, "AERONET - A federated instrument network and data archive for aerosol characterization," *Remote Sens. Environ.*, vol. 66, no. 1, pp. 1–16, 1998.

[48] J. E. Nichol and M. Bilal, "Validation of MODIS 3 km resolution aerosol optical depth retrievals over Asia," *Remote Sens.*, vol. 8, no. 4, 2016.

[49] J. S. Long and L. H. Ervin, "Using heteroscedasticity consistent standard errors in the linear regression model," *Am. Stat.*, vol. 54, no. May, pp. 217–224, 2000.

[50] L. A. Remer *et al.*, "The MODIS Aerosol Algorithm, Products, and Validation," *J. Atmos. Sci.*, vol. 62, 2005.

[51] P. Gupta and S. A. Christopher, "Particulate matter air quality assessment using integrated surface, satellite, and meteorological products: Multiple regression approach," *J. Geophys. Res. Atmos.*, vol. 114, no. 14, pp. 1–13, 2009.

[52] D. A. Chu, Y. J. Kaufman, C. Ichoku, L. A. Remer, D. Tanré, and B. N. Holben, "Validation of MODIS aerosol optical depth retrieval over land," *Geophys. Res. Lett.*, vol. 29, no. 12, pp. MOD2-1-MOD2-4, 2002.

[53] US EPA, "Fairbanks Air Quality Plan," *United States Environmental Protection Agency*, 2017. [Online]. Available: https://www.epa.gov/ak/fairbanks-air-quality-plan#nonattainment. [Accessed: 4-Nov-2018].

[54] E. W. Butt *et al.*, "Global and regional trends in particulate air quality and attributable health burden over the past 50 years," 2017.

[55] S. A. Christopher and P. Gupta, "Journal of the Air & Waste Management Association Satellite Remote Sensing of Particulate Matter Air Quality: The Cloud-Cover Problem Satellite Remote Sensing of Particulate Matter Air Quality: The Cloud-Cover Problem," *J. Air Waste Manage. Assoc.*, vol. 60, no. 5, pp. 596–602, 2010.

[56] P. Gupta and S. A. Christopher, “Seven year particulate matter air quality assessment from surface and satellite measurements,” *Atmos. Chem. Phys. Atmos. Chem. Phys.*, vol. 8, pp. 3311–3324, 2008.

[57] P. Gupta and S. A. Christopher, “An evaluation of Terra-MODIS sampling for monthly and annual particulate matter air quality assessment over the Southeastern United States,” *Atmos. Environ.*, vol. 42, no. 26, pp. 6465–6471, 2008.

[58] EPA, “Air Quality System Data Mart,” 2015. [Online]. Available: https://aqs.epa.gov/api. [Accessed: 20-Jan-2018].

[59] NASA, “Level 1 and Atmosphere Archive and Distribution System (LAADS),” *LAADS Web*, 2018. [Online]. Available: https://ladsweb.modaps.eosdis.nasa.gov/search/. [Accessed: 25-Jan-2018].

[60] Y. Liu, C. J. Paciorek, and P. Koutrakis, “Estimating regional spatial and temporal variability of PM2.5 concentrations using satellite data, meteorology, and land use information,” *Environ. Health Perspect.*, vol. 117, no. 6, pp. 886–892, 2009.

[61] S. Aggarwal, R. Jain, and J. D. Marshall, “Real-time prediction of size-resolved ultrafine particulate matter on freeways,” *Environ. Sci. Technol.*, vol. 46, no. 4, pp. 2234–2241, 2012.

## 1.7 Tables and Figures

Table 1.1. EPA designated maintenance and nonattainment areas in Alaska.

| Location | Pollutant | EPA Designation | NAAQS, Averaging Time | Year of Designation | 2010 Population |
|---|---|---|---|---|---|
| Anchorage | Carbon Monoxide | Maintenance | 9 ppm, 8 hour | 2002 | 286227 |
| Eagle River | PM10 | Maintenance | 150 μg/m$^3$, 24 hour | 2013 | 219193 |
| FNSB[1] | PM2.5 | Non-attainment | 35 μg/m$^3$, 24 hours | 2009 | 87456 |
| FNSB | Carbon Monoxide | Maintenance | 9 ppm, 8 hour | 2004 | 46211 |
| Juneau | PM10 | Maintenance | 150 μg/m$^3$, 24 hour | 1994 | 14030 |

[1] Fairbanks North Star Borough

Table 1.2. Air quality studies in various Alaskan regions that investigated particulate matter (PM) sources spanning a period of 1986-2012.

| *Region* | *Location* | *Reference* | *Pollutant* | *Sources of PM* | *Study Period* |
|---|---|---|---|---|---|
| *Interior* | FNSB | Ward et al. 2012 | PM2.5 | Secondary Sulfate, Ammonium Nitrate, Diesel, Gasoline, Wood Smoke | 2005-2012 |
| | FNSB | Wang & Hopke 2014 | PM2.5 | Secondary Sulfate, Ammonium Nitrate, Diesel, Gasoline, Wood Smoke | Nov-Feb 2008-2011 |
| | FNSB | Tran & Moelders 2012 | PM2.5 | Residential Wood Burning | Oct. 2008-Apr. 2009 |
| *Southcentral* | Anchorage | Kim & Hopke 2008 | PM2.5 | Gasoline Vehicle Emissions | 2002-2003 |
| | The Gulf of Alaska | Moelders et al. 2010 | PM2.5 | Ship Emissions | 2006 |
| | Palmer (Butte) | ADEC 2011 | PM10, PM2.5 | Dust, Wood smoke | 1999-2010 |
| | Big Lake | ADEC 2012 | PM2.5 | Transport | 2000-2002 |
| | Homer | ADEC 2013 | PM10 | Wood smoke | 2000-2001 |
| | Seward | ADEC 2013 | PM10 | Dust | 1/2011-5/2012 |
| *Northwest* | National Parks | Polissar et al. 1998 | PM2.5 | Arctic Haze | 1986-1995 |
| | Northwest Arctic Borough | ADEC 2011 | PM10 | Wood Smoke, Fugitive Road Dust | Feb-Sep 2003-2005 |
| *Southeast* | | Moelders et al. 2013 | PM2.5, PM10 | Ship Emissions | 2008 |
| | Juneau | ADEC 2010 | PM2.5 | Wood Smoke, Vehicle Emissions | 1993-2009 |
| | Skagway | ADEC 2007 | PM2.5 | Wood Smoke, Road Dust, Railroad Emissions, Ship Emissions | 2004-2005 |
| *National Parks* | | Polissar et al. 1998 | PM2.5 | Wildfires, vehicle emissions, salt, dust, anthropogenic | 1986-1995 |

Table 1.3. Results of source apportionment studies in Fairbanks North Star Borough region investigating significant contributors to PM2.5.

| Reference | Method | Location | Years | Months | Secondary Sulfate | Ammonium Nitrate | Diesel | Gasoline | Wood Smoke | Unexplained | Road Salt | Soil |
|---|---|---|---|---|---|---|---|---|---|---|---|---|
| Ward et al. 2012 | CMB[1] | Fairbanks/ North Pole | 2008-2011 | Nov-Feb | 8-20% | 3-11% | ND[3]-10% | ND-7% | 63-80% | 0-1% | | |
| | | Fairbanks State Office Building | | | 17.3-20% | 8.1-8.9% | ND-2.2% | 1.9-6.8% | 63.1 - 72.4% | 0.02-0.8% | | |
| Wang & Hopke 2014 | PMF[2] | Fairbanks State Office Building | 2005-2012 | Dec-Feb | 25.2% | 4.6% | 18.6% | 9.7% | 39.6% | | 1.9% | 0.4% |
| | | | | Mar-May | 21.5% | 5.7% | 8.9% | 20.9% | 33.3% | | 1.4% | 8.3% |
| | | | | Jun-Aug | 5.4% | 2.9% | 2.1% | 29.7% | 52.5% | | 0.4% | 7.1% |
| | | | | Sep-Nov | 14.5% | 4.2% | 18.3% | 17.6% | 41.1% | | 1.3% | 3.0% |
| | | | | Average | 19.5% | 4.5% | 14.3% | 16.3% | 40.5% | | 1.5% | 3.4% |

[1] Chemical Mass Balance, [2] Positive Matrix Factorization, [3] Non-detect

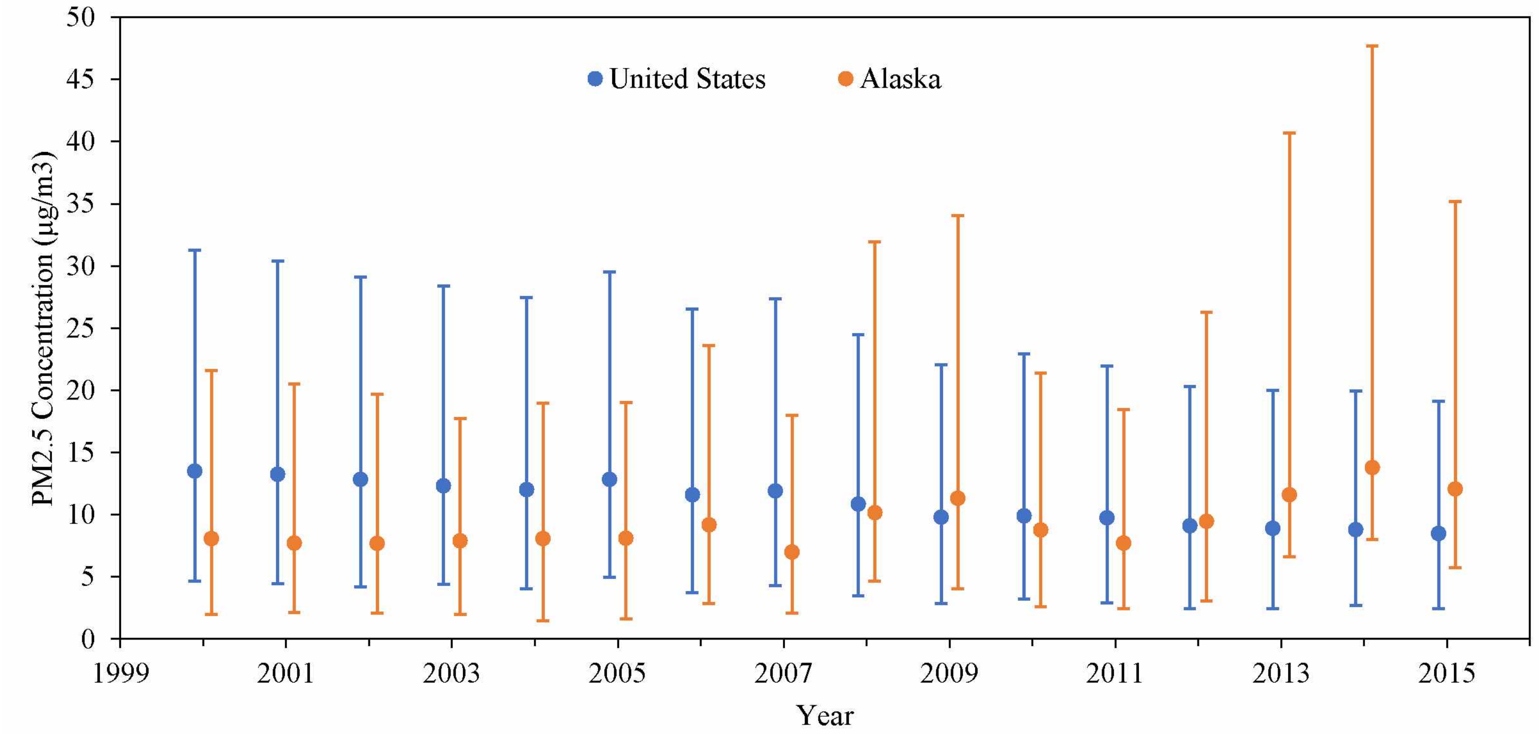


Figure 1.1. A comparison of trends in weighted mean average annual PM2.5 concentrations for Alaska (Anchorage Borough, Juneau Borough, Fairbanks North Star Borough, Matanuska-Susitna Borough) with error bars showing the maximum and minimum mean annual PM2.5 concentration and the United States (481 sites) based on air quality data from the EPA (www.epa.gov) with error bars showing 10th and 90th percentile mean annual PM2.5 concentration.

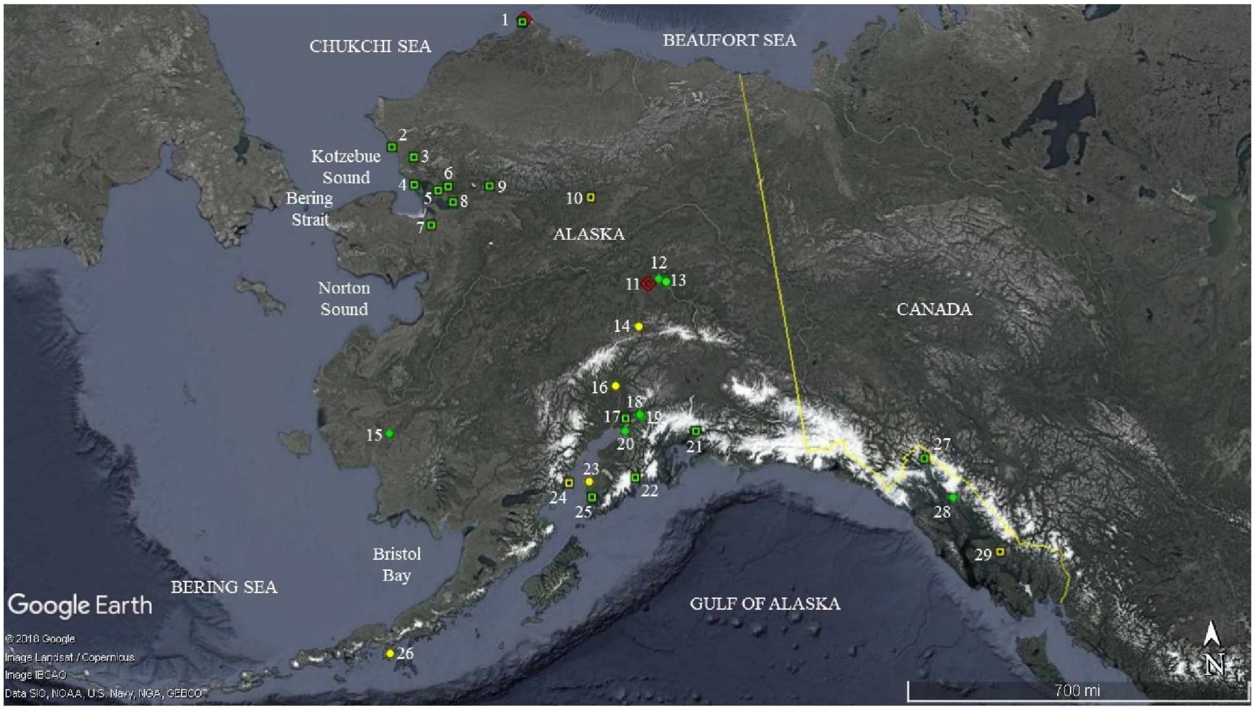


Figure 1.2. Locations of active PM2.5 and PM10 air quality monitors (circles), locations of AERONET stations (red diamonds), locations of past PM2.5 and PM10 studies and/or monitors (squares). Yellow symbols indicate monitors from the IMPROVE network. The following locations are shown: 1. Utqiagvik, 2. Kivalina, 3. Noatak, 4. Kotzebue, 5. Noorvik, 6. Kiana, 7. Buckland, 8. Selawik, 9. Ambler, 10. Gates of the Arctic National Park and Preserve, 11. Bonanza Creek, 12. Fairbanks, 13. North Pole, 14. Denali National Park and Preserve, 15. Bethel, 16. Trapper Creek, 17. Big Lake, 18. Palmer, 19. Butte, 20. Anchorage, 21. Valdez, 22. Seward, 23. Kenai, 24. Tuxedni, 25. Homer, 26. Simeonof, 27. Skagway, 28. Juneau, 29. Petersburg.

Chapter 2 Evaluation of MODIS-Retrieved Aerosol Optical Depth in Alaska: A Comparison of MODIS-Retrieved and AERONET-Retrieved AOD[2]

**Abstract**

The air quality monitoring network in Alaska is currently limited to ground-based observations in urban areas and national parks, leaving a large proportion of the state unmonitored. The use of Moderate Resolution Imaging Spectroradiometer MODIS aerosol optical depth (AOD) to estimate ground-level particulate pollution concentrations has been successfully demonstrated around the world and could potentially be used in Alaska. In this work, MODIS AOD measurements at 550 nm were validated against AOD derived from two ground-based Aerosol Robotic Network (AERONET) sunphotometers in Alaska, located at Utqiagvik (previously known as Barrow) and Bonanza Creek, to determine if MODIS AOD from the Terra and Aqua satellites could be used to estimate ground-level particulate pollution concentrations. The MODIS AOD was obtained from MODIS collection 6 using the dark target Land and Ocean algorithms from years 2000 to 2014. MODIS data could only be obtained between the months of April and October; therefore, it was only evaluated for those months. Individual and combined Terra and Aqua MODIS data were considered. The results showed that MODIS collection 6 products at 10-km resolution for Terra and Aqua combined are not valid over land but are valid over the ocean. Note that the individual Terra and Aqua MODIS collection 6 AOD products at 10-km resolution are valid over land individually but not when combined. Results also suggest the MODIS collection 6 AOD products at 3-km resolution are valid over land and ocean and perform better over land than the 10-km product. These findings indicate that MODIS collection 6 AOD products can be used quantitatively in air quality applications in Alaska during the summer months.

## 2.1 Introduction

Exposure to fine particulate matter (PM) air pollution adversely affects cardiopulmonary health and is associated with increased morbidity and premature mortality [1], [2]. Fine particulate pollution consists of particulates smaller than 2.5 μm (PM2.5) in aerodynamic diameter. A risk analysis of the public health impacts of exposure to ambient PM2.5 estimated that 130,000 PM2.5-related deaths in the continental United States would result from PM2.5 concentration levels in 2005 [3]. Alaska is not immune to the effects of PM pollution. Between the years of 2003 and 2008 in Fairbanks, AK, each 10 $\mu g/m^3$ increase in the mean 24-hour PM2.5 was associated with a 6% to 7% increase in the risk for cerebrovascular disease-coded

[2] McPhetres, A., Aggarwal, S. An Evaluation of MODIS-Retrieved Aerosol Optical Depth over AERONET Sites in Alaska. *Remote Sensing*. 2018, 10, 1384.

and respiratory tract-coded hospital visits the following day [4]. Air quality monitoring is essential for monitoring exposure, determining sources of pollutants, and providing air quality alerts to the public [5].

The air quality monitoring (AQM) network in Alaska is currently limited to urban areas (Fairbanks, Palmer, Anchorage, Juneau) and national parks. Figure 2.1 shows a map of the air quality index and monitoring network used to provide current air quality to the public by AirNow.gov [6].

Moderate Resolution Imaging Spectroradiometer (MODIS) derived aerosol optical depth (AOD) has been used successfully around the world to estimate ground-level PM air pollution [7]–[11], and it could potentially be used to estimate ground-level particulate pollution in Alaska and thus enhance the spatial coverage to fill the gaps beyond what is covered by the state's AQM network.

MODIS currently acquires data across 36 spectral bands, and it has been on-board the Terra and Aqua satellites since 1999 and 2002, respectively. The MODIS Collection 6 (C6) aerosol algorithm consists of three separate algorithms that are used to retrieve AOD from MODIS-observed spectral reflectance: the dark target (DT) ocean algorithm, the DT land algorithm, and the Deep Blue (DB) algorithm [12]–[16]. The DT ocean algorithm retrieves AOD over the ocean across seven wavelengths (470, 550, 660, 870, 1200, and 2100 nm) [12], [17]. The DT land algorithm retrieves AOD over vegetated and dark-soiled land in three visible wavelengths (470 nm, 550 nm, and 660 nm) [12], [17]. Both the DT algorithm products are available at 10-km and 3-km resolution.

MODIS collection 6 AOD has been validated at 550 nm globally for Aqua at 10-km resolution, but not for Terra at 3-km resolution; moreover, none of the studies have considered Alaska specifically [12], [13], [18], [19]. Therefore, to determine whether MODIS AOD can be used to estimate ground-level particulate pollution in Alaska, the 10-km and 3-km resolution products must first be validated against ground-based sunphotometers to determine if there is an agreement between MODIS AOD and AERONET AOD in Alaska. Thus, the overarching goal of this study is to determine if MODIS measurements of aerosol optical depth reflect the actual conditions based on ground-based measurements of aerosol optical depth. If at least 67% of the collocated ground-based and satellite-based measurements are highly correlated (Pearson correlation coefficient greater than 0.7) and within the estimated uncertainty determined from global validation studies (Table 2.1) [12], then it is indicative that MODIS AOD measurements reflect actual ground conditions. If the relationship is weak to non-existent, MODIS AOD does not reflect surface AOD [7], [20]–[22].

## 2.2 Validation Methods

### 2.2.1 AERONET AOD ($\tau_A$)

The Aerosol Robotic Network (AERONET) (http://aeronet.gsfc.nasa.gov) is a ground-based global network of sunphotometers that measure aerosol properties using measurements of solar direct and diffuse radiances [23], [24]. Measurements are obtained and recorded by AERONET sunphotometers at intervals of approximately 3 min. AOD is determined from direct measurements of solar radiance using the Beer-Lambert-Bouguer equation [19], [24]. Due to the low level of uncertainty of AERONET AOD measurements (0.01 to 0.02), AERONET data is commonly used for the validation of satellite-derived MODIS AOD products [19], [24]–[27].

The Alaska AERONET sites of Bonanza Creek and Utqiagvik (previously known as Barrow) were used for the validation of the MODIS AOD product over Alaska. Table 2.2 lists the locations of the two sites. The sunphotometers in Utqiagvik (Barrow) and Bonanza Creek measure direct solar radiance. The AERONET measurements are then used to determine AOD at the following wavelengths: 340, 380, 440, 500, 675, 870, and 1020 nm. The AERONET level 2.0 version 2.0 (cloud-screened and quality-assured) dataset was used to interpolate the AOD at 550 nm in the Multi-sensor Aerosol Products Sampling System (MAPSS) [23]. MAPSS is a framework that collects samples and generates the spatial statistics of various satellites (e.g., MODIS) over AERONET sites and other locations of interest and integrates them with ground-based measurements to facilitate validation [23]. Interpolated AOD at 550 nm, available via the MAPSS between the years 2000 and 2014, was used in this study. The AOD is interpolated using a quadratic fit on a log-log scale [23], [28].

### 2.2.2 MODIS AOD ($\tau_M$)

The MODIS C6 DT products for land and ocean provide AOD with 10-km and 3-km spatial resolutions at nadir at a wavelength of 550 nm at both the Bonanza Creek and Utqiagvik AERONET sites [12], [23]. The MODIS dark target land algorithm was used to determine AOD over the Bonanza Creek site, and the MODIS dark target ocean algorithm was used to determine AOD over the Utqiagvik site as little to no data existed over land for the Utqiagvik site. Terra AOD with mode quality assurance (QA) values of 3 (highest quality) of pixels within the collocation area and Aqua AOD with QA values of 3 were used for the validation of the DT land algorithm-derived MODIS AOD. Terra AOD with mode QA values greater than 0 within the collocation area and for Aqua AOD with QA values greater than 0 were used for the validation of the DT ocean algorithm-derived MODIS AOD. Previous validation studies have also used MODIS AOD with QA of 3 over land and QA greater than 0 over the ocean [12], [19], [25], [26], [28]. AOD data was obtained from Terra between the years 2000 and 2014 and from Aqua between the years 2002 and 2014. Table 2.1 lists the error envelope (EE) for each satellite and the dark target land and ocean algorithms derived from global validation studies for collection 6 [12], [18], [26], [29]. The EE was computed relative to AERONET 550 nm AOD ($\tau_A$).

### 2.2.3 Collocation

Spatially and temporally collocated MODIS and AERONET AOD measurements were obtained from the MAPSS. In MAPSS, AERONET AOD measurements taken within 30 min before or after the satellite overpass time were considered temporally collocated with the MODIS measurements. This was consistent with the previously described methods of temporal collocation [19], [23], [25]. MODIS pixels in MAPSS were sampled if the distance between the AERONET site and the MODIS pixels did not exceed 27.5 km [23]. Terra AOD was used only if the mode QA of the collocated product was 3, and Aqua AOD was used only for products with QA of 3. In MAPSS, the QA of 3 could only be specified for Aqua and not Terra at the time of the analysis; thus, Terra AOD was selected based on a mode of QA 3. The minimum number of collocated AERONET and MODIS pixels was set as one to increase the number of coincidences as described in the validation study by Sherman et al. [19].

### 2.2.4 Analysis

The validation study was performed using spatially and temporally collocated AOD from AERONET and MODIS (Terra and Aqua) obtained from MAPSS. AERONET and MODIS AOD were plotted against each other with MODIS AOD on the y-axis and AERONET AOD on the x-axis. Linear regressions (MODIS_AOD = AERONET_AOD*m + b) were calculated using ordinary least squares (OLS) for all AOD, for AERONET AOD less than 0.15, and for AERONET AOD greater than 0.15. The value of 0.15 was selected, because lower values of AOD are more susceptible to sensor uncertainties [25], [26]. Previous studies found that ordinary least squares could be used to calculate statistically significant coefficients but could not be used to calculate standard errors when the residuals were heteroscedastic; therefore, heteroscedasticity consistent errors were used to avoid incorrect interpretation of the data when heteroscedasticity (non-constant variance of errors) was present [30]. The residuals were tested for heteroscedasticity (non-constant variance) using White's test for heteroscedasticity. If the residuals were heteroscedastic, standard errors, significance tests, and confidence intervals were corrected using a heteroscedasticity consistent covariance matrix (HCCM) referred to as type 3 heteroscedasticity consistent (HC3) at a significance level of 0.05 [30]. If the residuals were not heteroscedastic, the standard errors calculated using OLS regression were used in the analysis.

The error envelopes (EE) for the Terra 10-km land, 3-km land, and 3-km ocean products were assumed to be equal to those of Aqua [12], [18]. Root mean square error (RMSE) was calculated using equation (2.1), in which $\tau_M$ is the MODIS AOD, $\tau_A$ is the AERONET AOD, and N was the number of collocations.

$$\mathrm{RMSE} = \sqrt{\frac{\sum(\tau_M - \tau_A)^2}{N}} \tag{2.1}$$

The median and mean bias were also calculated based on the difference between MODIS AOD and the AERONET AOD. The fraction of data within EE was also calculated as done in similar studies [19], [26]. The data validity was evaluated based on the following three criteria.

- **Criterion 1**: The slopes of the linear regressions of MODIS AOD versus AERONET AOD for AOD less than 0.15 and for AERONET AOD greater than 0.15 cannot be statistically different.

- **Criterion 2**: MODIS AOD and AERONET AOD (all and AERONOT AOD greater than 0.15) must be highly correlated (Pearson correlation coefficient greater than 0.7). MODIS AOD and AERONET AOD for AERONET AOD less than 0.15 must be moderately correlated (Pearson correlation coefficient between 0.5 and 0.7), because lower values of AOD have a greater level of uncertainty [25], [31], [32].
- **Criterion 3**: At least 67% of the MODIS AOD versus AERONET AOD datasets must lie within the EE. The value of 67% was selected based on the findings of Remer et al., in which 68% of the retrievals at 550 nm fit within the EE, and the fact that the prelaunch expectation was 66% [31]. It was also used in the validation study by Sherman et al. [19].

## 2.3 Results and Discussion

### 2.3.1 Bonanza Creek

MODIS AOD cannot be obtained in the presence of snow or clouds due to the high reflectivity of snow and clouds. Due to the presence of snow in Alaska during winter months, MODIS AOD data could only be obtained between the months of April and October; therefore, the validation is only effective for the end of April through early October. Table 2.3 lists the slopes of the linear regressions of MODIS AOD versus AERONET AOD at the Bonanza Creek site at 10-km and 3-km resolutions. The errors were heteroscedastic based on White's test for heteroscedasticity; therefore, HC3 was used to calculate the standard errors used in the *t*-tests. Chu et al. (2002) established that the departure of the slope from unity was representative of systematic bias, and that the y-intercept represented the error in the estimate of the surface reflectance [26]. The systematic errors could also be due to aerosol model assumptions, instrument calibration, or measurement selection [26]. While the slopes of the linear regressions for the 10-km datasets were lower than those of the 3-km datasets, the relative difference between the slopes of the regressions for the 10-km data were greater than those of the 3-km data. For example, the slopes of the linear regressions of the 10-km Terra, Aqua, and combined Aqua and Terra datasets ranged from 1.40 to 1.49, while those of the 3-km resolution MODIS AOD datasets ranged from 1.41 to 1.42 (Figure 2.2). Also, in Figure 2.2, the 3-km (Figure 2.2d–f) data appeared to be more scattered than the 10-km data (Figure 2.2a–c), which was presumably due to the higher resolution of the 3-km data. The higher resolution appears to enable the capture of more data, as evidenced by the number of collocated samples (Table 2.3). As such, it is possible that more data at higher AOD was able to be retrieved at 3-km resolution than 10-km resolution.

#### *2.3.1.1 Criterion 1: Linear Regression*

As listed in Table 2.3, all the 3-km resolution MODIS AOD data satisfied criterion 1. The slopes of the stratified (divided into two datasets with 0.15 as the breaking point) combined Aqua and Terra MODIS AOD at 10-km resolution were significantly different ($p < 0.05$; *t*-test), which indicated that combined Aqua and Terra AOD at 10 km resolution should not be used over Alaska. Similarly, the *p*-value for the stratified individual Terra MODIS AOD at 10-km resolution was relatively low at 0.06, indicating difference. For stratified individual Aqua MODIS AOD at 10-km resolution, slopes were not significantly different ($p$ = 0.35). Based on these, individual Aqua MODIS AOD at 10-km resolution could be used. For all the 3-km data stratified by AERONET AOD (Terra and Aqua combined or individual), slopes were not significantly different ($p > 0.8$; Table 2.3), indicating that the 3-km datasets could be used in Alaska. Overall, the 3-km dataset appeared to perform better than the 10-km dataset, because the difference in slope when the data were stratified by AERONET AOD was not significant. The lower relative difference between slopes in the 3-km datasets could be due to the higher spatial resolution of the data. Combined Terra and Aqua MODIS AOD can be used to estimate ground-level air quality at a resolution of 3-km.

#### *2.3.1.2 Criterion 2: Correlation*

Overall, the full MODIS and AERONET AOD datasets were highly correlated with Pearson correlation coefficients (Figure 2.3) and thereby satisfied criterion 2. In Figure 2.2, the MODIS AOD and AERONET AOD do appear to be highly correlated, which is consistent with the calculated correlations shown in Figure 2.3. The Pearson correlation coefficients at 10-km resolution ranged from 0.95 to 0.97 for all AERONET AOD and AERONET AOD greater than or equal to 0.15, indicating high correlation. The Pearson correlation coefficient at 10-km resolution for AERONET AOD less than 0.15 ranged from 0.71 to 0.76 (highly correlated). The Pearson correlation coefficients of the 3-km data for all AERONET AOD and AERONET AOD greater than or equal to 0.15 ranged from 0.89 to 0.93 (highly correlated). The Pearson correlation coefficients for AERONET AOD less than 0.15 at 3-km resolution ranged from 0.64 to 0.66 (moderately correlated). The lower correlation coefficients for AERONET AOD less than 0.15 were most likely due to the greater uncertainty associated with lower AOD [31], [32].

#### *2.3.1.3 Criterion 3: Error Envelope (EE)*

More than 67% of the data from both AQUA and TERRA were within the error envelope (Figure 2.4). The total percentage of the 10-km resolution and 3-km resolution combined Aqua and Terra data within the EE were 83.3% and 78.7%, respectively. The amount of data within the EE satisfied the validation requirements for a fraction of data within the EE used in various validation studies [12], [19], [25], [26].

#### *2.3.1.4 Error and Bias*

The Aqua and Terra MODIS AOD datasets appeared to have a negative bias (y-intercept) at both the 10-km (−0.035 to −0.020) and 3-km resolutions (−0.018 to 0.006). The negative bias, indicated by the y-intercept, of MODIS AOD is consistent with the findings of Sherman et al., Levy et al., and Sioris et al. [12], [19], [33]. Also, the RMSE of the Bonanza Creek 10-km data was slightly lower than that of the 3-km data. The difference in RMSE is likely due to the larger number of retrievals at higher concentrations of AOD, because the variance appears to increase with AOD. The RMSE is also more affected by larger values than smaller values of AOD. A validation study over Asia found that Aqua 3-km data was less reliable than the 10-km data, as only 55% of retrievals were within the estimated error [18]; however, global studies show that MODIS AOD performance varies by region and terrain [12]. Due to the high correlation between MODIS AOD and AERONET AOD, the high proportion of data points within the EE, and the consistency of the results of the linear regression and the MODIS AOD 10-km and 3-km resolution data can be used in when employing the dark target land and ocean algorithm in Alaska. Based on the overall performance of the 10-km and 3-km resolution data, it is recommended that only the Aqua 10-km data be used of the 10-km datasets. All of the 3-km MODIS AOD data are valid for use in Alaska between the months of April and October.

Overall, the following collection 6 Dark Target land products was determined to be valid: 10-km Aqua MODIS AOD, 3-km combined Aqua and Terra MODIS AOD, 3-km Aqua MODIS AOD, and 3-km Terra MODIS AOD. Potential sources of error include the incorrect identification of clouds in the masking process of the dark target land algorithm [31]. Another source of error could be the incorrect assumption of the surface brightness by the dark target algorithm [12]. The use of the mode of quality assurance value from the pixels used to calculate each AOD could also be another source of error; however, the error between MODIS Aqua AOD with QA 3 and mode QA 3 when collocated with the Bonanza Creek site was approximately 0.

### 2.3.2 Utqiagvik (Barrow)

MODIS AOD was derived for Utqiagvik, previously known as Barrow, over the ocean using the Dark Target Ocean Algorithm. As with the Bonanza Creek site, data was only available between the months of April and October; therefore, this validation study only applies between those months. Table 2.4 lists the results of the linear regression analysis of the relationship between MODIS AOD and AERONET AOD. White's test for heteroscedasticity revealed that the errors were heteroscedastic; therefore, HC3 was used to calculate the heteroscedasticity robust standard errors.

#### *2.3.2.1 Criterion 1: Linear Regression*

All of the AOD data for the Utqiagvik AERONET site satisfied the criterion that the slopes of the linear regressions of MODIS AOD versus AERONET AOD greater than or equal to 0.15 and AERONET AOD less than 0.15 could not be significantly different. The slopes of the least squares regressions of the 10-km resolution MODIS AOD datasets versus AERONET AOD ranged from 0.96 to 0.97 (Table 2.4, Figure 2.5a–c), indicating low systematic bias (slopes of 1 would indicate no systematic bias). The slopes from the least squares regression of the 3-km MODIS AOD data versus AERONET AOD ranged from 1.00 to 1.02 for the full datasets (Table 2.4, Figure 2.5d–f). The greatest relative difference between slopes of the 10-km and 3-km data stratified by AERONET AOD were 0.21 (Terra) and 0.03 (Aqua), respectively (Table 2.4). Based on *t*-tests with a significance level of 0.05, the slopes of the all of the 10-km and 3-km data stratified by AERONET AOD were not significantly different ($p > 0.08$; Table 2.4). The proximity of the slopes to one indicated low systematic bias [29]. The MODIS AOD datasets at 10-km and 3-km were positively biased with values ranging from 0.030 to 0.032 and 0.031 to 0.035, respectively, for the full datasets based on the y-intercepts of the linear regressions [29].

#### *2.3.2.2 Criterion 2: Correlation*

Another requirement for validation is that MODIS AOD and AERONET AOD are highly correlated [19]. For the Utqiagvik site, MODIS AOD and AERONET AOD appeared to be moderately to highly correlated with most points with an AERONET AOD of less than 0.2 (Figure 2.5). The correlation coefficients for the full MODIS AOD datasets were greater than 0.7, indicating that MODIS AOD and AERONET AOD were strongly correlated. For AERONET AOD less than 0.15, MODIS AOD and AERONET AOD were moderately correlated with correlation coefficients ranging from 0.51 to 0.58 (Figure 2.6). For AERONET AOD greater than or equal to 0.15, correlation coefficients greater than 0.75 indicated a strong correlation between MODIS AOD and AERONET AOD (Figure 2.6). The large difference in Pearson correlation coefficients indicates that the strength of correlation is impacted by the few larger values. A moderate to strong relationship was evident in the correlation coefficients and Figure 2.6, therefore, the recommended requirement of correlation to determine validity was satisfied.

#### *2.3.2.3 Criterion 3: Error Envelope (EE)*

The final requirement for validity is that more than 67% of the collocated data be within the error envelope (Figure 2.7). The error envelope for Terra was assumed to be equal to that of Aqua, which was expected to be the same [12]. The lowest percentage within the error envelope was 67.3% for Terra MODIS AOD at 3-km resolution, and the greatest percentage was 74.5% for Aqua MODIS AOD at 3-km resolution (Figure 2.7). When stratified by AERONET AOD, a larger percentage of the collocated data was within the error envelope for AERONET AOD less than 0.15 (67.8–74.9%) than that for AERONET AOD greater than or equal to 0.15 (58.7–67.3%) (Figure 2.6). As the requirement of a minimum of 67% was for the full dataset, the requirement was satisfied.

#### *2.3.2.4 Error and Bias*

Overall, all of the MODIS AOD collection 6 Dark Target Ocean products satisfied the requirements for validity and are thus considered valid for use in Alaska between the months of April and October over the ocean. Based on the linear regression over the Utqiagvik and Bonanza Creek sites, the Utqiagvik data appeared to have less systematic bias than the Bonanza Creek site (Tables 2.3 and 2.4). Potential sources of error could include incorrect assumptions in the Dark Target algorithm, such as incorrect identification of clouds or surface brightness [12]. The error between MODIS Aqua AOD with QA 1, 2, 3 and mode QA 1, 2, 3 when collocated with the Bonanza Creek site was approximately 0. Future analysis could use weighted least squares regression and compare the results to the findings in this study. The use of weighted least squares may result in a different estimation of bias and systematic error based on the regression.

**2.4 Conclusion**

The Aqua MODIS AOD 10-km and all of the 3-km MODIS AOD products are valid between the months of April and October over the Bonanza Creek and Utqiagvik (Barrow) sites. All of the collection 6 dark target ocean MODIS AOD products are valid over the ocean in Alaska. The successful validation of the MODIS AOD at Bonanza Creek and Utqiagvik indicates that the collection 6 dark target MODIS AOD reflects actual conditions based on ground-based measurements of aerosol optical depth over the two sites in Alaska [7], [19]. Further research in Alaska should be done to model the relationship between summertime particulate pollution and MODIS AOD to determine if MODIS AOD can be used to estimate ground-level PM2.5 concentrations. Care should be taken when modeling the relationship between particulate pollution and MODIS AOD in Alaska, because the validity of MODIS AOD may not be accurate at other locations in Alaska [12], [19]. Therefore, a clear relationship between MODIS AOD and particulate pollution should be evident prior to use outside of the regions of the AERONET sites in Alaska, and models should undergo significant testing and evaluation for robustness. Other validation studies could be done using other satellite platforms to determine which platform will work best in Alaska. Finally, if modeling of the relationship between particulate pollution and MODIS AOD is successful, MODIS AOD could be used to monitor air quality in the areas of Alaska that do not have ground-level air quality monitors, such as much of rural Alaska.

**Author Contributions:** The research was conceptualized and written by A.M. and S.A. The study design and data analyses were undertaken by A.M. under the supervision of S.A. Additionally, S.A. provided project oversight, supervision, and funding resources.

**Funding:** This material is based in part upon work supported by the Alaska National Aeronautics and Space Administration (NASA) Established Program to Stimulate Competitive Research (EPSCoR) Program (N NNX15AK31A).

**Acknowledgments:** Authors would like to acknowledge assistance from Pawan Gupta at NASA Goddard Centre and support from department of Civil and Environmental Engineering at University of Alaska Fairbanks.

**Conflicts of Interest:** The authors declare no conflict of interest. The funding sponsors had no role in the design of the study; in the collection, analyses, or interpretation of data; in the writing of the manuscript; or in the decision to publish the results.

**2.5 References**

[1] C. A. Pope and D. W. Dockery, "Health Effects of Fine Particulate Air Pollution: Lines that Connect," *J. Air Waste Manage. Assoc.*, vol. 56, no. 6, pp. 709–742, 2006.

[2] J. Lelieveld, J. S. Evans, M. Fnais, D. Giannadaki, and A. Pozzer, "The contribution of outdoor air pollution sources to premature mortality on a global scale," *Nature*, vol. 525, no. 7569, pp. 367–371, 2015.

[3] N. Fann, A. D. Lamson, S. C. Anenberg, K. Wesson, D. Risley, and B. J. Hubbell, "Estimating the National Public Health Burden Associated with Exposure to Ambient PM2.5 and Ozone," *Risk Anal.*, vol. 32, no. 1, pp. 81–95, Jan. 2012.

[4] L. McLaughlin, Joe; Castrodale, "Association between Air Quality and Hospital Visits—Fairbanks, 2003–2008," *State Alaska Epidemiol. Bull.*, no. 26, 2010.

[5] D. Ware, J. Lewis, S. Hopkins, B. Boyer, C. Noonan, and T. Ward, "Sources and perceptions of indoor and ambient air pollution in rural Alaska," *J. Community Health*, vol. 38, no. 4, pp. 773–780, 2013.

[6] US EPA, "AirNow - Alaska Air Quality," *Environmental Protection Agency*. [Online]. Available: https://www.airnow.gov/index.cfm?action=airnow.local_state&stateid=2&mapcenter=1&tabs=1. [Accessed: 07-Aug-2018].

[7] P. Gupta, S. a. Christopher, M. a. Box, and G. P. Box, "Multi year satellite remote sensing of particulate matter air quality over Sydney, Australia," *Int. J. Remote Sens.*, vol. 28, no. November 2014, pp. 4483–4498, 2007.

[8] S. Dey and L. Di Girolamo, "A decade of change in aerosol properties over the Indian subcontinent," *Geophys. Res. Lett.*, vol. 38, no. 14, pp. 1–5, 2011.

[9] Y. Xie, Y. Wang, K. Zhang, W. Dong, B. Lv, and Y. Bai, "Daily Estimation of Ground-Level PM2.5 Concentrations over Beijing Using 3 km Resolution MODIS AOD," *Environ. Sci. Technol.*, vol. 49, no. 20, pp. 12280–12288, 2015.

[10] Z. Ma *et al.*, "Satellite-based spatiotemporal trends in PM2.5concentrations: China, 2004-2013," *Environ. Health Perspect.*, vol. 124, no. 2, pp. 184–192, Jul. 2016.

[11] A. van Donkelaar *et al.*, "Global estimates of ambient fine particulate matter concentrations from satellite-based aerosol optical depth: Development and application," *Environ. Health Perspect.*, vol. 118, no. 6, pp. 847–855, Mar. 2010.

[12] R. C. Levy *et al.*, "The Collection 6 MODIS aerosol products over land and ocean," *Atmos. Meas. Tech.*, vol. 6, pp. 2989–3034, 2013.

[13] A. M. Sayer, N. C. Hsu, C. Bettenhausen, and M. J. Jeong, "Validation and uncertainty estimates for MODIS Collection 6 'deep Blue' aerosol data," *J. Geophys. Res. Atmos.*, vol. 118, no. 14, pp. 7864–7872, 2013.

[14] N. C. Hsu *et al.*, "Enhanced Deep Blue aerosol retrieval algorithm: The second generation," *J. Geophys. Res. Atmos.*, vol. 118, no. 16, pp. 9296–9315, Aug. 2013.

[15] A. M. Sayer, L. A. Munchak, N. C. Hsu, R. C. Levy, C. Bettenhausen, and M.-J. Jeong, "MODIS Collection 6 aerosol products: Comparison between Aqua's e-Deep Blue, Dark Target, and ``merged'' data sets, and usage recommendations," *J. Geo-phys. Res. Atmos*, vol. 119, pp. 965–978, 2014.

[16] A. M. Sayer, N. C. Hsu, C. Bettenhausen, M.-J. Jeong, and G. Meister, "Effect of MODIS Terra radiometric calibration improvements on Collection 6 Deep Blue aerosol products: Validation and Terra/Aqua consistency," *J. Geophys. Res. Atmos.*, vol. 120, no. 23, p. 12,157-12,174, Dec. 2015.

[17] R. Levy, "Dark Target Aerosol Retrieval Algorithm," *Nasa*, 2018. [Online]. Available: https://darktarget.gsfc.nasa.gov/. [Accessed: 07-Aug-2018].

[18] J. E. Nichol and M. Bilal, "Validation of MODIS 3 km resolution aerosol optical depth retrievals over Asia," *Remote Sens.*, vol. 8, no. 4, 2016.

[19] J. P. Sherman, P. Gupta, R. C. Levy, and P. J. Sherman, "An Evaluation of MODIS-Retrieved Aerosol Optical Depth over a Mountainous AERONET Site in the Southeastern US," *Aerosol Air Qual. Res.*, vol. 16, pp. 3243–3255, 2016.

[20] I. Kloog *et al.*, "Estimating daily PM2.5and PM10across the complex geo-climate region of Israel using MAIAC satellite-based AOD data," *Atmos. Environ.*, vol. 122, pp. 409–416, Dec. 2015.

[21] Y. Guo, N. Feng an, S. A. Christopher, P. Kang, F. B. Zhan, and S. Hong, "Satellite remote sensing of fine particulate matter (PM2.5) air quality over Beijing using MODIS," *Int. J. Remote Sens.*, vol. 35, pp. 6522–6544, 2014.

[22] S. A. Christopher and P. Gupta, "Satellite remote sensing of particulate matter air quality: the cloud-cover problem," *Journal of the Air and Waste Management Association*, vol. 60, no. 5. pp. 596–602, 2010.

[23] M. Petrenko, C. Ichoku, and G. Leptoukh, "Multi-sensor Aerosol Products Sampling System (MAPSS)," *Atmos. Meas. Tech*, vol. 5, pp. 913–926, 2012.

[24] B. N. Holben *et al.*, "AERONET - A federated instrument network and data archive for aerosol characterization," *Remote Sens. Environ.*, vol. 66, no. 1, pp. 1–16, 1998.

[25] C. Ichoku *et al.*, "A spatio-temporal approach for global validation and analysis of MODIS aerosol products," *Geophys. Res. Lett.*, vol. 29, no. 12, pp. 1–4, 2002.

[26] L. A. Remer *et al.*, "Validation of MODIS aerosol retrieval over ocean," *Geophys. Res. Lett.*, vol. 29, no. 12, p. 8008, 2002.

[27] T. F. Eck *et al.*, "Wavelength dependence of the optical depth of biomass burning, urban, and desert dust aerosols," *J. Geophys. Res.*, vol. 104, no. D24, pp. 31333–31349, 1999.

[28] A. K. Georgoulias *et al.*, "Spatiotemporal variability and contribution of different aerosol types to the aerosol optical depth over the Eastern Mediterranean," *Atmos. Chem. Phys.*, vol. 16, no. 21, pp. 13853–13884, 2016.

[29] D. A. Chu, Y. J. Kaufman, C. Ichoku, L. A. Remer, D. Tanré, and B. N. Holben, "Validation of MODIS aerosol optical depth retrieval over land," *Geophys. Res. Lett.*, vol. 29, no. 12, pp. MOD2-1-MOD2-4, 2002.

[30] J. S. Long and L. H. Ervin, "Using heteroscedasticity consistent standard errors in the linear regression model," *Am. Stat.*, vol. 54, no. May, pp. 217–224, 2000.

[31] L. A. Remer *et al.*, "The MODIS Aerosol Algorithm, Products, and Validation," *J. Atmos. Sci.*, vol. 62, 2005.

[32] P. Gupta and S. A. Christopher, "Particulate matter air quality assessment using integrated surface, satellite, and meteorological products: Multiple regression approach," *J. Geophys. Res. Atmos.*, vol. 114, no. 14, pp. 1–13, 2009.

[33] C. E. Sioris, C. A. Mclinden, M. W. Shephard, V. E. Fioletov, and I. Abboud, "Assessment of the aerosol optical depths measured by satellite-based passive remote sensors in the Alberta oil sands region," *Atmos. Chem. Phys*, vol. 17, 1931.

## 2.6 Tables and Figures

Table 2.1. Estimated error for MODIS collection 6 dark target algorithm [12].

| **Resolution** | **10-km** | | **3-km** | |
|---|---|---|---|---|
| **Satellite** | AQUA | TERRA | AQUA | TERRA |
| **Land** | $\pm(0.05 + 0.15\tau_A)$ | $\pm(0.05 + 0.15\tau_A)$ | $\pm(0.05 + 0.2\tau_A)$ | NA |
| **Ocean** | $-0.02-0.1\tau_A$ | NA | $\pm(0.04 + 0.05\tau_A)$ | NA |

Table 2.2. Locations of AERONET stations.

| **Station** | **Location** | **Latitude (North)** | **Longitude (West)** | **Elevation (m)** | **Dates Operational** |
|---|---|---|---|---|---|
| **Utqiagvik (Barrow)** | Utqiagvik, AK | 71.31220° | 156.66500° | 0.0 | 30 July 1994–present |
| **Bonanza Creek** | Bonanza Creek, AK | 64.74281° | 148.31627° | 150.0 | 31 May 1994–present |

Table 2.3. Results of linear regression ($\tau_M = \tau_A$*m + b) and *t*-tests at a significance level of 0.05 for the Bonanza Creek AERONET site. The 95% confidence intervals are listed in parentheses, and se and N are the standard error of the slope and the number of samples, respectively. A p-value less than 0.05 indicates that the slopes are significantly different.

| Satellite | $\tau_A$ | Count | m | se | b | *p*-Value |
|---|---|---|---|---|---|---|
| **10-km Resolution** | | | | | | |
| **TERRA & AQUA** | all | 1490 | 1.45 (1.34, 1.57) | 0.06 | −0.027 (−0.038, −0.015) | NA |
| | <0.15 | 1232 | 1.29 (1.23, 1.36) | 0.03 | −0.013 (−0.018, −0.009) | 0.03 |
| | ≥0.15 | 258 | 1.48 (1.33, 1.63) | 0.08 | −0.052 (−0.101, −0.002) | |
| **TERRA** | all | 853 | 1.49 (1.33, 1.65) | 0.08 | −0.020 (−0.036, −0.005) | NA |
| | <0.15 | 713 | 1.32 (1.23, 1.40) | 0.04 | −0.005 (−0.010, 0.001) | 0.06 |
| | ≥0.15 | 140 | 1.53 (1.32, 1.73) | 0.10 | −0.058 (−0.121, 0.005) | |
| **AQUA** | all | 637 | 1.40 (1.26, 1.54) | 0.07 | −0.035 (−0.050, −0.020) | NA |
| | <0.15 | 519 | 1.31 (1.21, 1.40) | 0.05 | −0.028 (−0.035, −0.021) | 0.35 |
| | ≥0.15 | 118 | 1.41 (1.21, 1.61) | 0.10 | −0.040 (−0.110, 0.030) | |
| **3-km Resolution** | | | | | | |
| **TERRA & AQUA** | all | 2494 | 1.41 (1.29, 1.53) | 0.06 | −0.005 (−0.017, 0.007) | NA |
| | <0.15 | 2091 | 1.38 (1.31, 1.46) | 0.04 | −0.004 (−0.009, 0.001) | 0.84 |
| | ≥0.15 | 403 | 1.40 (1.25, 1.55) | 0.08 | 0.009 (−0.043, 0.062) | |
| **TERRA** | all | 1352 | 1.41 (1.22, 1.59) | 0.09 | 0.006 (−0.012, 0.024) | NA |
| | <0.15 | 1146 | 1.38 (1.28, 1.48) | 0.05 | 0.007 (0.000, 0.014) | 0.87 |
| | ≥0.15 | 206 | 1.40 (1.16, 1.63) | 0.12 | 0.015 (−0.067, 0.096) | |
| **AQUA** | all | 1142 | 1.42 (1.26, 1.58) | 0.08 | −0.018 (−0.034, −0.001) | NA |
| | <0.15 | 945 | 1.43 (1.32, 1.54) | 0.06 | −0.021 (−0.028, −0.013) | 0.83 |
| | ≥0.15 | 197 | 1.40 (1.20, 1.60) | 0.10 | 0.004 (−0.065, 0.073) | |

Table 2.4. Results of linear regression ($\tau_M = \tau_A$*m + b) and t-tests at a significance level of 0.05 for the Utqiagvik (Barrow) AERONET site. The 95% confidence intervals are listed in parenthesis, and se is the standard error of the slope. A p-value less than 0.05 indicates that the slopes are significantly different.

| **Satellite** | **$\tau_A$** | **N** | **m** | **se** | **b** | ***p*-Value** |
|---|---|---|---|---|---|---|
| 10-km Resolution | | | | | | |
| TERRA & AQUA | all | 1490 | 1.45 (1.34, 1.57) | 0.06 | −0.027 (−0.038, −0.015) | NA |
| | <0.15 | 1232 | 1.29 (1.23, 1.36) | 0.03 | −0.013 (−0.018, −0.009) | 0.03 |
| | ≥0.15 | 258 | 1.48 (1.33, 1.63) | 0.08 | −0.052 (−0.101, −0.002) | |
| TERRA | all | 853 | 1.49 (1.33, 1.65) | 0.08 | −0.020 (−0.036, −0.005) | NA |
| | <0.15 | 713 | 1.32 (1.23, 1.40) | 0.04 | −0.005 (−0.010, 0.001) | 0.06 |
| | ≥0.15 | 140 | 1.53 (1.32, 1.73) | 0.10 | −0.058 (−0.121, 0.005) | |
| AQUA | all | 637 | 1.40 (1.26, 1.54) | 0.07 | −0.035 (−0.050, −0.020) | NA |
| | <0.15 | 519 | 1.31 (1.21, 1.40) | 0.05 | −0.028 (−0.035, −0.021) | 0.35 |
| | ≥0.15 | 118 | 1.41 (1.21, 1.61) | 0.10 | −0.040 (−0.110, 0.030) | |
| 3-km Resolution | | | | | | |
| TERRA & AQUA | all | 2494 | 1.41 (1.29, 1.53) | 0.06 | −0.005 (−0.017, 0.007) | NA |
| | <0.15 | 2091 | 1.38 (1.31, 1.46) | 0.04 | −0.004 (−0.009, 0.001) | 0.84 |
| | ≥0.15 | 403 | 1.40 (1.25, 1.55) | 0.08 | 0.009 (−0.043, 0.062) | |
| TERRA | all | 1352 | 1.41 (1.22, 1.59) | 0.09 | 0.006 (−0.012, 0.024) | NA |
| | <0.15 | 1146 | 1.38 (1.28, 1.48) | 0.05 | 0.007 (0.000, 0.014) | 0.87 |
| | ≥0.15 | 206 | 1.40 (1.16, 1.63) | 0.12 | 0.015 (−0.067, 0.096) | |
| AQUA | all | 1142 | 1.42 (1.26, 1.58) | 0.08 | −0.018 (−0.034, −0.001) | NA |
| | <0.15 | 945 | 1.43 (1.32, 1.54) | 0.06 | −0.021 (−0.028, −0.013) | 0.83 |
| | ≥0.15 | 197 | 1.40 (1.20, 1.60) | 0.10 | 0.004 (−0.065, 0.073) | |

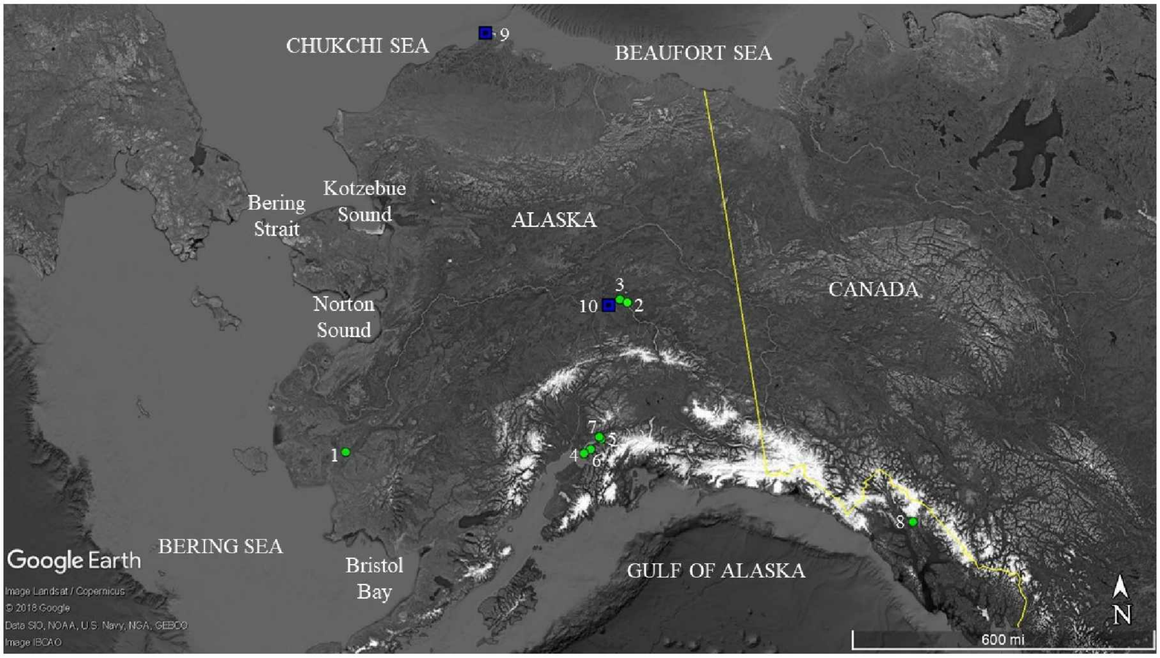

Figure 2.1. Alaska's air quality monitoring (AQM) network used by AirNow.gov to provide current air quality index to the public on 22 August 2018 [6]. Green dots signify locations with good air quality. The following AQM locations are shown: (1) Bethel, (2) North Pole, (3) Fairbanks, (4) Anchorage, (5) Butte, (6) Eagle River, (7) Palmer, and (8) Juneau. The blue squares signify locations of the two AERONET stations, (9) Utqiagvik (Barrow), and (10) Bonanza Creek. Yellow line highlights the border between USA and Canada.

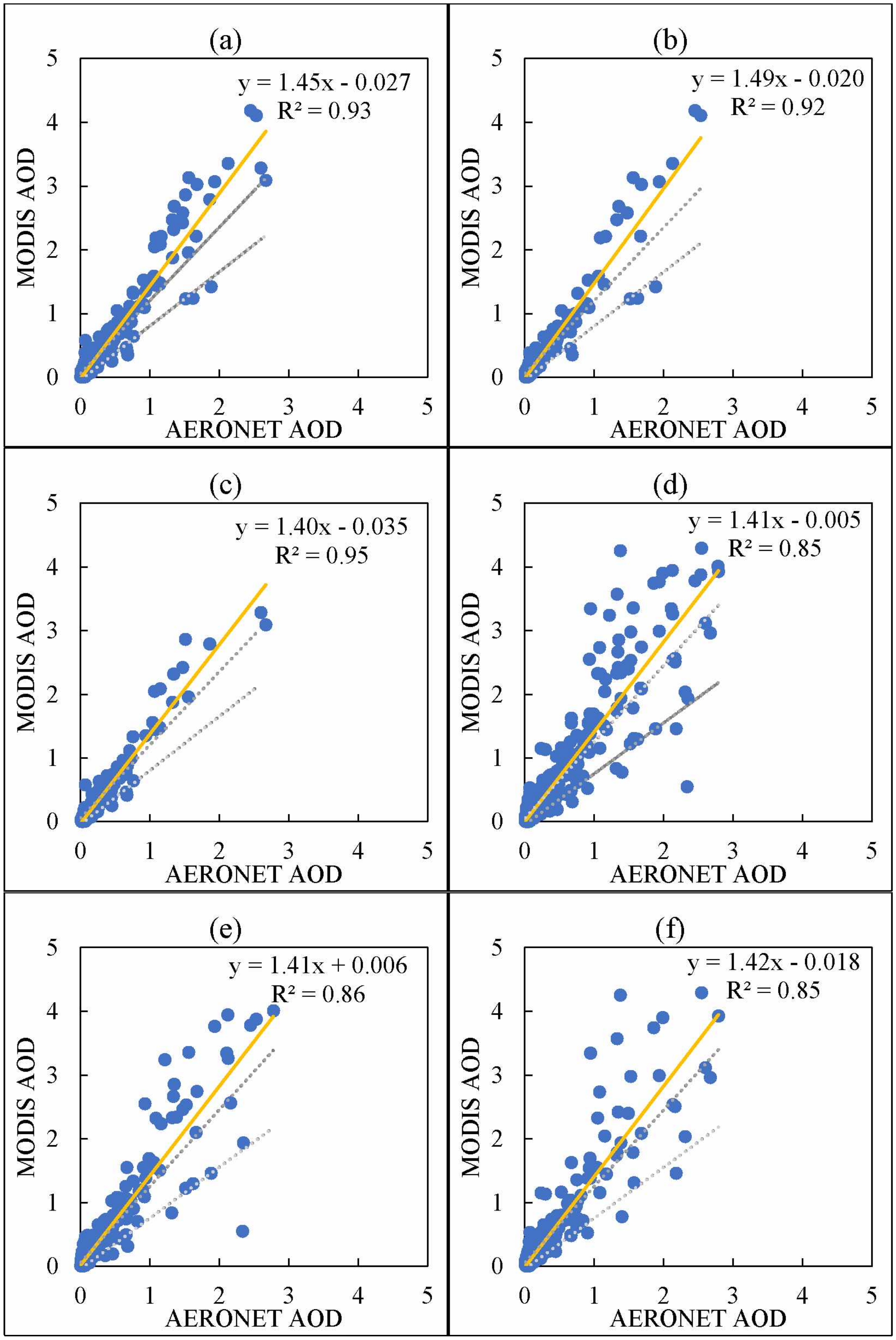


Figure 2.2. MODIS AOD versus AERONET AOD at the Bonanza Creek AERONET site with linear regression as solid yellow line and the dashed gray line as the error envelope where the following figures are for (a) Terra and Aqua 10-km combined, (b) Terra 10-km, (c) Aqua 10-km, (d) Terra and Aqua 3-km combined, (e) Terra 3-km, and (f) Aqua 3-km.

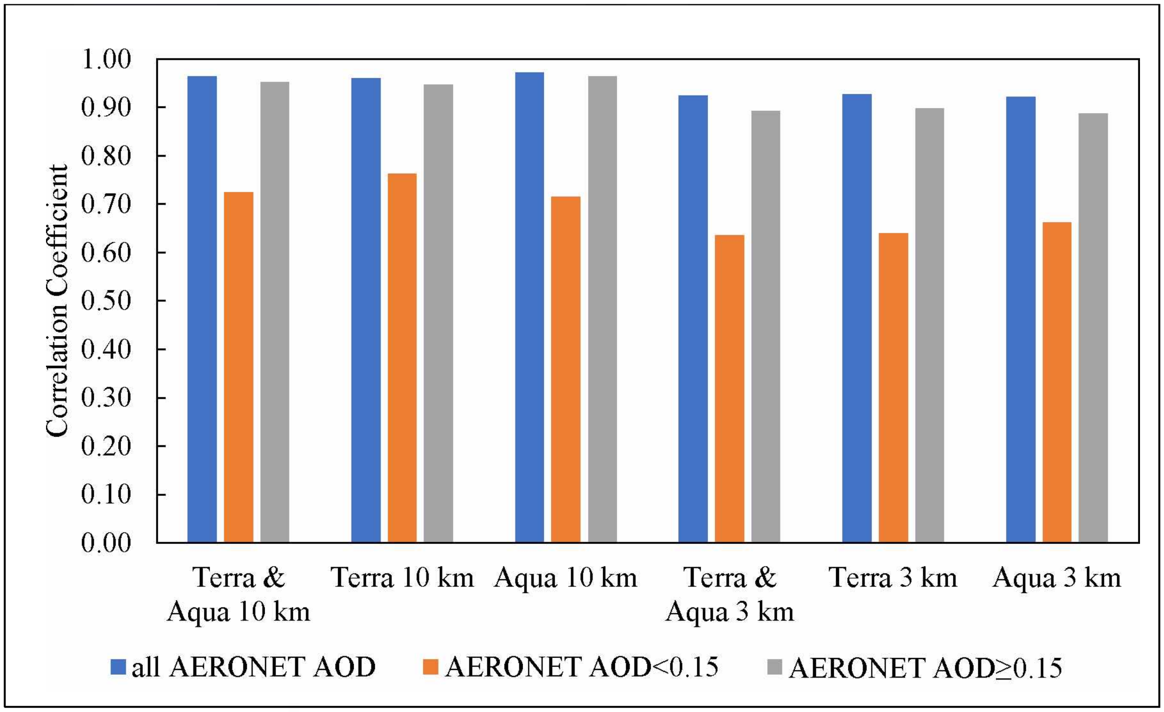


Figure 2.3. A comparison of the correlation coefficients for MODIS AOD versus AERONET AOD over the Bonanza Creek AERONET site. Criterion 2 is satisfied if the correlation coefficient is greater than 0.5 for AERONET AOD less than 0.15; and correlation coefficient is greater than 0.7 for all AERONET AOD as well as for AERONET AOD greater than or equal to 0.15.

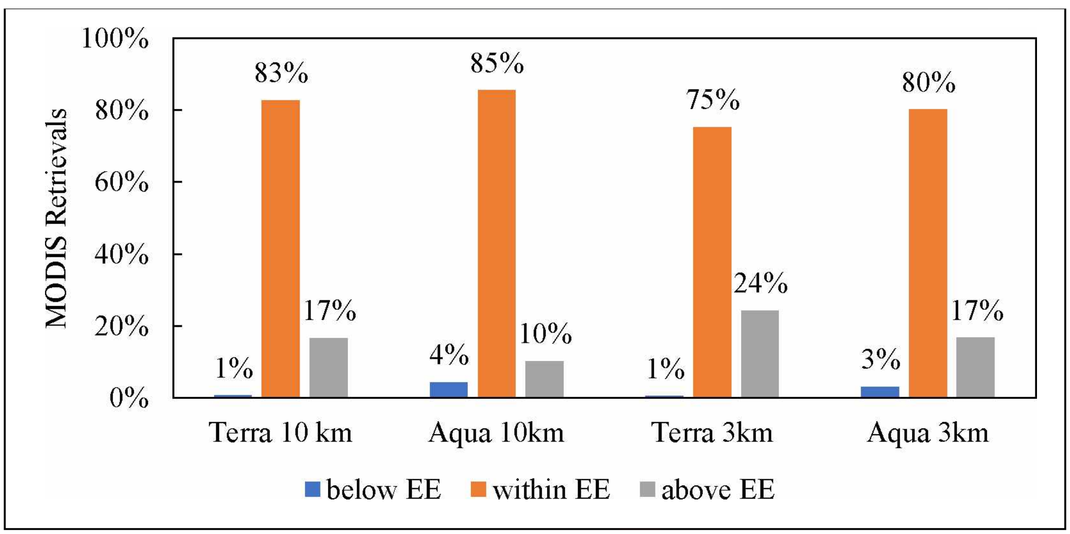


Figure 2.4. A comparison of the percentage of MODIS land retrievals over the Bonanza Creek AERONET site from Aqua and Terra with 3-km and 10-km resolutions below, within, and above the error envelope (EE). The MODIS Collection 6 error envelopes for land are listed in Table 2.1. Criterion 3 for validation is satisfied if 67% of MODIS retrievals are within the error envelope.

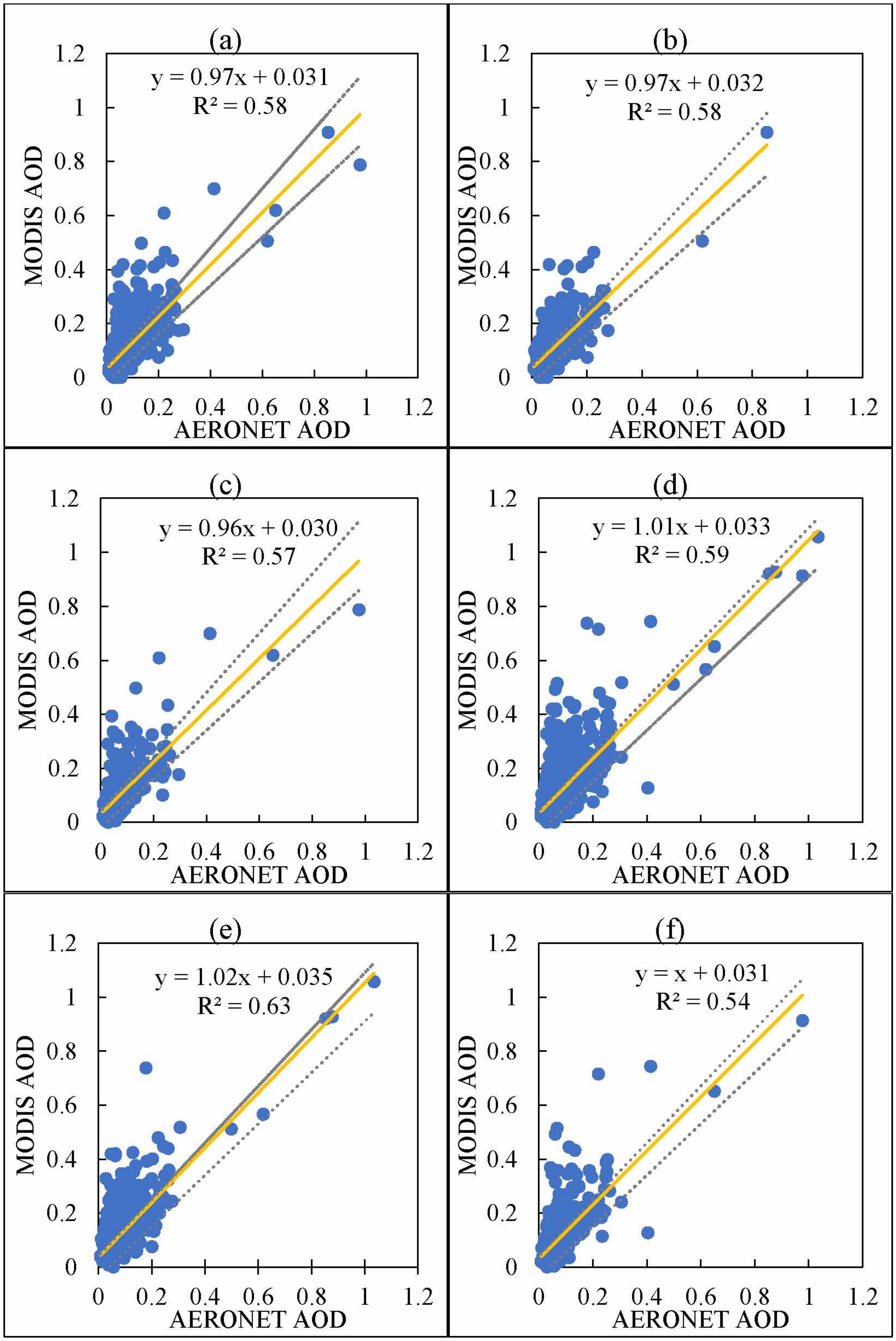


Figure 2.5. MODIS AOD versus AERONET AOD at the Utqiagvik (Barrow) AERONET site with linear regression as solid yellow line and the dashed gray line as the error envelope where the following figures are for (a) Terra and Aqua 10-km combined, (b) Terra 10-km, (c) Aqua 10-km, (d) Terra and Aqua 3-km combined, (e) Terra 3-km, and (f) Aqua 3-km.

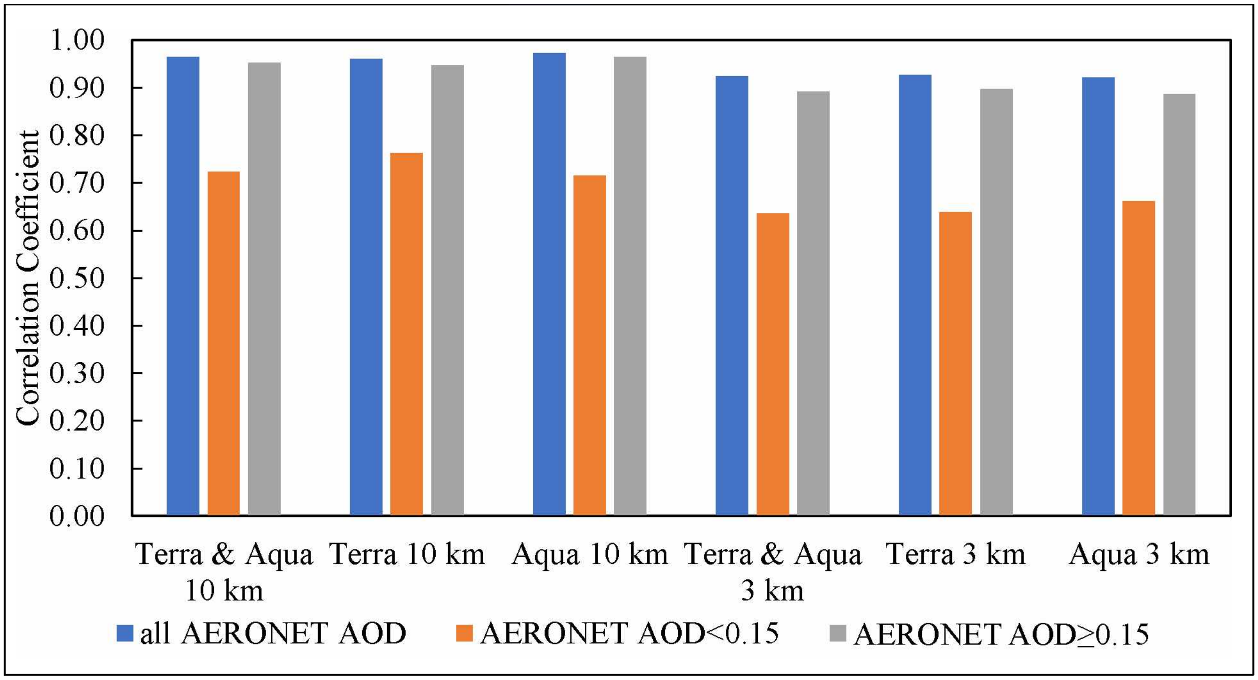


Figure 2.6. A comparison of the correlation coefficients for MODIS AOD versus AERONET AOD over the Utqiagvik (Barrow) AERONET site. Criterion 2 was satisfied if the correlation coefficient was greater than 0.5 for AERONET AOD less than 0.15 and greater than 0.7 for all AERONET AOD and AERONET AOD greater than 0.15.

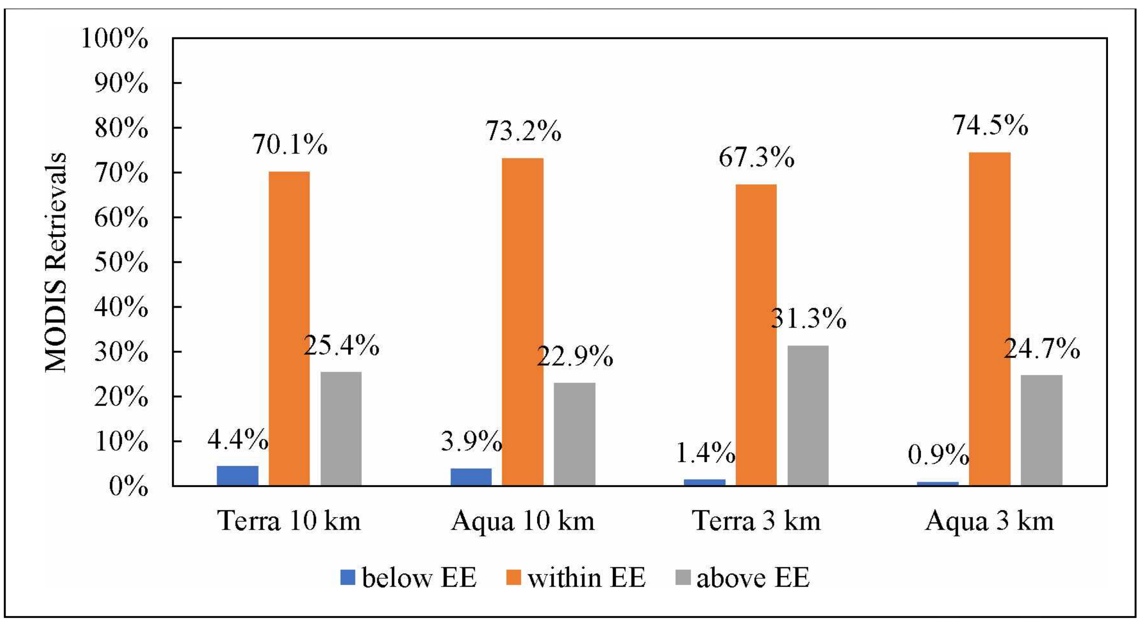


Figure 2.7. A comparison of the percentage of MODIS land retrievals over the Utqiagvik (Barrow) AERONET site from Aqua and Terra with 3-km and 10-km resolutions below, within, and above the error envelope (EE). The MODIS Collection 6 error envelopes for land are listed in Table 2.1. Criterion 3 for validation was satisfied if 67% of MODIS retrievals were within the error envelope

Chapter 3 Assessing the Relationship Between Moderate Resolution Imaging Spectroradiometer (MODIS) Aerosol optical depth (AOD) and Fine Particulate Matter (PM2.5) in Alaska's Urban Area[3]

**Abstract**

MODIS AOD has been successfully used throughout the world to estimate ground-level PM2.5 concentrations and monitor long-term trends. The purpose of this research is to determine if a multilinear regression model with MODIS AOD and meteorological parameters as predictors can be used to estimate mean ground-level PM2.5 concentrations in Alaska.

The MODIS data was first evaluated by determining the amount of available data and the magnitude of the error and bias introduced to the model by comparing PM2.5 data retrieved by ground-based air quality monitors (AQMs) on satellite retrieval days (AquaTerraPM, TerraPM, AquaPM) to all ground-based PM2.5 retrievals (AllPM). Juneau, Alaska had the lowest retrieval rates and highest RMSE. On average, the highest retrieval rates occur from May to September, particularly in interior Alaska. Wintertime retrieval rates were much lower than summertime retrieval rates for both interior and southcentral Alaska with zero usable MODIS data in December. The low retrieval rates in the winter months are likely due to extensive snow and cloud cover. Based on RMSE data and retrieval rates, no model should be developed for Juneau or for the winter months.

Predictive models for PM2.5 were then developed for southcentral and interior Alaska using MODIS AOD and meteorological data as independent variables in a multilinear regression (MLR) framework. Low $R^2$ values (<0.30) and high mean square errors (13-121 μg/m$^3$) for each model indicate that the models perform poorly. Model performance, however, appears to increase with quantile. Quantile regression of the data indicate the ordinary least squares model may not adequately represent upper quantiles (75$^{th}$ and 90$^{th}$). And quantile regressions of the 25$^{th}$ and 75$^{th}$ percentiles are significantly different from each other. However, the moderate correlation between Aqua MODIS AOD and ground-level PM2.5 in interior Alaska indicates that further research using other models, such as mixed effects models, may be promising. More air quality monitors are essential for developing adequate models for estimating ground-based PM2.5 concentrations.

## 3.1 Introduction

Exposure to PM2.5 adversely affects cardiopulmonary health and is associated with premature mortality [1]–[3]. Due to the ill-effects of PM2.5 exposure on human health, air quality monitoring is necessary to provide air quality alerts to the public and monitor exposure. The Fairbanks North Star

---

[3] McPhetres, A., Aggarwal, S. *Assessing the Relationship Between Moderate Resolution Imaging Spectroradiometer (MODIS) Aerosol optical depth (AOD) and Fine Particulate Matter (PM2.5) in Alaska's Urban Area*. Unpublished Manuscript. 2018.

Borough in Alaska was re-classified as a serious non-attainment area on April 28, 2017 for 24-hour PM2.5 National Ambient Air Quality Standard [4]. Fairbanks was first classified as a non-attainment area in 2009 [4]. Currently, Alaska's air quality monitoring network is limited primarily to major urban areas (Fairbanks, Juneau, Anchorage) and national parks [5].

The low spatial resolution of the air quality network in Alaska limits the ability of regulators to monitor air quality exposure and provide alerts to the public. A possible solution to improving the spatial resolution of Alaska's air quality monitoring network is the use of satellite remote sensing in conjunction with ground-based air quality monitors. Data obtained with the Moderate Resolution Imaging System (MODIS) onboard both the Terra and Aqua satellites has been successfully used throughout the globe to identify wildfire locations, estimate ground-level PM2.5 concentrations, and to monitor long-term trends in ground-level PM2.5 concentrations [6]–[10].

The purpose of this research is to determine if MODIS AOD may be used to estimate and monitor ground-level PM2.5 concentrations in Alaska. The first step is to determine the magnitude of bias and error introduced by only using PM2.5 concentrations from satellite retrieval days. MODIS AOD is only retrieved in relatively cloud- and snow-free conditions [10]. This analysis can then be used to determine if potential models could be used to monitor long-term trends in PM2.5 concentrations. It is also used to determine if there is sufficient data to develop models of the relationship between MODIS AOD and ground-level PM2.5. The second step of this research is to develop models of PM2.5 versus MODIS AOD and meteorological data using multilinear regression for Fairbanks, Anchorage, and Juneau, if possible. The models are the final step in evaluating whether MODIS AOD can be used to estimate ground-level PM2.5 concentrations in Fairbanks, Juneau, and Anchorage.

## 3.2 Data

### 3.2.1 PM2.5 Mass Concentration Data

Daily mean PM2.5 mass concentrations were obtained from seven ground-level air quality monitors in southcentral, interior, and southeast Alaska from January 1, 2012 to December 31, 2016 from the United States (US) Environmental Protection Agency (EPA) Air Quality System (AQS) Data Mart [11]. The instruments used to obtain the data were BAM-1020 air quality monitors (Beta Attenuation Monitor). Table 3.1 lists the air quality monitoring stations and their respective locations.

### 3.2.2 MODIS Data

The Moderate Resolution Imaging Spectroradiometer (MODIS) instrument acquires data daily across 36 spectral bands and is located on-board the Terra and Aqua satellites, which were launched in 1999 and 2002, respectively [12]. Collection 6 MODIS data at three-kilometer resolution was obtained from the Level-1 Atmosphere Archive & Distribution System (LAADS) Distributed Active Archive Center (DAAC) [13]. The MODIS data was processed using the dark target algorithm

"Optical_Depth_Land_And_Ocean" standard dataset to obtain data for high quality pixels [12], [14]. High quality pixels have a quality assurance value of three for land and quality assurance value greater than zero for ocean [14]. MODIS AOD is only retrieved in relatively cloud and snow free conditions (when the surface reflectance in the 2.1 μm channel is less than 0.4) [10]. The MODIS and PM2.5 data were then collocated by centering a five-by-five group of three-kilometer pixels over each air quality monitoring station. The practice of centering a five-by-five group of pixels over a point is a common method of collocation employed in many studies that use MODIS AOD [10], [15].

### 3.2.3 Meteorological Data

Meteorological daily-averaged data was obtained from the National Climatic Data Center (NCDC) for the following locations: Fairbanks International Airport, Ted Stevens International Airport, Palmer Municipal Airport, and Juneau International Airport. The daily meteorological data included the following: relative humidity (RH; %), average wind speed (WS; m/s), temperature (Temp; K), precipitation, and air pressure (AP; kPa). The precipitation data was converted to a factor variable (Rain) divided into precipitation days (value of 1) and non-precipitation days (value of 0). Meteorological data from the nearest airport with the greatest temporal coverage of the January 1, 2012 to December 31, 2016 time range was used to develop the models for each region.

## 3.3 Methods

### 3.3.1 Bias Analysis

The data was first evaluated to determine the feasibility of developing a model based on possible bias and error introduced by limited retrievals and insufficient MODIS data due to snow and cloud cover using similar methods to those employed by Gupta et al. [10]. Total mean and monthly mean PM2.5 mass concentrations were compared for all PM2.5 mass concentrations measurements, ALLPM, and PM2.5 mass concentrations measured on MODIS retrieval days for Aqua, Terra, and Aqua and Terra combined, (AquaPM, TerraPM, AquaTerraPM). The monthly means were first calculated for each year. The calculated monthly means were then used to calculate the root mean square error (RMSE) and mean of the ratio of monthly ALLPM to satellite PM (AquaPM, TerraPM, AquaTerraPM). The average bias was also calculated for each month by subtracting ALLPM from satellite PM (AquaPM, TerraPM). The monthly retrieval frequency was calculated by dividing the number of satellite retrieval days (Aqua Days, Terra Days, Aqua Terra Days) by the number of PM2.5 retrieval days (PM Days). The percentiles were calculated for AllPM, AquaPM, and TerraPM for each month and region then plotted. The percentile plots were used to evaluate if AquaPM and TerraPM captured the various levels of PM2.5. The calculated results were then used to determine the best time of year for which to develop models for each region based on retrieval rates, error, and bias.

### 3.3.2 Regression Analysis

#### *3.3.2.1 Data*

Only MODIS data with MODIS AOD standard deviations below 0.5 and composed of at least three pixels were used to develop the models [16]. Quantile plots indicate that both the AOD and PM2.5 data have log-normal distributions; therefore, log-transforms were applied to both AOD and PM2.5 after adding a constant to both AOD and PM2.5 to ensure that all log-transformed values would be defined and to prevent possible bias introduced by eliminating negative values of PM2.5 and AOD [14]. Previous research also indicated that model fit improved with the addition of meteorological parameters when estimating ground-level PM2.5 concentrations; therefore, the following were evaluated as possible model parameters: temperature (Temp), WS (wind speed), AP (air pressure), RH (relative humidity), cloud fraction (CF) and rain [16], [17].

#### *3.3.2.2 Model Development*

Multilinear regression (MLR) and quantile regression were performed in R version 3.4.3. MLR models were developed for each region from May to September to estimate mean ground-level PM2.5 concentrations (response) based on MODIS AOD and weather parameters (predictors). The initial parameters to be included in the best fit model were selected using stepwise regression, which employs a combination of both backwards and forwards regression with the "step" function in R version 3.4.3 [18]. Bootstrap resampling was then applied using the "boot" package in R version 3.4.3 to estimate bootstrap percentile confidence intervals at a significance level of 0.05 and the standard errors [19], [20]. All insignificant predictors except AOD were removed from the model. AOD was not removed from the model because the purpose of this research is to evaluate the relationship between MODIS AOD and ground-level concentrations of PM2.5. All parameters included in the final best fit model were significant at a significance level of 0.05. A total of three MLR models were developed for each region and satellite platform (Aqua or Terra) with PM2.5 as the response variable. The best fit model was selected using stepwise regression and included only significant variables and AOD. The following two regressions were also performed, where C1 is a constant, C2 is the coefficient of log(AOD+0.06), C3 is the coefficient of cloud fraction (CF), C4 is the coefficient of temperature (Temp), C5 is the coefficient of relative humidity (RH), C6 is the coefficient of air pressure (AP), C7 is the coefficient of the factor variable rain when precipitation is greater than zero, and C8 is the coefficient of wind speed.

$$\log(PM2.5+5)=C1+C2*\log(AOD+0.06)+C3*CF+C4*Temp+C5*RH+C6*AP+C7*rain+C8*WS \quad (3.1)$$

$$\log(PM2.5+5)=C1+C2*\log(AOD+0.06) \quad (3.2)$$

Quantile regression (QR) was then performed in R version 3.4.3 using the "quantreg" package using the same parameters used in the associated MLR models for the following quantiles: 0.1, 0.25, 0.5, 0.75, and

0.90 [21]. The coefficients and pseudo-$R^2$ of the QR models were then compared to the MLR models to evaluate the representativeness of the MLR models of the various quantile ranges. ANOVA (analysis of variance) was also used to determine if models for each quantile were significantly different from each other.

#### *3.3.2.3 Validation*

K-fold (k=5) cross validation was used to validate the MLR models. K-fold cross validation (CV) was performed using the “cv.lm” function in the “DAAG” packing in R [22]. The cross validate r-squared value (CV-$R^2$) was calculated by squaring the correlation coefficient, r, of the CV predicted and observed values of log(PM2.5+5) (response). The mean square error (MSE) and root mean square error (RMSE) were also calculated to evaluate the performance of the MLR models.

## 3.4 Results & Discussion

The performance of MODIS AOD for the estimation of ground-level PM2.5 concentrations was evaluated for each platform (Aqua, Terra) and three regions using seven ground stations in Alaska based on retrieval rates, bias, RMSE, and MLR models. The three regions for which MODIS AOD was evaluated were southeast (Juneau), southcentral (Matanuska-Susitna Valley and Municipality of Anchorage), and interior Alaska (Fairbanks North Star Borough). The statistics for each station for AOD and PM2.5 are listed in Table 3.2.

### 3.4.1 Retrieval Rates

The ratio of the number of satellite retrieval days (Aqua, Terra, and AquaTerra days) to the number of PM days for each month is first calculated to determine the best time periods for which to develop models for each station. For example, no MODIS AOD was retrieved over the stations during the month of December; therefore, no model can be developed for the month of December. Overall, the monthly ratio of AquaTerra days to PM days is the highest, ranging from 0 to 0.66 with an overall retrieval rate of 0.26. Terra has the next highest maximum monthly retrieval rate ranging from 0 to 0.59 with an overall retrieval rate of 0.22. Aqua has the lowest monthly retrieval rates, which range from 0 to 0.56 with an overall retrieval rate of 0.17. The retrieval rate for AquaTerra is not additive of the retrieval rates for Aqua and Terra; the maximum retrieval rate for AquaTerra is only 0.07 greater than that for Terra and 0.10 greater than that for Aqua. This indicates that both Aqua and Terra tend to retrieve (or not retrieve) MODIS AOD on the same days despite being separate platforms and having different overpass times. Overpass times vary by location, satellite, and day. The difference in retrieval rates between MODIS AOD may be due to changes in cloud cover during the day such that it may have been cloudy during the overpass of one satellite but not the other.

On average, the highest retrieval rates occur from May to September (Figure 3.1), particularly in interior Alaska. Wintertime retrieval rates were much lower than summertime retrieval rates for both interior and southcentral Alaska with zero usable MODIS data in December. The low retrieval rates in the winter months are likely due to extensive snow and cloud cover. As mentioned previously, the algorithm only retrieves data when the surface reflectance in the 2.1 um channel is less than 0.4, in snow-free conditions [10]. The stations located within the same region have similar retrieval rates (Figure 3.1). Juneau has the lowest overall retrieval rates (Figure 3.1). Juneau is located along the southeast coast of Alaska and has a particularly rainy climate. Normal annual precipitation (1981-2010) for Juneau is 62.27 inches (224 precipitation days) while those for Anchorage (southcentral) and Fairbanks (interior) are 16.58 inches (114 precipitation days) and 10.81 inches (114 precipitation days), respectively [23], [24].The low overall retrieval of MODIS data over Juneau is likely due to cloud contamination. Juneau has an average of 280 cloudy, 41 partly cloudy, and 44 clear days per year [24]. In comparison, Fairbanks has an average of 210 cloudy, 86 partly cloudy, and 70 clear days; and Anchorage has an average of 239 cloudy, 65 partly cloudy, and 61 clear days per year. Previous research found that MODIS has difficulty retrieving AOD over coastal areas and in mountainous regions [10], [25], [26]. While Juneau has the lowest overall retrieval rates, Juneau has the highest retrieval rates in the winter months (November, January, February, March), which is likely due to it typically having less snow cover in winter months than both interior and southcentral Alaska. Juneau has 137 freezing degree days while Fairbanks and Anchorage have 226 and 192 freezing degree days, respectively [24].

Interior Alaska has the highest retrieval rates in summer months (May through September; Figure 3.1). Southcentral Alaska most likely has lower summertime retrieval rates than interior Alaska because it is a coastal, mountainous region. As mentioned previously, MODIS has difficulty retrieving data over mountainous and coastal regions [10], [25], [26].

### 3.4.2 Root Mean Square Error

The root mean square error (RMSE) of calculated monthly average PM2.5 is then examined to determine the magnitude of error associated with only using ground-level PM2.5 data that was collected on satellite retrieval days instead of all PM2.5 measurement days. Despite southeast (Juneau) Alaska having a maximum PM2.5 concentration of 23.44 $\mu g/m^3$ and interior (NCORE) and southcentral (Garden) Alaska having maximum PM2.5 concentrations of 169.81 $\mu g/m^3$ and 57.71 $\mu g/m^3$, southeast (Juneau) Alaska has the highest monthly RMSE. The RMSE for Juneau ranges from 1.45 $\mu g/m^3$ for AquaPM to 15.53 $\mu g/m^3$ for AquaTerraPM. The RMSE for AquaPM ranges from 0.29 $\mu g/m^3$ (Butte) to 12.45 $\mu g/m^3$ (Juneau). The RMSE for TerraPM ranges from 0.32 $\mu g/m^3$ (Garden) to 14.48 $\mu g/m^3$ (Juneau). The RMSE for AquaTerraPM ranges from 0.34 $\mu g/m^3$ (Parkgate) to 15.53 $\mu g/m^3$ (Juneau). RMSE is highest from November to February with no retrievals in December (Figure 3.2). The relatively high RMSE for Juneau is likely due to low satellite retrieval rates.

### 3.4.3 Bias

The average ratio monthly AllPM to AquaPM and TerraPM is then calculated to determine the amount of bias associated with only using PM2.5 data on satellite retrieval days (Figure 3.3). Values less than one indicate positive bias while values greater than one indicate negative bias. The ratio of AllPM to AquaPM (Figure 3.3) ranged from 0.42 (January) to 0.74 (March) for Juneau, 0.78 (September) to 2.90 (November) for southcentral, and 0.80 (September) to 1.20 (April) for interior Alaska. The ratio of AllPM to TerraPM range from 0.49 (January) to 1.0 (February) for Juneau, 0.51 (January) to 1.11 (April) for southcentral, and 0.88 (September) to 1.18 (April) for interior Alaska.

The average monthly error is also calculated to quantify the amount of bias associated with only using PM2.5 data on satellite retrieval days (Figure 3.4). The average difference between monthly means for AquaPM and AllPM (Figure 3.4) ranges from 1.80 $\mu g/m^3$ (May) to 12.2 $\mu g/m^3$ (January) for Juneau, -3.18 $\mu g/m^3$ (November) to 3.76 $\mu g/m^3$ (February) for southcentral, and -0.74 $\mu g/m^3$ (April) to 1.02 $\mu g/m^3$ (September) for interior Alaska. The average difference between monthly means of TerraPM and AllPM (Figure 3.4) range from 1.11 $\mu g/m^3$ (February) to 11.4 $\mu g/m^3$ (January) for Juneau, -0.78 $\mu g/m^3$ (February) to 5.86 $\mu g/m^3$ (January) for southcentral, and -0.68 $\mu g/m^3$ (July) to 0.61 $\mu g/m^3$ (September) for interior Alaska. As evidenced in Figures 3.3 through 3.6, determinations of whether monthly AquaPM and TerraPM are biased low or high occasionally differs between methods of determining bias due to the nature of the tests.

In both sets of bias evaluation, monthly averages of AquaPM and TerraPM are positively biased for Juneau, while those for both southcentral and interior Alaska tend to be low biased, centered around zero for the analysis of differences and close to one for the ratio analysis. Overall, the period with the lowest amount of bias for southcentral and interior Alaska is between April and October (MODIS AOD is only available between April and October for interior Alaska). The monthly bias tends to vary more in direction and be greater magnitude in the winter months for southcentral Alaska (no data is available for interior Alaska), which is consistent with the RMSE analysis. Positive bias is likely because MODIS AOD can only be retrieved in cloud free conditions, which means that data is not typically obtainable in rainy conditions when ground-level PM2.5 concentrations may be suppressed by rainfall. Higher PM2.5 concentrations tend to be associated with hot, dry conditions in the summertime.

Based on analysis of RMSE values and retrieval rates, models of the relationship between PM2.5 and AOD should not be developed during the winter months (November through March) in Alaska due to snow cover. Models should only be developed for months with historically higher retrieval rates, relatively low RMSE, and relatively low bias, such as the months of May through September for southcentral and interior Alaska. Based on the high RMSE, relatively high bias and low retrieval rates of MODIS, a model should not be developed for southeast Alaska (Juneau) at this time.

### 3.4.4 Multilinear Models

Three models were developed for each region and platform (Aqua and Terra): a best fit model (includes significant variables), the model outlined by equation 3.1 and the model outlined by equation 3.2. The best fit model of the relationship between MODIS AOD, meteorological parameters and mean ground-based PM2.5 measurements is then selected for each region and satellite (Aqua and Terra) using both backward and forward stepwise regression and the subsequent removal of insignificant parameters. A model was not developed for Juneau due primarily to low retrieval rates and relatively high bias of retrievals on satellite retrieval days. The percentile plots of AllPM, AquaPM, and TerraPM for the processed data, PM2.5 data associated with AOD with standard deviations less than 0.5, for each month are shown in figures 3.5, 3.6 and 3.7. The AquaPM and TerraPM appear to be most representative of ALLPM data between the $10^{th}$ and $90^{th}$ percentile for the months of April to October for Southcentral and Interior Alaska. For the 24-hour PM2.5 NAAQS, the $98^{th}$ percentile of PM2.5 concentrations averaged over three years is used to determine exceedances. Based on the percentile plots, the satellite retrievals days are not capturing the $98^{th}$ percentile.

Overall, the MLR models for interior Alaska had higher $R^2$ values than those for southcentral Alaska. Table 3.3 lists the multilinear regression results for interior and southcentral Alaska. Cross-validated r-squared (CV-$R^2$) values ranged from 0.20 to 0.27 for interior Alaska and 0.054 to 0.16 for southcentral Alaska. The highest CV-$R^2$ (0.27) and adjusted $R^2$ (0.28) were for the interior model only including Aqua AOD as a predictor. All CV-$R^2$ values were close to those of the adjusted $R^2$ values which indicates that the adjusted $R^2$ is a good measure of the goodness of fit. The model for interior Alaska that only included significant values had lower r-squared values than the model that only included AOD as the predictor. The disparity in r-squared values may be due to the higher number of coincidences between AOD and PM2.5 measurements than models that include meteorological parameters. AOD also appears to account for a greater amount of variance in interior Alaska than in the models for southcentral Alaska. The CV-$R^2$ for the interior model with only Terra AOD as a predictor is the same as those for the models including Terra AOD and meteorological parameters (0.20). This indicates that AOD has the greatest impact on model fit in interior Alaska. For southcentral Alaska models, the models with AOD as a predictor had CV-$R^2$ of 0.054 (Aqua) and 0.085 (Terra) while models with cloud fraction, temperature, rain and air pressure had CV-$R^2$ of 0.15 for both Terra and Aqua. The poor performance of AOD as a predictor in southcentral models is likely due to it being located on the coast and in mountainous terrain [25], [27]. Previous research indicates that MODIS AOD performs poorly in coastal zones and in mountainous terrain [25], [27].

The models with the highest CV-$R^2$ (interior Alaska) have more PM2.5 retrievals and a larger range of PM2.5 concentrations. The low CV-$R^2$ at lower concentrations of PM2.5 could be due to higher uncertainties in AOD, which is consistent with the findings in previous studies [16], [26]. It is likely that some error can be attributed to instrumental error (MODIS and ground AQM) and other variables not accounted for in the model, such as location, wind direction, and land-use information. To develop a good model, it is necessary to have a wide range of values. The southcentral model appears to be a poor fit for the data because there are no elevated (greater than 35 $\mu g/m^3$) measurements of ground-level PM2.5 on satellite retrieval days and only one PM2.5 measurement day. The adjusted r-squared values of the models for interior Alaska appear to be higher due to the larger number of higher concentration (greater than 35 $\mu g/m^3$) PM2.5 measurements. The maximum PM2.5 concentration detected during the period of May through September for southcentral was 57.7 $\mu g/m^3$ (Garden), while the maximum concentration detected in interior Alaska was 160.2 $\mu g/m^3$. Previous studies in Alaska comparing BAM 1020 AQMs to the FRM (federal reference method) found similar issues. The DEC determined that the poor correlations with FRMs were likely due to a lack of data for higher concentrations of PM2.5 [28]. Other sources of error may be the widespread locations of the AQMs in Southcentral AK, different sources of PM2.5, and missing data.

The coefficients for rain, relative humidity (RH), and cloud fraction are typically negative, indicating that they are negatively correlated with PM2.5 concentration. The coefficients of AOD, temperature, air pressure (AP) are positive indicating that they are positively correlated with PM2.5 concentration. This indicates that between the months of May and September, higher PM2.5 concentrations are associated with hot, dry days while lower PM2.5 concentrations are associated with cold, humid (rainy) days.

Tables 3.4 through 3.7 list the results of quantile regressions using the same predictors as those used to develop the models listed in Table 3.3. For interior Alaska, quantile regressions of the 90$^{th}$ percentile have the highest pseudo-$R^2$ (0.21-0.26) while those of the 10$^{th}$ percentile have the lowest (0.024-0.098) pseudo-$R^2$. For southcentral Alaska, the quantile regressions with the highest pseudo-$R^2$ vary between the 50$^{th}$, 75$^{th}$, and 90$^{th}$ percentiles (Tables 3.6 and 3.7). In addition, the values of the regression coefficients and the constants tend to increase with each increase in quantile (Appendix B). ANOVA indicates that quantile regressions of the 50$^{th}$, 75$^{th}$, and 90$^{th}$ percentiles are significantly different from those of the 10$^{th}$ and 25$^{th}$ percentiles for southcentral Alaska, while it indicates that the quantile regressions of the 75$^{th}$ and 90$^{th}$ percentiles are significantly different from the 10$^{th}$, 25$^{th}$, and 50$^{th}$ percentiles for interior Alaska. Results from the QR approach indicate that for interior Alaska modeling mean PM2.5 values using ordinary least squares may not adequately represent all quantiles with lower quantiles regressions being significantly different from those of upper quantiles. These findings are consistent with previous research that found that there is a higher level of uncertainty associated with lower aerosol loadings [14]. Based on a comparison between the multilinear regressions and the quantile regressions, the use of quantile regression or an alternate method of modeling (e.g.,mixed-effects modeling) may be required to adequately represent the data.

Table 3.8 lists the slope and intercept of the estimated versus observed values of log(PM2.5+5) and the MSE of the estimated and observed values of PM2.5. Plots of the estimated versus observed values of log(PM2.5+5) are shown in Figures 3.8 and 3.9. The cross-validated mean square error (MSE-CV) of the observed and estimated PM2.5 concentrations are quite high. The MSE-CV of the models for interior Alaska range from 51.1 to 121.4 $\mu g/m^3$, where the lowest MSE-CV is for the model with only Aqua AOD as a predictor and the highest MSE-CV is for the model with only Terra AOD as a predictor. The MSE-CV of the models for southcentral Alaska range from 13.5 to 16.1 $\mu g/m^3$, where the lowest MSE-CV is for the model with only significant predictors and Terra AOD; and the highest MSE-CV is for the model with only Aqua AOD as a predictor. The lower MSE-CV of the southcentral models is likely due to the lower range of PM2.5 concentrations used to develop the southcentral models as compared to interior Alaska. In general, the high MSE and low $R^2$ values indicate that the models fit the data poorly and are not adequate for accurate prediction of ground-level PM2.5 concentrations. In addition, the slopes of the fitted versus observed values of log(PM2.5+5) are all below 0.3 which indicates that the models severely underpredict ground-level PM2.5 concentrations. The models would not be useful for identifying exceedances of air quality standards due to severe underprediction of ground-level PM2.5.

### 3.4.5 Discussion

The MLR models developed of the relationship between ground level PM2.5, meteorological data, and MODIS AOD do not perform well with high MSE and low CV-$R^2$. The poor performance of the data appears to be due to the limited availability of MODIS AOD data in Alaska and missingness (missing data). The limited range of data (PM2.5 values) also is factor in the poor performance of the models; approximately 75 percent of the available PM2.5 data between May and September are below five $\mu g/m^3$. Note that models for each region did not truly encompass the entire regions for which the models were developed. For example, the interior model was only developed using one air quality monitoring station each from the cities of North Pole and Fairbanks.

Overall, the relationship between Aqua MODIS AOD and PM2.5 is strongest in interior Alaska. There is little to no relationship between MODIS AOD and PM2.5 in southcentral Alaska. While MODIS AOD has been validated against ground-based (AERONET) measurements of AOD in Bonanza Creek (near Fairbanks) Alaska [29]. No validation study has been performed for southcentral (Palmer, Anchorage) or southeast (Juneau) Alaska due to a lack of AERONET stations in those areas [29]. The low CV-$R^2$ values of southcentral Alaska could be due to poor agreement between MODIS AOD and ground-based AOD because validation studies in other mountainous and coastal regions indicate that there is poor agreement between satellite-based and ground-based measurements of AOD in those regions [25], [30].

Linear regressions of the relationship between MODIS AOD (Terra and Aqua v. 5.2.6) and PM2.5 for EPA regions one through ten had correlation coefficients (R) that ranged from 0.26 to 0.67 with the highest R for region four, three, two, and one (East U.S.) and lowest for regions ten, nine, and eight (West U.S.) [7]. The CV-R (0.53) of the linear regression of the log-transformed Aqua MODIS AOD and PM2.5 in interior Alaska is between the R values found for regions five and seven, which are also non-coastal regions in the continental U.S. [7]. The CV-R for the interior model only including Terra MODIS AOD (0.45) is between the R values found for regions five and six, which are primarily non-coastal regions. The CV-R (0.29) for southcentral Alaska models with only Terra MODIS AOD is between those found for regions ten (0.33) and eight (0.28) [7]. Region ten is coastal and mountainous and region eight also has mountainous terrain [7]. The CV-R (0.23) for the southcentral model with only Aqua AOD much lower than the range of R values found for the linear regressions of MODIS AOD and PM2.5 for EPA regions one through ten, where the lowest for Aqua is 0.28 for region nine (coastal and mountainous region) [7]. Gupta et al. also assessed the relationship between MODIS AOD and PM2.5 over multiple locations in India, Australia, Hong Kong, Switzerland, and U.S. (New York) [31]. The CV-R values for India, Australia, Hong Kong, Switzerland and U.S. (New York) ranged from 0.24 to 0.85, 0.11 to 0.48, 0.24 to 0.54, 0.21 to 0.45, and 0.48 to 0.75, respectively [31]. Overall, the CV-R values found for southcentral and interior Alaska appear to be consistent with those found during global studies and studies of the U.S.

Further research should be done using alternative modeling methods for MODIS AOD and PM2.5 in interior Alaska. The higher correlation between PM2.5 and MODIS AOD at higher PM2.5 concentrations is evident in both figures and models using Aqua MODIS AOD in interior Alaska. Therefore, MODIS AOD may be used qualitatively to identify areas of high PM2.5 concentrations but may not be used to estimate AQI or ground level PM2.5 concentrations. More air quality monitors are essential for developing adequate models for predicting ground-based PM2.5 concentrations.

Due to limited availability of MODIS data in Alaska, the use of MODIS AOD via multilinear regressions to evaluate ground level PM2.5 concentrations over time is not recommended. Future analyses using collocated weather stations and AQMs could possibly improve the fit of the models, but more MODIS AOD data is necessary to develop an applicable model. The use of mixed-effects models may improve the prediction accuracy of the models [32]. A review of various modeling methods indicates of the modeling methods attempted using AOD to estimate ground-level PM2.5 concentrations, mixed-effects models may improve prediction performance [32].

### 3.5 Conclusion

MODIS AOD data may be used qualitatively to identify areas of high PM2.5 concentrations but has limited applicability for quantitatively estimating ground-level PM2.5 concentrations in Alaska due to low retrieval rates and limited ranges of PM2.5 concentrations with which to develop models of the relationship between MODIS AOD and PM2.5. Little to no MODIS AOD data is retrieved in the winter time in Alaska, which is likely due to cloud- and snow-cover. Low retrieval rates are associated with higher RMSE and bias. In addition, upper quantiles of PM2.5 measurements are not captured by MODIS AOD due to low retrieval rates. Multilinear and quantile regression models of PM2.5 versus Aqua MODIS AOD in interior Alaska indicate that the correlation between the two variables increases with PM2.5 concentration (aerosol loading). Other modeling methods and may prove better for the data due to the high level of missingness. Also, model application and range are limited due to the limited availability of air quality monitors in Alaska with which to develop models. In addition to the need for more data, further work using alternative modeling methods, such as mixed-effects modeling, may be needed to develop more robust models.

### 3.6 References


[1] C. A. Pope and D. W. Dockery, "Health Effects of Fine Particulate Air Pollution: Lines that Connect," *J. Air Waste Manage. Assoc.*, vol. 56, no. 6, pp. 709–742, 2006.

[2] E. W. Butt *et al.*, "Global and regional trends in particulate air quality and attributable health burden over the past 50 years," *Environ. Res. Lett.*, vol. 12, no. 10, 2017.

[3] R. Kossover, "Association between Air Quality and Hospital Visits — Fairbanks , 2003 – 2008," *State of Alaska Epidemiology Bulletin*, Anchorage, AK, p. 99503, 30-Aug-2010.

[4] US EPA, "Fairbanks Air Quality Plan," *United States Environmental Protection Agency*, 2017. [Online]. Available: https://www.epa.gov/ak/fairbanks-air-quality-plan#nonattainment. [Accessed: 4-Nov-2018].

[5] ADEC, "Alaska Department of Environmental Conservation Annual Air Quality Monitoring Network Plan," *Alaska Department of Environmental Conservation: Air Quality Division Air Monitoring and Quality Assurance Program*, 2015. [Online]. Available: http://dec.alaska.gov/air/am/2015_Air_Monitoring_plan.pdf. [Accessed: 24-Jan-2017].

[6] P. Gupta, S. A. Christopher, M. A. Box, and G. P. Box, "Multi year satellite remote sensing of particulate matter air quality over Sydney, Australia," *Int. J. Remote Sens.*, vol. 28, no. 20, pp. 4483–4498, 2007.

[7] H. Zhang, R. M. Hoff, and J. A. Engel-Cox, "The Relation between Moderate Resolution Imaging Spectroradiometer (MODIS) Aerosol Optical Depth and PM2.5 over the United States: A Geographical Comparison by U.S. Environmental Protection Agency Regions," *J. Air Waste Manag. Assoc,* vol. 59, no.11, pp. 1358-13569, 2009.

[8] S. A. Christopher and P. Gupta, "Satellite Remote Sensing of Particulate Matter Air Quality: The Cloud-Cover Problem Satellite Remote Sensing of Particulate Matter Air Quality: The Cloud-Cover Problem," *J. Air Waste Manage. Assoc.*, vol. 60, no. 5, pp. 596–602, 2010.

[9] P. Gupta and S. A. Christopher, "Seven year particulate matter air quality assessment from surface and satellite measurements," *Atmospheric Chemistry and Physics.*, vol. 8, pp. 3311–3324, 2008.

[10] P. Gupta and S. A. Christopher, "An evaluation of Terra-MODIS sampling for monthly and annual particulate matter air quality assessment over the Southeastern United States," *Atmos. Environ.*, vol. 42, no. 26, pp. 6465–6471, 2008.

[11] EPA, "Air Quality System Data Mart," 2015. [Online]. Available: https://aqs.epa.gov/api. [Accessed: 20-Jan-2018].

[12] R. Levy, "Dark Target Aerosol Retrieval Algorithm," *Nasa*, 2018. [Online]. Available: https://darktarget.gsfc.nasa.gov/. [Accessed: 07-Aug-2018].

[13] NASA, "Level 1 and Atmosphere Archive and Distribution System (LAADS)," *LAADS Web*, 2018. [Online]. Available: https://ladsweb.modaps.eosdis.nasa.gov/search/. [Accessed: 25-Jan-2018].

[14] R. C. Levy *et al.*, "The Collection 6 MODIS aerosol products over land and ocean," *Atmos. Meas. Tech.*, vol. 6, pp. 2989–3034, 2013.

[15] C. Ichoku *et al.*, "A spatio-temporal approach for global validation and analysis of MODIS aerosol products," *Geophys. Res. Lett.*, vol. 29, no. 12, pp. 1–4, 2002.

[16] P. Gupta and S. A. Christopher, "Particulate matter air quality assessment using integrated surface, satellite, and meteorological products: Multiple regression approach," *J. Geophys. Res. Atmos.*, vol. 114, no. 14, pp. 1–13, 2009.

[17] Y. Liu, C. J. Paciorek, and P. Koutrakis, "Estimating regional spatial and temporal variability of PM2.5 concentrations using satellite data, meteorology, and land use information," *Environ. Health Perspect.*, vol. 117, no. 6, pp. 886–892, 2009.

[18] W.N. Venables, B.D. Ripley, *Modern Applied Statistics with S*, 4$^{th}$ ed. New York, NY: Springer, 2002.

[19] S. Aggarwal, R. Jain, and J. D. Marshall, "Real-time prediction of size-resolved ultrafine particulate matter on freeways," *Environ. Sci. Technol.*, vol. 46, no. 4, pp. 2234–2241, 2012.

[20] A. Canty, B. Ripley, "boot: Bootstrap R (S-Plus) Functions," R Package version 1.3-20. 2017.

[21] R. Koenker, "quantreg: Quantile Regression," R Package version 5.36. 2018.

[22] J. H. Maindonald and W. J. Braun, "DAAG: Data Analysis and Graphics Data and Functions," R Package version 1.22. 2015.

[23] "1981-2010 Normals | Data Tools | Climate Data Online (CDO) | National Climatic Data Center (NCDC)." [Online]. Available: https://www.ncdc.noaa.gov/cdo-web/datatools/normals. [Accessed: 13-Aug-2018].

[24] "Comparative Climatic Data for the United States through 2015," National Oceanic and Atmospheric Administration. [Online]. Available: http://ncd.noaa.gov/data-access/quick-links#ccd. [Accessed: 18-Oct-2018].

[25] J. P. Sherman, P. Gupta, R. C. Levy, and P. J. Sherman, "An Evaluation of MODIS-Retrieved Aerosol Optical Depth over a Mountainous AERONET Site in the Southeastern US," *Aerosol Air Qual. Res.*, vol. 16, pp. 3243–3255, 2016.

[26] L. A. Remer, Y. J. Kaufman, D. Tanré, S. Mattoo, D. A. Chu, K. V. Martins, R. R. Li, C. Ichoku, R. C. Levy, R. G. Kleidman, T. F. Eck, E. Vermote, B. N. Holben, "The MODIS Aerosol Algorithm, Products, and Validation," *J. Atmos. Sci.*, vol. 62, 2005.

[27] D. A. Chu, Y. J. Kaufman, C. Ichoku, L. A. Remer, D. Tanré, and B. N. Holben, "Validation of MODIS aerosol optical depth retrieval over land," *Geophys. Res. Lett.*, vol. 29, no. 12, pp. MOD2-1-MOD2-4, 2002.

[28] ADEC, "Assessment of the continuous PM 2.5 Met One BAM 1020 sampler performance in the State of Alaska Air monitoring Network," *Alaska Department of Environmental Conservation: Air Quality Division Air Monitoring and Quality Assurance Program*, 2014. [Online]. Available: http://dec.alaska.gov/air/anpms/projects-reports/DOCS/Alaska-PM2.5-FRM-FEM-Correlations-Report.pdf. [Accessed: 24-Jan-2017].

[29] A. McPhetres and S. Aggarwal, "Evaluation of MODIS-Retrieved Aerosol Optical Depth in Alaska : Implications for Surface Air Quality Applications," *Remote Sens.*, vol. 10, no. 9, pp. 1–14, 2018.

[30] A. M. Sayer, N. C. Hsu, C. Bettenhausen, and M. J. Jeong, "Validation and uncertainty estimates for MODIS Collection 6 'deep Blue' aerosol data," *J. Geophys. Res. Atmos.*, vol. 118, no. 14, pp. 7864–7872, 2013.

[31] P. Gupta, S. A. Christopher, J. Wang, R. Gehrig, Y. Lee, and N. Kumar, "Satellite remote sensing of particulate matter and air quality assessment over global cities," *Atmospheric Environment*, vol. 40, pp. 5880-5892, 2006.

[32] Y. Chu *et al.*, "A Review on Predicting Ground PM2.5 Concentration Using Satellite Aerosol Optical Depth," *Atmosphere (Basel)*, vol. 7, no. 10, p. 129, 2016.

### 3.7 Tables and Figures

Table 3.1. Locations of air quality monitoring stations (AQM) [11].

| Region | Site Name | Latitude* | Longitude* | AQS[1] Identification |
|---|---|---|---|---|
| Southcentral | Garden | 61.206 | -149.825 | 02-020-0018 |
| | Laurel | 61.181 | -149.834 | 02-020- 0051 |
| | Parkgate | 61.327 | -149.570 | 02-020-1004 |
| | Butte | 61.534 | -149.035 | 02-170-0008 |
| | Palmer | 61.599 | -149.104 | 02-170-0012 |
| Interior | NCORE | 64.845 | -147.726 | 02-090-0034 |
| | North Pole Fire Station #3 (NPFS3) | 64.763 | -147.310 | 02-090-0035 |
| Southeast | Floyd Dryden Middle School | 58.389 | -134.566 | 02-110-0004 |

*Coordinates for latitude and longitude are consistent with the World Geodetic System (WGS 84).
[1]Environmental protection agency air quality system identification number

Table 3.2. PM2.5 retrieval statistics for air quality monitoring stations in Alaska from May to September.

| Station | Parameter | $N_{MS}$ | PM2.5 ($\mu g/m^3$) | | | | | AOD | |
|---|---|---|---|---|---|---|---|---|---|
| | | | Min | Average | SD | Median | Max | Average | SD |
| Butte | AllPM | 727 | -3.08 | 2.49 | 3.30 | 2.04 | 40.79 | NA | NA |
| | AquaPM | 212 | -1.67 | 3.49 | 2.85 | 3.08 | 20.38 | 0.15 | 0.15 |
| | TerraPM | 271 | -1.91 | 3.20 | 2.82 | 2.75 | 20.38 | 0.21 | 0.20 |
| | AquaTerraPM | 318 | -1.91 | 3.10 | 2.78 | 2.68 | 20.38 | 0.18 | 0.17 |
| Palmer | AllPM | 704 | -1.63 | 4.55 | 3.85 | 3.81 | 23.44 | NA | NA |
| | AquaPM | 213 | -0.42 | 5.93 | 4.27 | 5.04 | 23.44 | 0.16 | 0.16 |
| | TerraPM | 272 | -1.46 | 5.34 | 4.33 | 4.44 | 23.44 | 0.20 | 0.17 |
| | AquaTerraPM | 310 | -1.46 | 5.35 | 4.27 | 4.33 | 23.44 | 0.19 | 0.17 |
| Parkgate | AllPM | 745 | -0.75 | 4.00 | 3.23 | 3.29 | 41.54 | NA | NA |
| | AquaPM | 220 | -0.58 | 5.05 | 3.98 | 4.00 | 32.63 | 0.13 | 0.10 |
| | TerraPM | 299 | -0.58 | 4.88 | 3.65 | 3.92 | 32.63 | 0.22 | 0.24 |
| | AquaTerraPM | 336 | -0.58 | 4.73 | 3.54 | 3.79 | 32.63 | 0.19 | 0.21 |
| Garden | AllPM | 748 | -0.42 | 4.75 | 3.54 | 4.17 | 57.71 | NA | NA |
| | AquaPM | 201 | 0.63 | 6.12 | 3.80 | 5.22 | 22.46 | 0.18 | 0.21 |
| | TerraPM | 306 | -0.25 | 5.94 | 4.64 | 5.10 | 57.71 | 0.25 | 0.23 |
| | AquaTerraPM | 337 | -0.25 | 5.80 | 4.51 | 5.04 | 57.71 | 0.23 | 0.23 |
| NCORE | AllPM | 743 | -0.17 | 5.54 | 11.29 | 3.33 | 169.81 | NA | NA |
| | AquaPM | 287 | -0.17 | 6.18 | 11.00 | 3.83 | 126.16 | 0.13 | 0.20 |
| | TerraPM | 380 | -0.17 | 5.97 | 10.66 | 3.72 | 126.16 | 0.18 | 0.27 |
| | AquaTerraPM | 420 | -0.17 | 5.97 | 10.62 | 3.66 | 126.16 | 0.16 | 0.21 |
| NPFS3 | AllPM | 568 | -4.14 | 6.73 | 13.47 | 3.85 | 160.21 | NA | NA |
| | AquaPM | 263 | -3.65 | 7.96 | 13.93 | 4.84 | 160.21 | 0.15 | 0.28 |
| | TerraPM | 305 | -3.65 | 7.40 | 11.44 | 4.69 | 96.30 | 0.18 | 0.31 |
| | AquaTerraPM | 332 | -3.65 | 7.83 | 14.16 | 4.68 | 160.21 | 0.17 | 0.29 |
| Juneau | AllPM | 704 | -1.63 | 4.55 | 3.85 | 3.81 | 23.44 | NA | NA |
| | AquaPM | 110 | -1.50 | 7.80 | 4.51 | 7.02 | 23.44 | 0.24 | 0.21 |
| | TerraPM | 183 | -1.29 | 7.01 | 4.59 | 6.33 | 23.44 | 0.26 | 0.22 |
| | AquaTerraPM | 217 | -1.50 | 6.87 | 4.52 | 6.13 | 23.44 | 0.25 | 0.22 |

NPFS3-North Pole Fire Station 3; SD-Standard Deviation; $N_{MS}$-number of retrievals from May to September.

Table 3.3. Multilinear regressions for interior and southcentral Alaska where log(PM2.5+5) is the response variable and the standard error is listed in parentheses.

| Region | Platform | N | Model Coefficients | | | | | | | | Adj. $R^2$ | CV-$R^2$ |
|---|---|---|---|---|---|---|---|---|---|---|---|---|
| | | | Constant | log(AOD+0.06) | CF | Temp | WS | Rain | AP | RH | | |
| South-central | Terra | 707 | -5.1 (1.8) | 0.17 (0.035) | -0.17 (0.072) | 0.0062* (0.0031) | -0.029 (0.012) | -0.12 (0.038) | 0.061 (0.016) | -0.0026* (0.0014) | 0.16 | 0.14 |
| | | 735 | -6.5 (1.7) | 0.18 (0.034) | -0.17 (0.071) | 0.0072 (0.0030) | | -0.15 (0.030) | 0.070 (0.016) | | 0.15 | 0.15 |
| | | 824 | 2.6 (0.059) | 0.16 (0.032) | | | | | | | 0.086 | 0.085 |
| | Aqua | 498 | -7.1 (2.4) | 0.18 (0.033) | -0.29 (0.054) | 0.012 (0.0037) | -0.017* (0.014) | -0.15 (0.046) | 0.062 (0.019) | 0.0010* (0.0017) | 0.16 | 0.13 |
| | | 518 | -7.8 (2.3) | 0.17 (0.033) | -0.30 (0.053) | 0.012 (0.0038) | | -0.14 (0.038) | 0.069 (0.020) | | 0.15 | 0.15 |
| | | 573 | 2.6 (0.059) | 0.16 (0.032) | | | | | | | 0.055 | 0.054 |
| Interior | Terra | 453 | 3.1* (2.7) | 0.40 (0.058) | -0.43 (0.13) | 0.0052* (0.0038) | -0.028* (0.016) | -0.19 (0.067) | -0.013* (0.023) | -0.00028* (0.0018) | 0.22 | 0.20 |
| | | 472 | 3.2 (0.089) | 0.42 (0.040) | -0.46 (0.10) | | | -0.18 (0.049) | | | 0.21 | 0.20 |
| | | 573 | 3.0 (0.096) | 0.44 (0.052) | | | | | | | 0.20 | 0.20 |
| | Aqua | 364 | 0.80 (3.4) | 0.32* (0.056) | -0.22 (0.090) | 0.0069* (0.0046) | -0.045 (0.016) | -0.21 (0.073) | 0.0034* (0.029) | -0.0011* (0.0021) | 0.23 | 0.21 |
| | | 381 | 3.1 (0.10) | 0.30 (0.051) | -0.24 (0.081) | | -0.039 (0.014) | -0.23 (0.054) | | | 0.24 | 0.23 |
| | | 458 | 3.1 (0.10) | 0.41 (0.050) | | | | | | | 0.28 | 0.27 |

*Not significant at a significance level of 0.05; AOD-aerosol optical depth; CF-cloud fraction; Temp-temperature (K); WS-wind speed (m/s); AP-air pressure (kPa); Rain-precipitation; RH-relative humidity (%).

Table 3.4. Quantile regression for interior Alaska PM2.5 measurements and Aqua AOD, where log(PM2.5+5) is the response and the standard error is listed in parentheses.

| Quantile | Model Coefficients | | | | | | | | Pseudo-$R^2$ |
|---|---|---|---|---|---|---|---|---|---|
| | Intercept | log(AOD+0.06) | CF | Temp | WS | Rain | RH | AP | |
| **0.1** | -5.6* (3.5) | 0.20 (0.041) | 0.018* (0.098) | 0.0081* (0.0055) | 0.0017* (0.015) | -0.013* (0.11) | -0.0059 (0.0024) | 0.059 (0.03) | 0.098 |
| **0.25** | -5.9 (2.6) | 0.25 (0.051) | -0.032* (0.093) | 0.01 (0.0046) | -0.014* (0.016) | -0.086* (0.071) | -0.0042 (0.0016) | 0.059 (0.024) | 0.11 |
| **0.5** | -2.0* (3.7) | 0.24 (0.041) | -0.22 (0.077) | 0.0068* (0.0054) | -0.053 (0.015) | -0.14 (0.063) | -0.0025* (0.0019) | 0.031* (0.028) | 0.13 |
| **0.75** | 5.7* (5.5) | 0.35 (0.1) | -0.48 (0.15) | 0.0093* (0.0065) | -0.068 (0.023) | -0.28 (0.11) | 0.0020* (0.0034) | -0.051* (0.048) | 0.16 |
| **0.9** | 15.2* (8.5) | 0.39 (0.11) | -0.35* (0.22) | 0.0089* (0.012) | -0.084 (0.04) | -0.52 (0.16) | 0.0066* (0.0042) | -0.14* (0.078) | 0.24 |
| **0.1** | 2.3 (0.062) | 0.21 (0.035) | 0.040* (0.079) | | 0.012* (0.014) | -0.12* (0.097) | | | 0.068 |
| **0.25** | 2.6 (0.12) | 0.25 (0.052) | -0.073* (0.10) | | -0.012 (0.013) | -0.16* (0.059) | | | 0.072 |
| **0.5** | 2.9 (0.075) | 0.28 (0.038) | -0.24 (0.052) | | -0.04 (0.014) | -0.2 (0.054) | | | 0.12 |
| **0.75** | 3.6 (0.19) | 0.42 (0.089) | -0.49 (0.13) | | -0.055 (0.021) | -0.21 (0.08) | | | 0.16 |
| **0.9** | 4 (0.19) | 0.47 (0.097) | -0.57 (0.23) | | -0.049* (0.04) | -0.44 (0.16) | | | 0.24 |
| **0.1** | 2.3 (0.061) | 0.23 (0.035) | | | | | | | 0.051 |
| **0.25** | 2.5 (0.089) | 0.24 (0.043) | | | | | | | 0.068 |
| **0.5** | 2.9 (0.12) | 0.31 (0.06) | | | | | | | 0.078 |
| **0.75** | 3.4 (0.18) | 0.45 (0.078) | | | | | | | 0.14 |
| **0.9** | 4.0 (0.12) | 0.56 (0.059) | | | | | | | 0.26 |

*Not significant at a significance level of 0.05; AOD-aerosol optical depth; CF-cloud fraction; Temp-temperature (K); WS-wind speed (m/s); AP-air pressure (kPa); Rain-precipitation; RH-relative humidity (%).

Table 3.5. Quantile regression for interior Alaska PM2.5 measurements and Terra AOD, where log(PM2.5+5) is the response and the standard error is listed in parentheses.

| **Quantile** | **Model Coefficients** | | | | | | | | **Pseudo-$R^2$** |
|---|---|---|---|---|---|---|---|---|---|
| | Intercept | log(AOD+0.06) | CF | Temp | WS | Rain | RH | AP | |
| **0.1** | -6.5* (4.1) | 0.25 (0.057) | -0.3 (0.15) | 0.0096* (0.0054) | 0.0065* (0.018) | -0.051* (0.086) | -0.0030* (0.0017) | 0.064* (0.034) | 0.072 |
| **0.25** | -4.3* (2.4) | 0.28 (0.051) | -0.42 (0.1) | 0.0098 (0.0036) | -0.0046* (0.017) | -0.067* (0.048) | -0.0017* (0.0015) | 0.043 (0.021) | 0.095 |
| **0.5** | 4.0* (3.1) | 0.27 (0.051) | -0.44 (0.11) | 0.0023* (0.0046) | -0.039 (0.016) | -0.13 (0.057) | -0.0021* (0.0019) | -0.015* (0.025) | 0.12 |
| **0.75** | 7.1* (4.1) | 0.36 (0.11) | -0.49 (0.14) | 0.0047* (0.0053) | -0.076 (0.021) | -0.24 (0.089) | 0.0011* (0.0025) | -0.051* (0.034) | 0.15 |
| **0.9** | 16.3 (5.1) | 0.59 (0.065) | -0.35* (0.23) | 0.00036* (0.0072) | -0.08 (0.026) | -0.3 (0.098) | 0.0012* (0.0033) | -0.12 (0.045) | 0.26 |
| **0.1** | 2.5 (0.14) | 0.24 (0.056) | -0.35 (0.12) | | | -0.17 (0.076) | | | 0.051 |
| **0.25** | 2.7 (0.12) | 0.30 (0.047) | -0.4 (0.13) | | | -0.13 (0.047) | | | 0.074 |
| **0.5** | 3.0 (0.10) | 0.31 (0.044) | -0.5 (0.11) | | | -0.14 (0.043) | | | 0.11 |
| **0.75** | 3.4 (0.20) | 0.41 (0.093) | -0.53 (0.15) | | | -0.21 (0.049) | | | 0.13 |
| **0.9** | 4.1 (0.11) | 0.59 (0.052) | -0.58 (0.23) | | | -0.27 (0.11) | | | 0.22 |
| **0.1** | 2.2 (0.077) | 0.192 (0.334) | | | | | | | 0.024 |
| **0.25** | 2.4 (0.082) | 0.25 (0.041) | | | | | | | 0.045 |
| **0.5** | 2.7 (0.094) | 0.28 (0.052) | | | | | | | 0.066 |
| **0.75** | 3.4 (0.18) | 0.52 (0.087) | | | | | | | 0.11 |
| **0.9** | 3.9 (0.081) | 0.64 (0.048) | | | | | | | 0.21 |

*Not significant at a significance level of 0.05; AOD-aerosol optical depth; CF-cloud fraction; Temp-temperature (K); WS-wind speed (m/s); AP-air pressure (kPa); Rain-precipitation; RH-relative humidity (%).

Table 3.6. Quantile regression for southcentral Alaska PM2.5 measurements and Aqua AOD, where log(PM2.5+5) is the response and the standard error is listed in parentheses.

| Quantile | Model Coefficients | | | | | | | | Pseudo-$R^2$ |
|---|---|---|---|---|---|---|---|---|---|
| | Intercept | log(AOD+0.06) | CF | Temp | WS | Rain | RH | AP | |
| **0.1** | -6.9* (4.4) | 0.053* (0.038) | -0.27 (0.11) | -0.0064* (0.0067) | -0.039* (0.024) | -0.077* (0.074) | 0.0022* (0.0036) | 0.11 (0.037) | 0.098 |
| **0.25** | -8.4 (2.9) | 0.11 (0.037) | -0.28 (0.075) | 0.0046* (0.0040) | -0.041* (0.022) | -0.091* (0.056) | -0.0014* (0.0019) | 0.096 (0.024) | 0.1 |
| **0.5** | -7.2 (3.0) | 0.19 (0.043) | -0.28 (0.065) | 0.012 (0.0045) | -0.033* (0.019) | -0.18 (0.056) | 0.0016* (0.0018) | 0.063 (0.023) | 0.13 |
| **0.75** | -6.3* (3.2) | 0.25 (0.059) | -0.30 (0.070) | 0.019 (0.0044) | -0.00039* (0.020) | -0.18 (0.075) | 0.0017* (0.0027) | 0.036* (0.030) | 0.12 |
| **0.9** | -5.6* (6.1) | 0.23 (0.072) | -0.26* (0.17) | 0.022 (0.01) | 0.030* (0.031) | -0.23 (0.12) | 0.0025* (0.0039) | 0.023* (0.047) | 0.087 |
| **0.1** | -6.8* (4.3) | 0.076 (0.037) | -0.22 (0.10) | -0.0045* (0.0083) | | -0.029* (0.0054) | | 0.10 (0.036) | 0.066 |
| **0.25** | -10 (3.2) | 0.099 (0.037) | -0.27 (0.068) | 0.0069* (0.0043) | | -0.090 (0.042) | | 0.10 (0.027) | 0.081 |
| **0.5** | -8.2 (3.2) | 0.18 (0.037) | -0.31 (0.065) | 0.014 (0.0045) | | -0.16 (0.043) | | 0.068 (0.026) | 0.12 |
| **0.75** | -7.3 (3.1) | 0.25 (0.06) | -0.30 (0.068) | 0.019 (0.0042) | | -0.14 (0.065) | | 0.048* (0.028) | 0.12 |
| **0.9** | -6.2* (5.9) | 0.25 (0.068) | -0.35 (0.16) | 0.022 (0.01) | | -0.15* (0.11) | | 0.032* (0.047) | 0.077 |
| **0.1** | 2.0 (0.060) | 0.051* (0.029) | | | | | | | 0.0092 |
| **0.25** | 2.2 (0.085) | 0.093 (0.043) | | | | | | | 0.013 |
| **0.5** | 2.6 (0.06) | 0.19 (0.028) | | | | | | | 0.047 |
| **0.75** | 3.0 (0.096) | 0.3 (0.055) | | | | | | | 0.048 |
| **0.9** | 3.2 (0.12) | 0.25 (0.065) | | | | | | | 0.037 |

*Not significant at a significance level of 0.05; AOD-aerosol optical depth; CF-cloud fraction; Temp-temperature (K); WS-wind speed (m/s); AP-air pressure (kPa); Rain-precipitation; RH-relative humidity (%).

Table 3.7. Quantile regression for southcentral Alaska PM2.5 measurements and Terra AOD, where log(PM2.5+5) is the response and the standard error is listed in parentheses.

| Quantile | Model Coefficients | | | | | | | | Pseudo-$R^2$ |
|---|---|---|---|---|---|---|---|---|---|
| | Intercept | log(AOD+0.06) | CF | Temp | WS | Rain | RH | AP | |
| **0.1** | -6.0* (3.4) | 0.072* (0.050) | -0.024* (0.11) | -0.0075 (0.0051) | -0.066 (0.025) | 0.00050* (0.089) | -0.0038* (0.0036) | 0.11 (0.028) | 0.097 |
| **0.25** | -5.3* (2.9) | 0.094 (0.044) | 0.011* (0.093) | 0.0025* (0.004) | -0.043 (0.012) | -0.073* (0.045) | -0.00087* (0.0017) | 0.069 (0.025) | 0.09 |
| **0.5** | -6.7 (2.1) | 0.15 (0.033) | -0.12 (0.063) | 0.01 (0.0037) | -0.04 (0.011) | -0.13 (0.036) | -0.00089* (0.0013) | 0.064 (0.019) | 0.12 |
| **0.75** | -2.3* (2.6) | 0.22 (0.063) | -0.18* (0.11) | 0.01 (0.0049) | -0.022* (0.017) | -0.18 (0.06) | -0.0020* (0.0018) | 0.024* (0.023) | 0.11 |
| **0.9** | -4.3* (3.8) | 0.27 (0.050) | -0.39 (0.12) | 0.0080* (0.0052) | -0.0099* (0.020) | -0.047* (0.087) | -0.0067 (0.0027) | 0.057* (0.034) | 0.14 |
| **0.1** | -10.5 (3.1) | 0.10 (0.052) | -0.054* (0.13) | -0.0033* (0.0057) | | -0.060* (0.052) | | 0.13 (0.027) | 0.07 |
| **0.25** | -8.2 (2.7) | 0.11 (0.047) | -0.018* (0.087) | 0.0055* (0.0038) | | -0.082* (0.041) | | 0.088 (0.023) | 0.074 |
| **0.5** | -8.1 (2.1) | 0.15 (0.033) | -0.15 (0.068) | 0.013 (0.0037) | | -0.15 (0.040) | | 0.068 (0.020) | 0.11 |
| **0.75** | -4.0* (2.5) | 0.21 (0.057) | -0.21* (0.096) | 0.011 (0.0049) | | -0.20 (0.052) | | 0.038* (0.022) | 0.1 |
| **0.9** | -5.1* (4.3) | 0.27 (0.053) | -0.45 (0.15) | 0.0097* (0.0062) | | -0.15* (0.078) | | 0.055* (0.044) | 0.12 |
| **0.1** | 2.1 (0.082) | 0.13 (0.044) | | | | | | | 0.025 |
| **0.25** | 2.3 (0.049) | 0.17 (0.029) | | | | | | | 0.039 |
| **0.5** | 2.6 (0.048) | 0.22 (0.029) | | | | | | | 0.052 |
| **0.75** | 2.9 (0.068) | 0.27 (0.038) | | | | | | | 0.057 |
| **0.9** | 3.2 (0.064) | 0.3 (0.038) | | | | | | | 0.079 |

*Not significant at a significance level of 0.05; AOD-aerosol optical depth; CF-cloud fraction; Temp-temperature (K); WS-wind speed (m/s); AP-air pressure (kPa); Rain-precipitation; RH-relative humidity (%).

Table 3.8. Goodness of fit parameters of multilinear regressions including the intercept and slope of estimated versus observed values of log(PM2.5+5) and mean square error of PM2.5.

| Platform | Predictors | Intercept | Slope | MSE ($\mu g/m^3$) | MSE-CV ($\mu g/m^3$) |
|---|---|---|---|---|---|
| **Southcentral** | | | | | |
| **Terra** | AOD, CF, Temp, Rain, AP, RH, WS | 1.9 | 0.17 | 13.3 | 13.7 |
| | AOD, CF, Temp, Rain, AP | 1.9 | 0.16 | 14.6 | 14.6 |
| | AOD | 1.9 | 0.17 | 13.6 | 13.3 |
| **Aqua** | AOD, CF, Temp, Rain, AP, RH, WS | 1.9 | 0.17 | 13.8 | 14.3 |
| | AOD, CF, Temp, Rain, AP | 1.9 | 0.16 | 13.9 | 14.1 |
| | AOD | 2.2 | 0.056 | 16.0 | 16.1 |
| **Interior** | | | | | |
| **Terra** | AOD, CF, Temp, Rain, AP, RH, WS | 1.8 | 0.22 | 56.2 | 57.4 |
| | AOD, CF, Rain | 1.8 | 0.22 | 55.3 | 56.3 |
| | AOD | 1.8 | 0.20 | 120.1 | 121.4 |
| **Aqua** | AOD, CF, Temp, Rain, AP, RH, WS | 1.8 | 0.25 | 50.4 | 51.8 |
| | AOD, CF, Rain, WS | 1.8 | 0.25 | 49.8 | 51.1 |
| | AOD | 1.7 | 0.28 | 87.2 | 89.3 |

AOD-aerosol optical depth; CF-cloud fraction; Temp-temperature (K); WS-wind speed (m/s); AP-air pressure (kPa); Rain-precipitation; RH-relative humidity (%); MSE-mean square error; MSE-CV-cross-validated MSE.

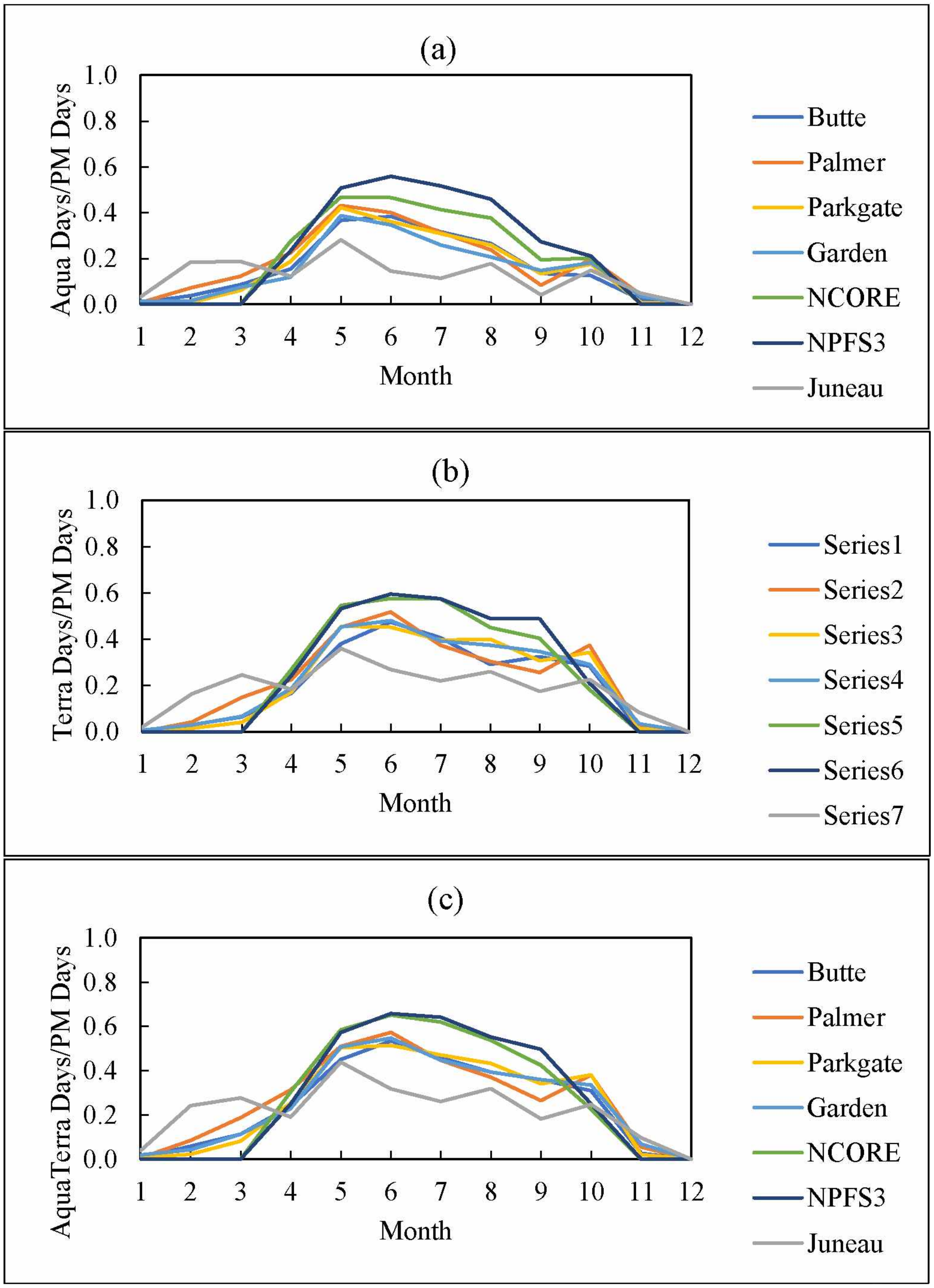


Figure 3.1. Cumulative retrieval rate per month from January (1) to December (12) for the years 2012 to 2016.

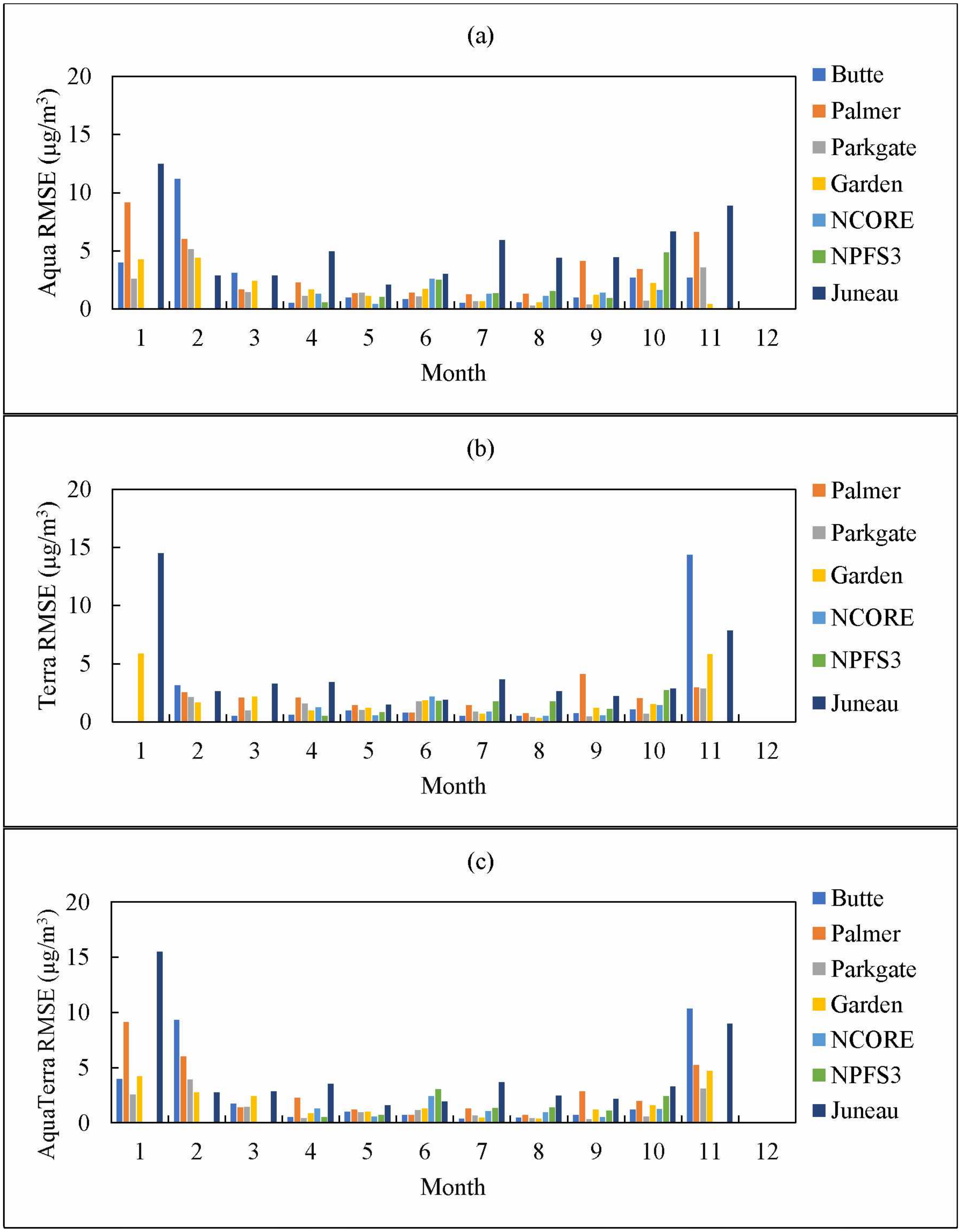


Figure 3.2. Bar charts showing RMSE of average monthly PM2.5 for Aqua, Terra, and AquaTerra retrieval days as compared to all PM2.5 retrieval days from January (1) to December (12) for the years 2012 to 2016.

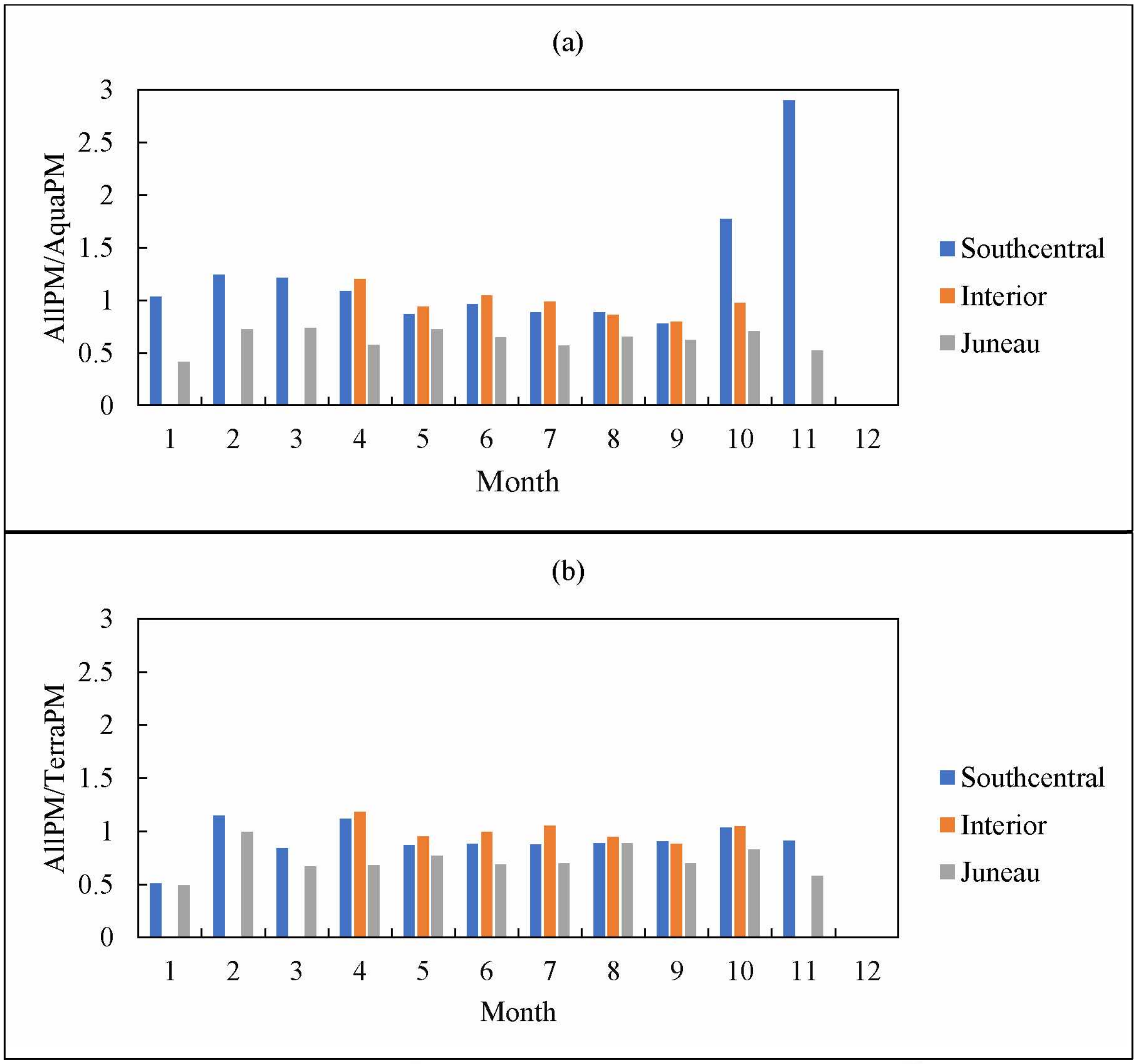

Figure 3.3. Ratio of monthly average of ALLPM to (a) AquaPM and (b) TerraPM for Southcentral, Interior, and Juneau, Alaska from January (1) to December (12) for the years 2012 to 2016.

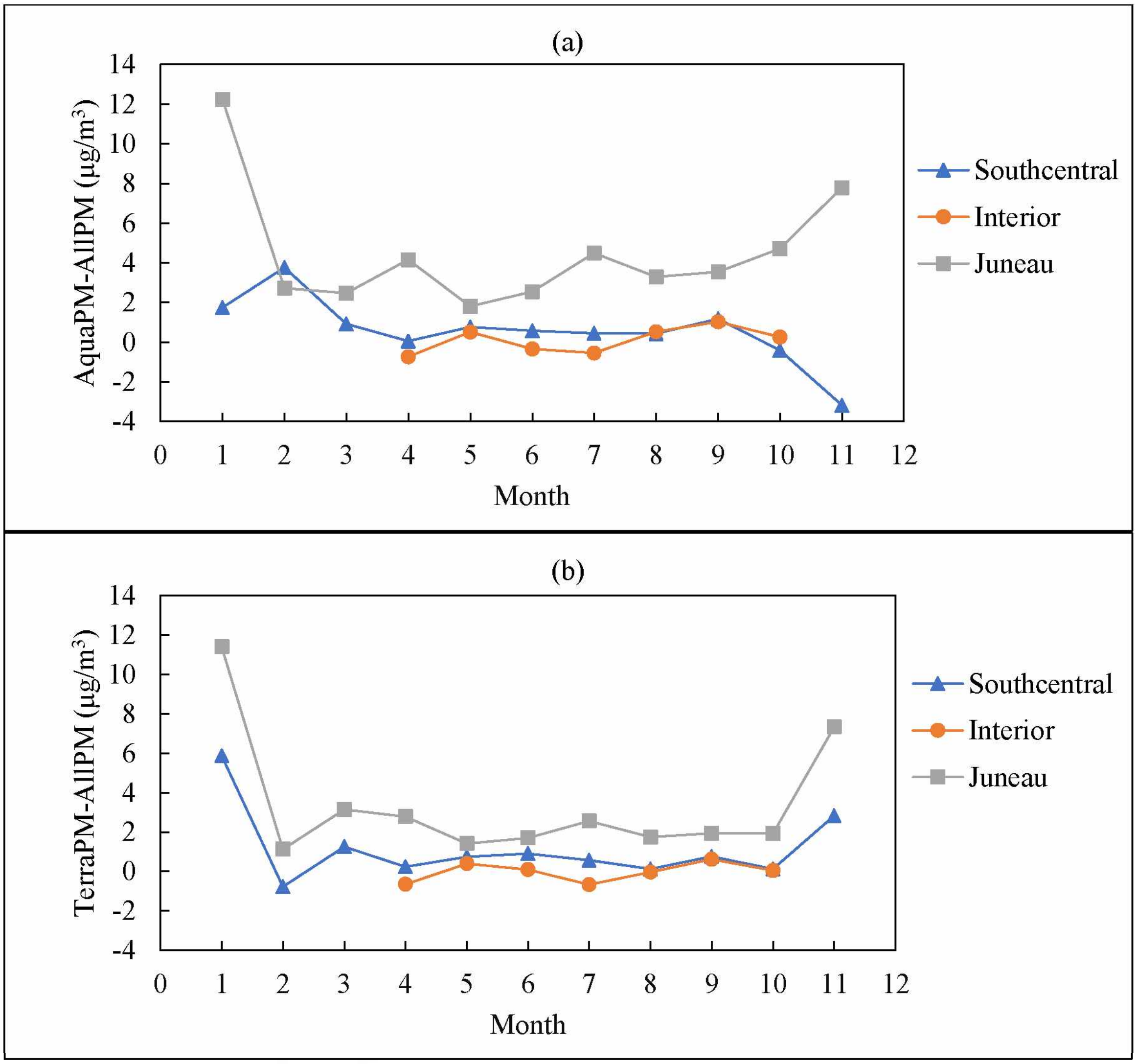


Figure 3.4. The mean of the difference between monthly average (a) AquaPM and AllPM and (b) TerraPM and AllPM from January (1) to December (12) for the years 2012 to 2016.

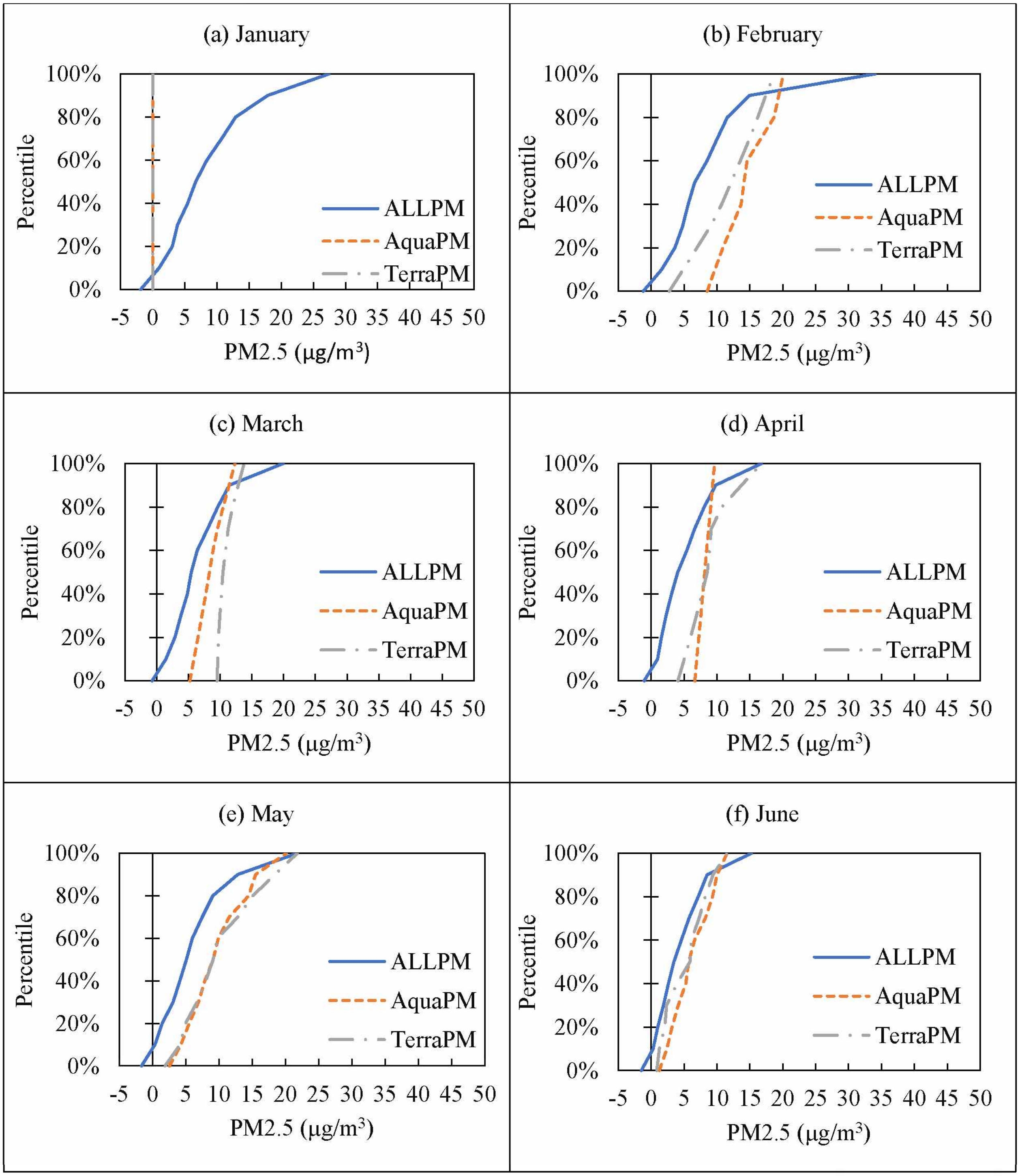


Figure 3.5. (a-l) Percentile versus ground level PM2.5 concentration in interior Alaska for the months of January through December. AllPM is all ground-based PM2.5 measurements. AquaPM and TerraPM are all ground-based PM2.5 measurements on Aqua MODIS AOD and Terra MODIS AOD retrieval days, respectively, where AOD has a maximum standard deviation of 0.5 and the number of retrieved pixels is at least three. Plots that are highlighted in gray indicate that there were no Aqua and/or Terra MODIS AOD retrievals with standard deviation less than 0.5 and at least 3 pixels.

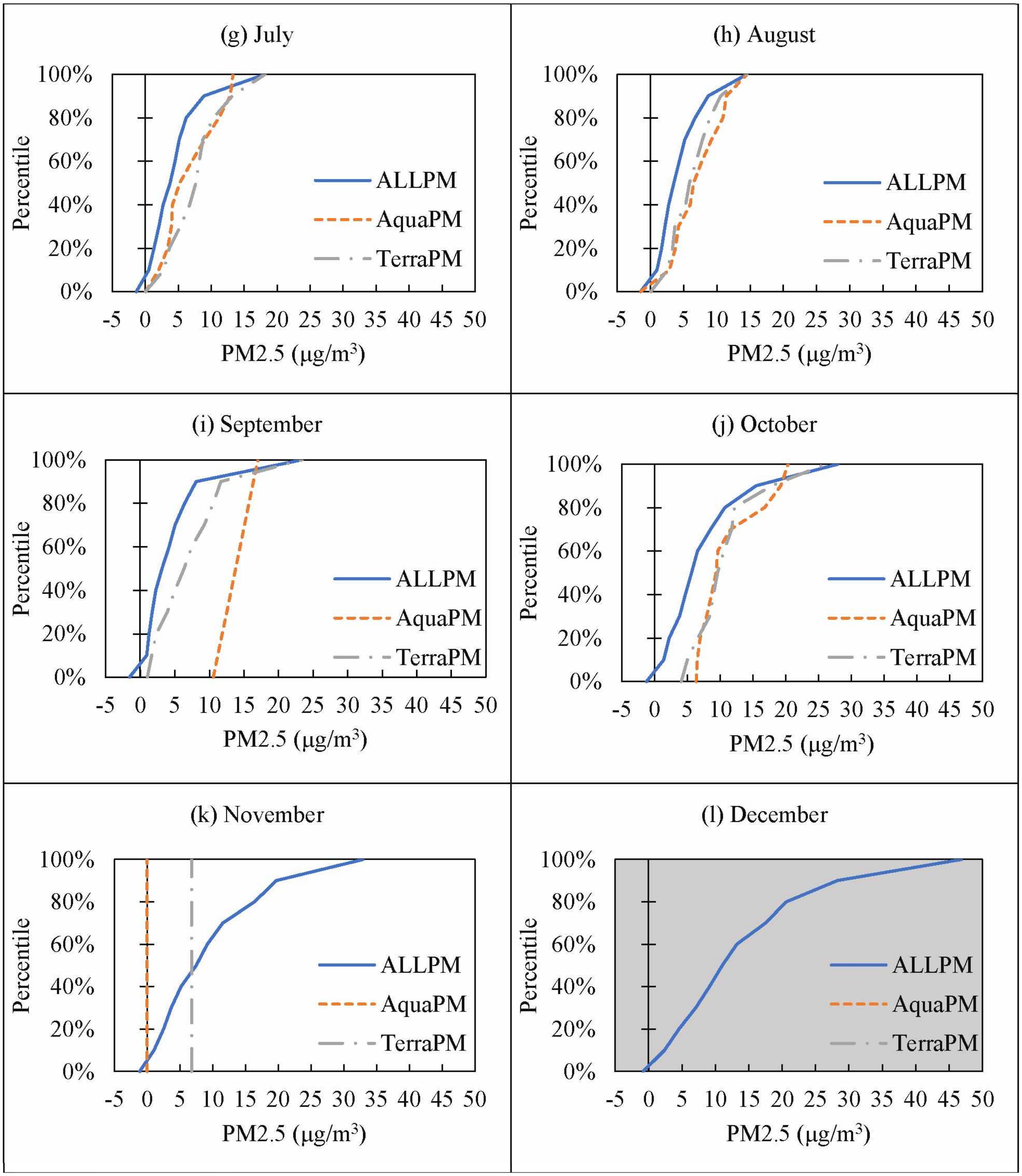

Figure 3.5 (continued)

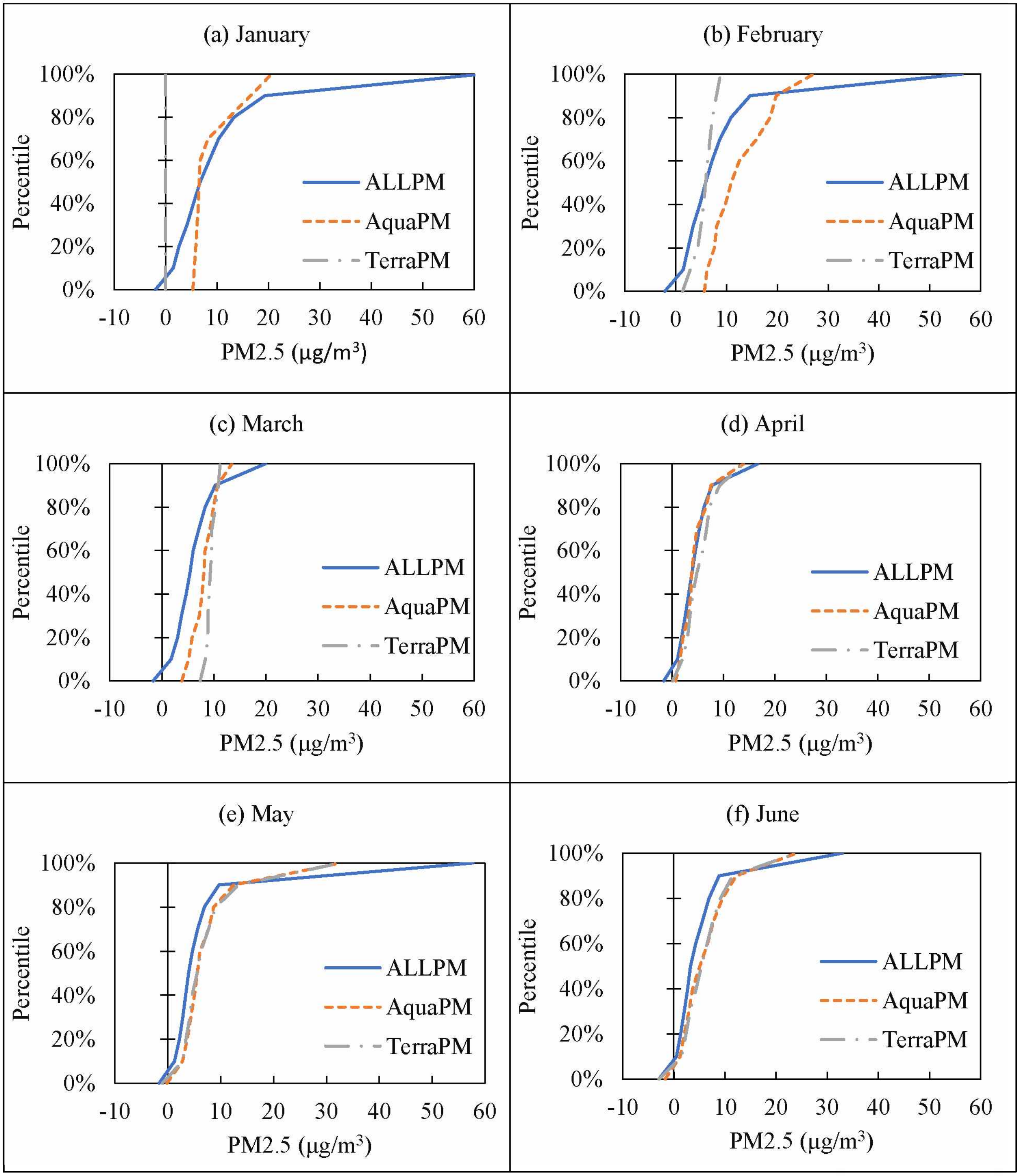


Figure 3.6. (a-l) Percentile versus ground level PM2.5 concentration in interior Alaska for the months of January through December. AllPM is all ground-based PM2.5 measurements. AquaPM and TerraPM are all ground-based PM2.5 measurements on Aqua MODIS AOD and Terra MODIS AOD retrieval days, respectively, where AOD has a maximum standard deviation of 0.5 and the number of retrieved pixels is at least three. Plots that are highlighted in gray indicate that there were no Aqua and/or Terra MODIS AOD retrievals with standard deviation less than 0.5 and at least 3 pixels.

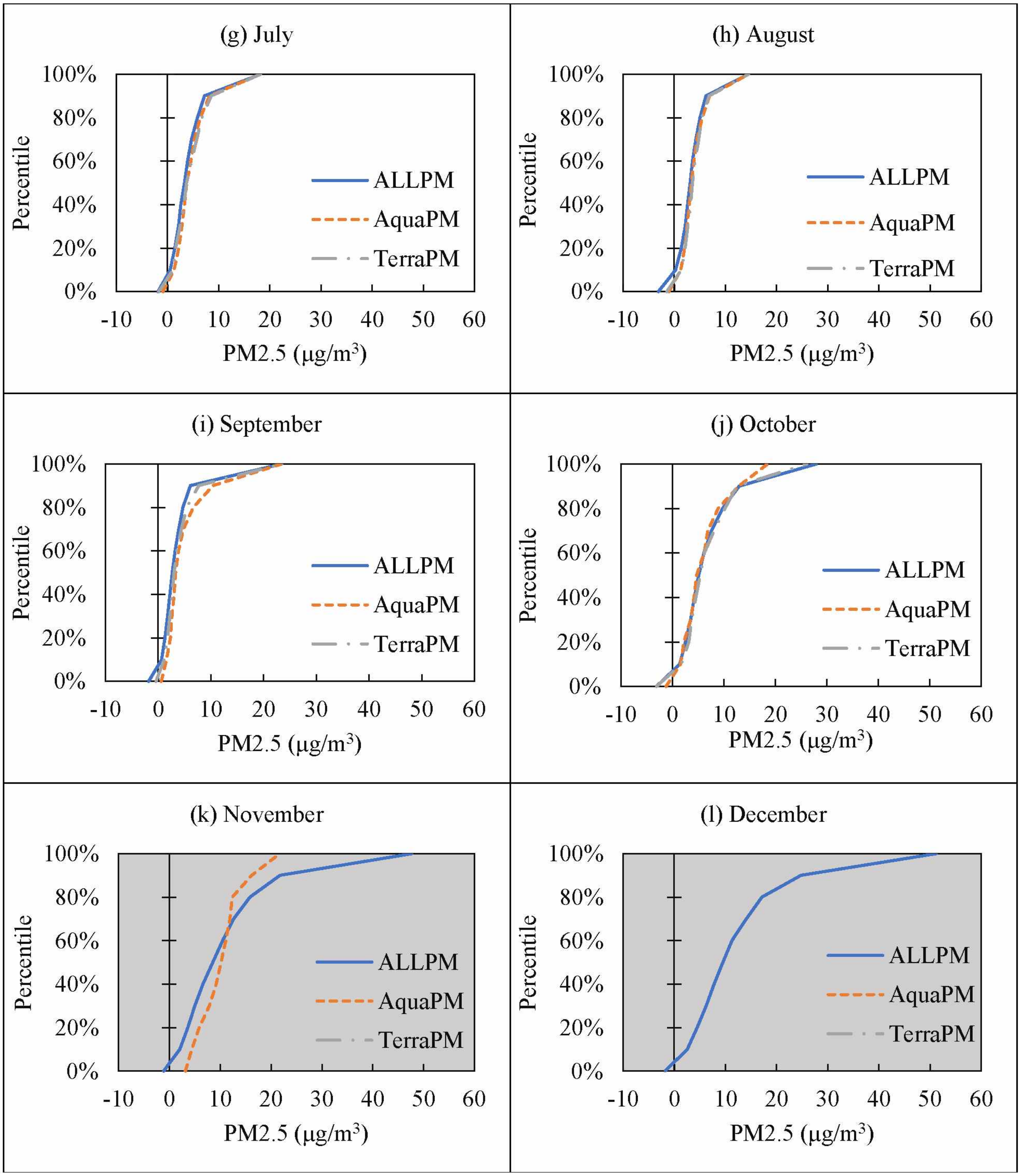


Figure 3.6 (continued)

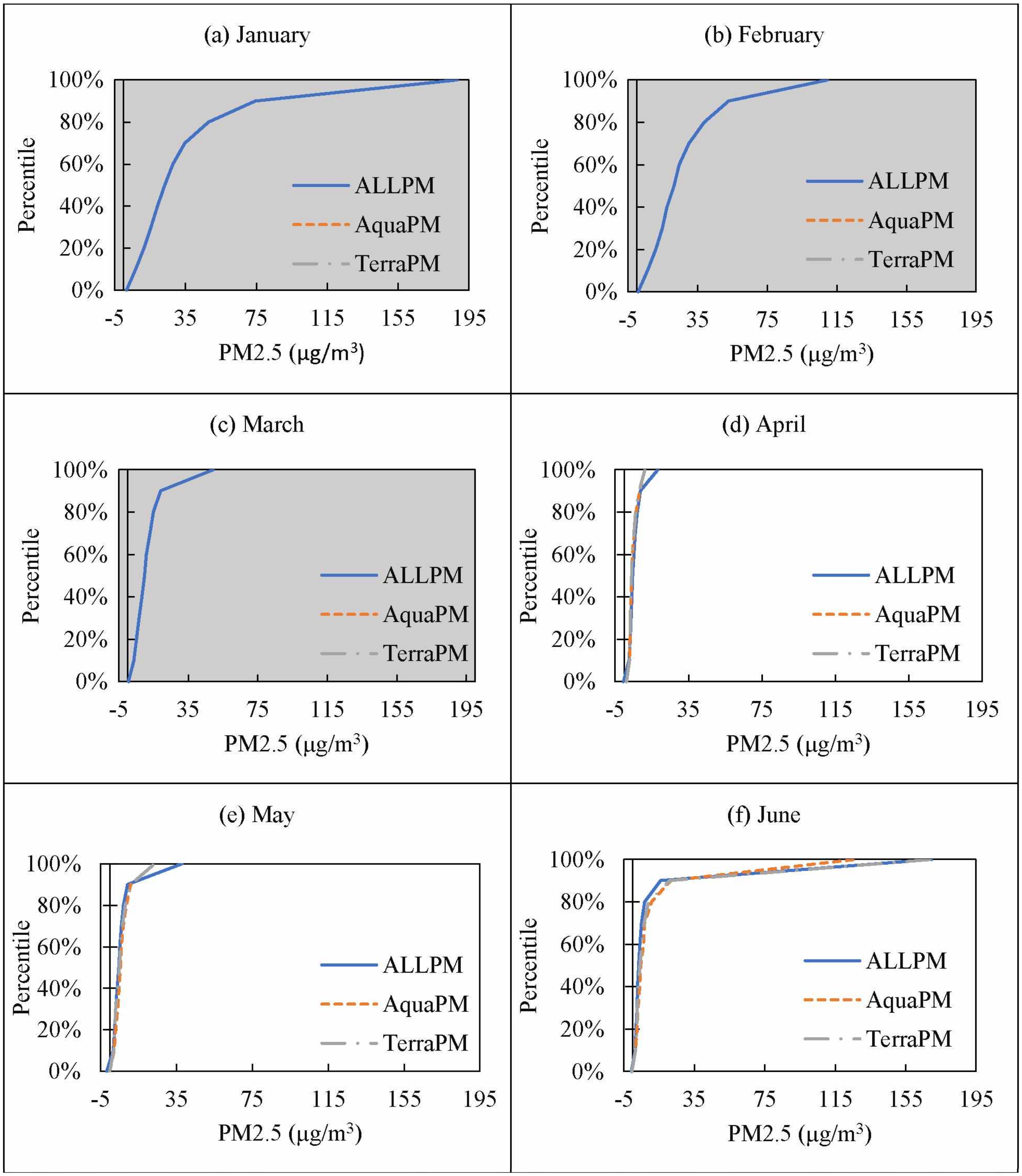


Figure 3.7. (a-l) Percentile versus ground level PM2.5 concentration in interior Alaska for the months of January through December. AllPM is all ground-based PM2.5 measurements. AquaPM and TerraPM are all ground-based PM2.5 measurements on Aqua MODIS AOD and Terra MODIS AOD retrieval days, respectively, where AOD has a maximum standard deviation of 0.5 and the number of retrieved pixels is at least three. Plots that are highlighted in gray indicate that there were no Aqua and/or Terra MODIS AOD retrievals with standard deviation less than 0.5 and at least 3 pixels.

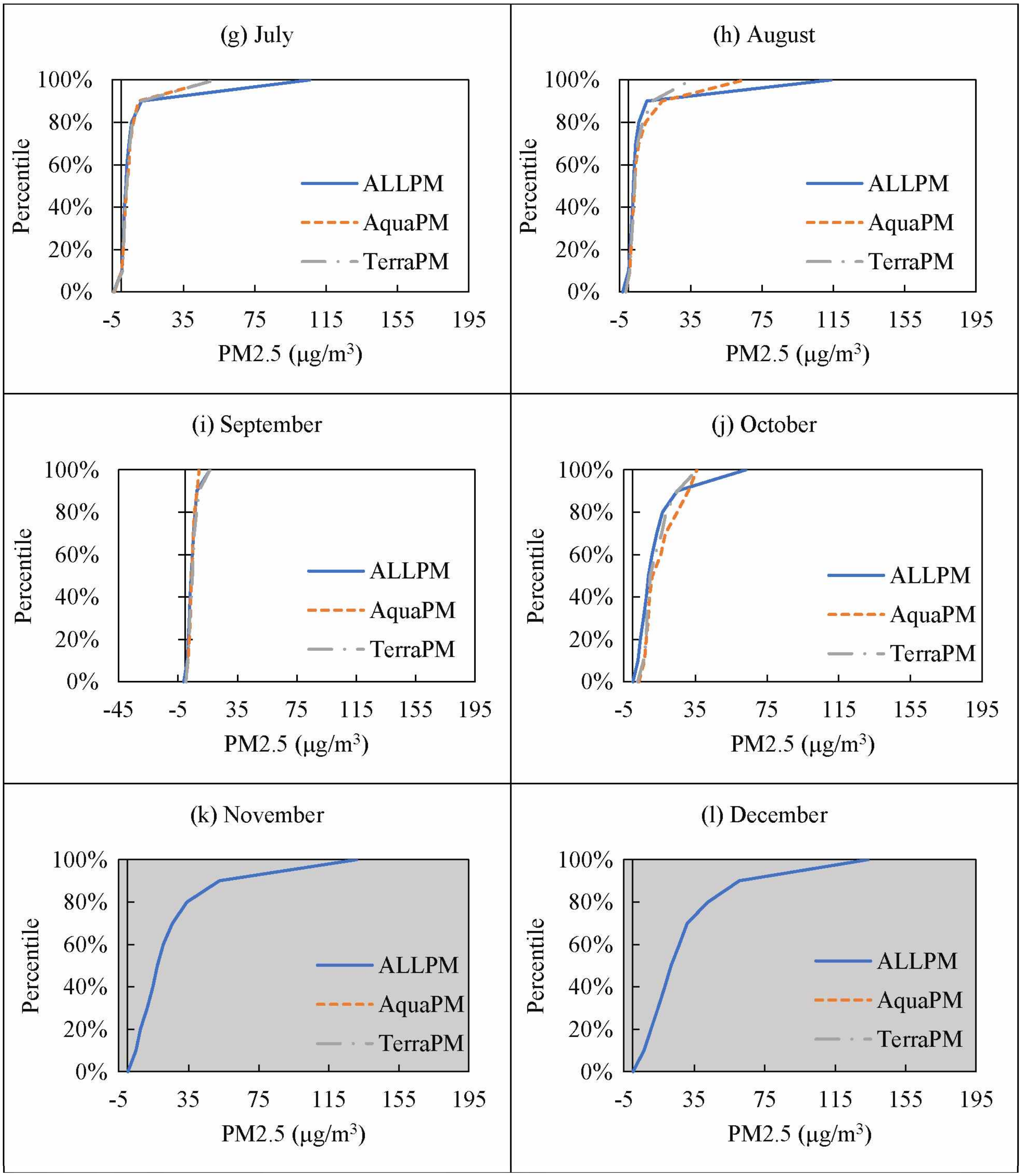


Figure 3.7 (continued)

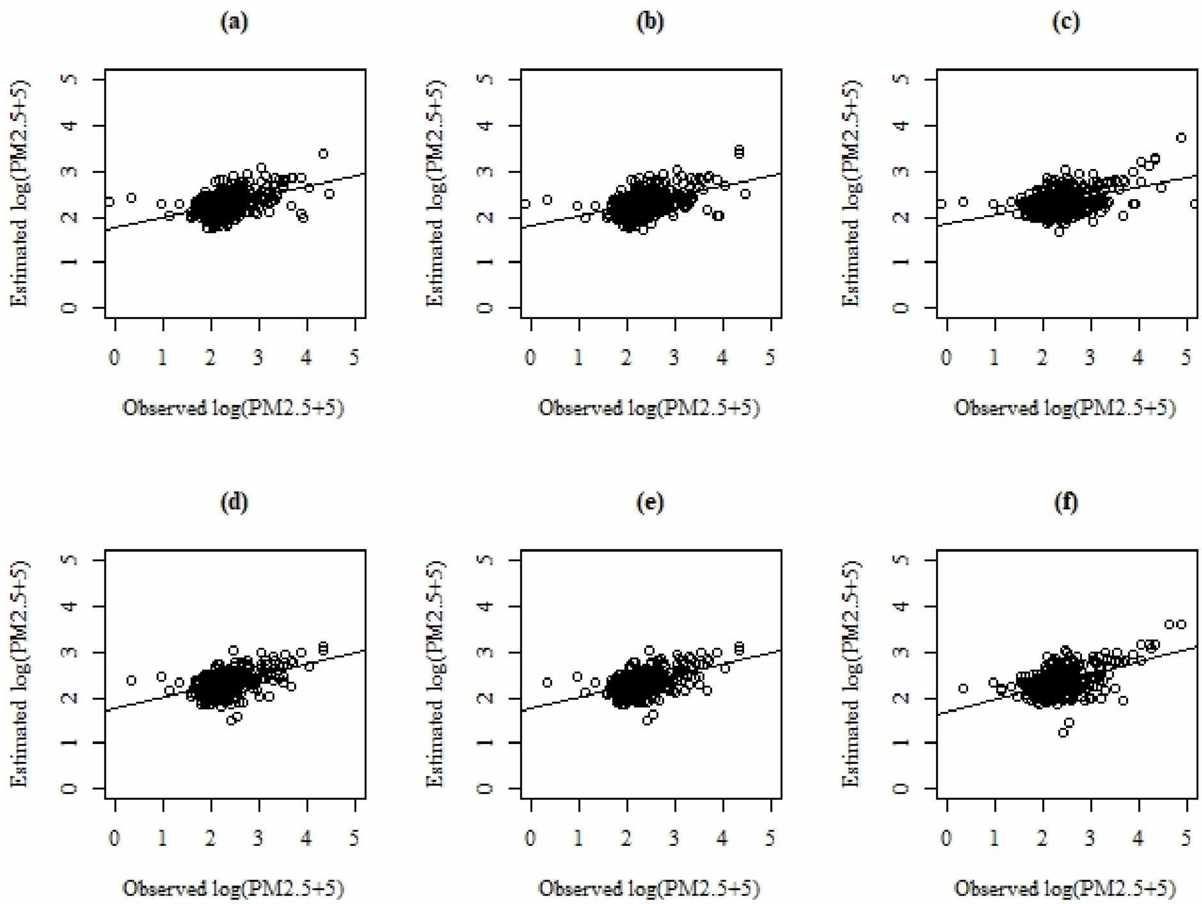


Figure 3.8. Plots of estimated versus observed log(PM2.5+5) for interior Alaska.
(a) Terra: log(PM2.5+5)~log(AOD+0.06)+CF+Temp+WS+Rain+AP+RH;
(b) Terra: log(PM2.5+5)~log(AOD +0.06)+CF+Rain;
(c) Terra: log(PM2.5+5)~log(AOD+0.06);
(d) Aqua: log(PM2.5+5)~log(AOD+0.06) +CF+Temp+WS+Rain+AP+RH;
(e) Aqua: log(PM2.5+5)~log(AOD+0.06)+CF+WS+Rain; (f) Aqua: log(PM2.5+5)~log(AOD+0.06).

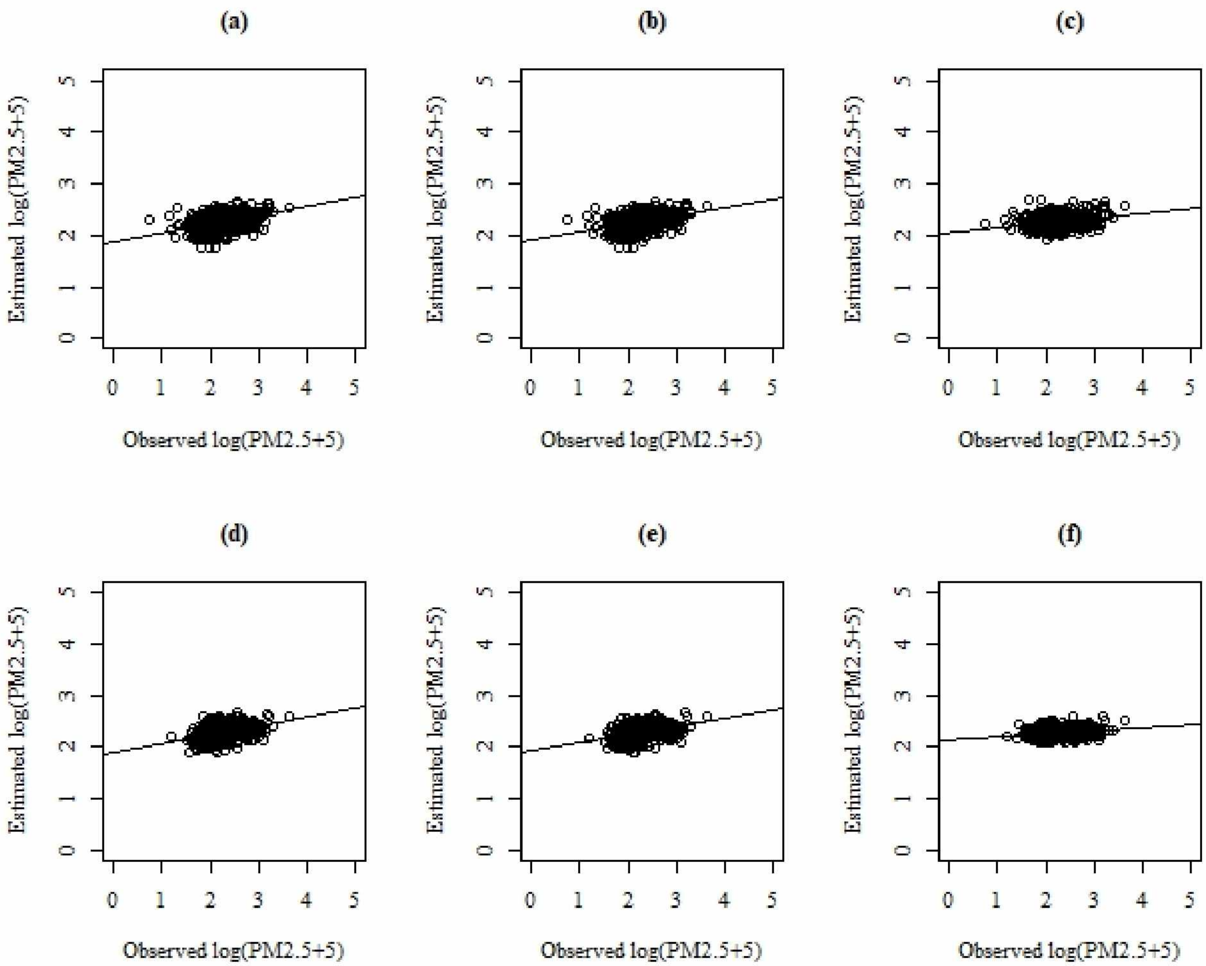


Figure 3.9. Plots of estimated versus observed log(PM2.5+5) for southcentral Alaska.
(a) Terra: log(PM2.5+5)~log(AOD+0.06)+CF+Temp+WS+Rain+AP+RH;
(b) Terra: log(PM2.5+5)~log(AOD +0.06)+CF+Temp+Rain+AP;
(c) Terra: log(PM2.5+5)~log(AOD+0.06);
(d) Aqua: log(PM2.5+5)~log(AOD+0.06) +CF+Temp+WS+Rain+AP+RH;
(e) Aqua: log(PM2.5+5)~log(AOD+0.06)+CF+Temp+Rain+AP;
(f) Aqua: log(PM2.5+5)~log(AOD+0.06).

## Conclusion

MODIS AOD cannot currently be used to quantitatively estimate ground-level air PM2.5 in Alaska. The air quality monitoring network in Alaska is limited spatially which poses a problem for both air quality monitoring and developing models using ground-based PM2.5 measurements. Models developed to predict PM2.5 using MODIS AOD are limited in application to the areas in which the air quality monitors used to develop the models are located. With respect to validation of MODIS AOD in Alaska, AERONET stations are only active in Utqiagvik and Bonanza Creek so MODIS AOD measurements cannot be validated for other regions and findings should not be extrapolated to other areas of Alaska. MODIS AOD retrievals are limited temporally. MODIS AOD measurements are retrieved at a rate of one to two measurements per day and can only be retrieved in relatively snow-free and cloud-free conditions. As a result, models using MODIS AOD are limited in application to the months of April or May to September or October in interior and southcentral Alaska.

In addition, the terrain and climates of Alaska also pose significant problems for developing models using MODIS AOD. MODIS AOD performs poorly in specific regions and climates, particularly coastal and mountainous areas and rainy (cloudy) climates, as evidenced by the poor performance of models in southcentral as compared to interior Alaska and the limited availability of data in southeast Alaska. MLR models indicate that there is little to no relationship between MODIS AOD and PM2.5 in southcentral Alaska. MODIS AOD should not be used over southcentral or southeast Alaska to estimate ground-level PM2.5 qualitatively or quantitatively. MLR models for southcentral and interior Alaska also severely underpredict ground-level PM2.5 concentrations; however, MODIS AOD is moderately correlated with PM2.5 in interior Alaska and may prove to be a good predictor when using different modeling methods, such as mixed-effects modeling. In addition, QR models indicate that models of the relationship between MODIS AOD and PM2.5 perform better at upper quantiles. Additional research and modeling of the upper quantiles of MODIS AOD and PM2.5 in interior Alaska may prove useful for identifying areas with elevated concentrations of PM2.5. Regulators could utilize this data to identify possible source areas of PM2.5 that may not have been identified previously as well as locations for placement of air quality monitors. In addition, models utilizing MODIS AOD to estimate ground-level PM2.5 could prove useful for identifying exposure areas and trends in summertime air quality in the interior.

Further research should be done using alternative modeling methods and remote sensing data, such as mixed-effects models, WRF-Chem, and data from CALIPSO. Due to the high percentage of cloudy and snow-covered days, CALIPSO may also prove an excellent solution to the resulting limited availability of MODIS AOD data because it is not dependent on reflectance and can be used to evaluate the distribution of particulate matter in the atmospheric column. The use of CALIPSO and MODIS AOD to predict ground-level PM2.5 concentrations could improve the number of possible retrievals, the temporal coverage, and the accuracy of the models. In addition, further research should be done using WRF-Chem and MODIS AOD in combination to estimate ground-level PM2.5 because WRF-Chem has been successfully used to forecast PM2.5 concentrations due to smoke from wildfires in Alaska [7], [8].

References


[1] C. A. Garcia, P.-S. Yap, H.-Y. Park, and B. L. Weller, "Association of long-term PM2.5 exposure with mortality using different air pollution exposure models: impacts in rural and urban California.," *Int. J. Environ. Health Res.*, vol. 26, no. 2, pp. 145–57, 2016.

[2] C. A. Pope and D. W. Dockery, "Health Effects of Fine Particulate Air Pollution: Lines that Connect," *J. Air Waste Manage. Assoc.*, vol. 56, no. 6, pp. 709–742, 2006.

[3] R. J. Singleton, R. C. Holman, A. M. Folkema, J. D. Wenger, C. A. Steiner, and J. T. Redd, "Trends in Lower Respiratory Tract Infection Hospitalizations among American Indian/Alaska Native Children and the General US Child Population," *YMPD*, vol. 161, p. 296–302.e2, 2012.

[4] ALA, "AMERICAN LUNG ASSOCIATION STATE OF THE AIR 2018," *American Lung Association,* 2018. [Online]. Available: https://www.lung.org/assets/documents/healthy-air/state-of-the-air/sota-2018-full.pdf. [Accessed: 11-Oct-2018].

[5] US EPA, "Fairbanks Air Quality Plan," *United States Environmental Protection Agency*, 2017. [Online]. Available: https://www.epa.gov/ak/fairbanks-air-quality-plan#nonattainment. [Accessed: 4-Nov-2018].

[6] ADEC, "Assessment of the continuous PM 2.5 Met One BAM 1020 sampler performance in the State of Alaska Air monitoring Network," *Alaska Department of Environmental Conservation: Air Quality Division Air Monitoring and Quality Assurance Program*, 2014. [Online]. Available: http://dec.alaska.gov/air/anpms/projects-reports/DOCS/Alaska-PM2.5-FRM-FEM-Correlations-Report.pdf. [Accessed: 24-Jan-2017].

[7] M. Stuefer, G. Grell, S. Freitas, and C. Waigl, "UAFSMOKE Wildfire Smoke Prediction for Alaska." [Online]. Available: http://smoke.alaska.edu/index.html. [Accessed: 23-Sep-2018].

[8] G. Grell, S. R. Freitas, M. Stuefer, and J. Fast, "Atmospheric Chemistry and Physics Inclusion of biomass burning in WRF-Chem: impact of wildfires on weather forecasts," *Atmos. Chem. Phys*, vol. 11, pp. 5289–5303, 2011.

[9] P. Gupta, S. a. Christopher, M. A. Box, and G. P. Box, "Multi year satellite remote sensing of particulate matter air quality over Sydney, Australia," *Int. J. Remote Sens.*, vol. 28, no. November 2014, pp. 4483–4498, 2007.

[10] Y. Xie, Y. Wang, K. Zhang, W. Dong, B. Lv, and Y. Bai, "Daily Estimation of Ground-Level PM2.5 Concentrations over Beijing Using 3 km Resolution MODIS AOD," *Environ. Sci. Technol.*, vol. 49, no. 20, pp. 12280–12288, 2015.

[11] H. Zhang, R. M. Hoff, and J. A. Engel-Cox, "The Relation between Moderate Resolution Imaging Spectroradiometer (MODIS) Aerosol Optical Depth and PM2.5 over the United States: A Geographical Comparison by U.S. Environmental Protection Agency Regions," *J. Air Waste Manag. Assoc.*

[12] A. M. Sayer, L. A. Munchak, N. C. Hsu, R. C. Levy, C. Bettenhausen, and M.-J. Jeong, "MODIS Collection 6 aerosol products: Comparison between Aqua's e-Deep Blue, Dark Target, and ``merged'' data sets, and usage recommendations," *J. Geo-phys. Res. Atmos*, vol. 119, pp. 965–978, 2014.

[13] R. Levy, "Dark Target Aerosol Retrieval Algorithm," *NASA*, 2018. [Online]. Available: https://darktarget.gsfc.nasa.gov/. [Accessed: 07-Aug-2018].

# Appendix A

## Chapter 2 Supplemental Data

Table A-1. Results of linear regression (**$\tau_M = \tau_A$*m+b**) for the Bonanza Creek site where r is the correlation coefficient and se is the standard error. The 95% confidence intervals are listed in parentheses.

| Satellite | $\tau_A$ | N | m | se | b | se | R2 | r | RMSE |
|---|---|---|---|---|---|---|---|---|---|
| | | | | | **10 KM Resolution** | | | | |
| **TERRA & AQUA** | all | 1490 | 1.45 (1.34, 1.57) | 0.06 | -0.027 (-0.038, -0.015) | 0.006 | 0.929 | 0.964 | 0.155 |
| | <0.15 | 1232 | 1.29 (1.23, 1.36) | 0.03 | -0.013 (-0.018, -0.009) | 0.002 | 0.524 | 0.724 | 0.042 |
| | ≥0.15 | 258 | 1.48 (1.33, 1.63) | 0.08 | -0.052 (-0.101, -0.002) | 0.025 | 0.906 | 0.952 | 0.362 |
| **TERRA** | all | 853 | 1.49 (1.33, 1.65) | 0.08 | -0.020 (-0.036, -0.005) | 0.008 | 0.922 | 0.960 | 0.171 |
| | <0.15 | 713 | 1.32 (1.23, 1.40) | 0.04 | -0.005 (-0.010, 0.001) | 0.003 | 0.581 | 0.762 | 0.042 |
| | ≥0.15 | 140 | 1.53 (1.32, 1.73) | 0.10 | -0.058 (-0.121, 0.005) | 0.032 | 0.896 | 0.947 | 0.410 |
| **AQUA** | all | 637 | 1.40 (1.26, 1.54) | 0.07 | -0.035 (-0.050, -0.020) | 0.008 | 0.945 | 0.972 | 0.132 |
| | <0.15 | 519 | 1.31 (1.21, 1.40) | 0.05 | -0.028 (-0.035, -0.021) | 0.003 | 0.512 | 0.715 | 0.042 |
| | ≥0.15 | 118 | 1.41 (1.21, 1.61) | 0.10 | -0.040 (-0.110, 0.030) | 0.036 | 0.929 | 0.964 | 0.295 |
| | | | | | **3 KM Resolution** | | | | |
| **TERRA & AQUA** | all | 2494 | 1.41 (1.29, 1.53) | 0.06 | -0.005 (-0.017, 0.007) | 0.006 | 0.854 | 0.924 | 0.208 |
| | <0.15 | 2091 | 1.38 (1.31, 1.46) | 0.04 | -0.004 (-0.009, 0.001) | 0.003 | 0.404 | 0.636 | 0.061 |
| | ≥0.15 | 403 | 1.40 (1.25, 1.55) | 0.08 | 0.009 (-0.043, 0.062) | 0.027 | 0.796 | 0.892 | 0.499 |
| **TERRA** | all | 1352 | 1.41 (1.22, 1.59) | 0.09 | 0.006 (-0.012, 0.024) | 0.009 | 0.859 | 0.927 | 0.199 |
| | <0.15 | 1146 | 1.38 (1.28, 1.48) | 0.05 | 0.007 (0.000, 0.014) | 0.003 | 0.408 | 0.639 | 0.065 |
| | ≥0.15 | 206 | 1.40 (1.16, 1.63) | 0.12 | 0.015 (-0.067, 0.096) | 0.042 | 0.806 | 0.898 | 0.486 |
| **AQUA** | all | 1142 | 1.42 (1.26, 1.58) | 0.08 | -0.018 (-0.034, -0.001) | 0.008 | 0.850 | 0.922 | 0.219 |
| | <0.15 | 945 | 1.43 (1.32, 1.54) | 0.06 | -0.021 (-0.028, -0.013) | 0.004 | 0.438 | 0.662 | 0.055 |
| | ≥0.15 | 197 | 1.40 (1.20, 1.60) | 0.10 | 0.004 (-0.065, 0.073) | 0.035 | 0.786 | 0.887 | 0.512 |

Table A-2. Fraction of data within, below, and above the error envelope (EE) and relative bias for the Bonanza Creek site.

| Satellite | $\tau_A$ | N | below EE | w/in EE | above EE | Median Bias | Mean Bias |
|---|---|---|---|---|---|---|---|
| **10 KM Resolution** | | | | | | | |
| **TERRA & AQUA** | all | 1490 | 2.3% | 83.8% | 13.9% | 0.006 | 0.036 |
| | <0.15 | 1232 | 1.9% | 90.0% | 8.0% | 0.000 | 0.007 |
| | ≥0.15 | 258 | 3.9% | 54.3% | 41.9% | 0.074 | 0.174 |
| **TERRA** | all | 853 | 0.7% | 82.6% | 16.6% | 0.017 | 0.046 |
| | <0.15 | 713 | 0.1% | 88.9% | 10.9% | 0.010 | 0.016 |
| | ≥0.15 | 140 | 3.6% | 50.7% | 45.7% | 0.082 | 0.195 |
| **AQUA** | all | 637 | 4.4% | 85.4% | 10.2% | -0.007 | 0.023 |
| | <0.15 | 519 | 4.4% | 91.5% | 4.0% | -0.012 | -0.006 |
| | ≥0.15 | 118 | 4.2% | 58.5% | 37.3% | 0.064 | 0.149 |
| **3 KM Resolution** | | | | | | | |
| **TERRA & AQUA** | all | 2494 | 1.7% | 77.5% | 20.8% | 0.018 | 0.055 |
| | <0.15 | 2091 | 1.4% | 82.5% | 16.0% | 0.011 | 0.022 |
| | ≥0.15 | 403 | 3.2% | 51.1% | 45.7% | 0.099 | 0.224 |
| **TERRA** | all | 1352 | 0.5% | 75.2% | 24.3% | 0.026 | 0.062 |
| | <0.15 | 1146 | 0.2% | 79.9% | 19.9% | 0.020 | 0.033 |
| | ≥0.15 | 206 | 2.4% | 49.0% | 48.5% | 0.105 | 0.225 |
| **AQUA** | all | 1142 | 3.2% | 80.1% | 16.7% | 0.005 | 0.046 |
| | <0.15 | 945 | 3.0% | 85.7% | 11.3% | -0.002 | 0.009 |
| | ≥0.15 | 197 | 4.1% | 53.3% | 42.6% | 0.088 | 0.223 |

Table A-3. Results of linear regression ($\tau_M = \tau_A*m+b$) for the Barrow site where $\tau_M$ is MODIS AOD, $\tau_A$ is AERONET AOD. m is the slope, and b is the y-intercept. The table also lists the correlation coefficients (r), root mean square errors (RMSE), and the standard errors (se). The 95% confidence intervals are listed in parentheses.

| Satellite | $\tau_A$ | N | m | se | b | se | $R^2$ | r | RMSE |
|---|---|---|---|---|---|---|---|---|---|
| | | | | | **10 KM Resolution** | | | | |
| **TERRA & AQUA** | all | 1327 | 0.97 (0.86, 1.07) | 0.06 | 0.031 (0.024, 0.039) | 0.004 | 0.58 | 0.76 | 0.058 |
| | <0.15 | 1233 | 1.10 (0.99, 1.20) | 0.05 | 0.023 (0.017, 0.029) | 0.003 | 0.33 | 0.58 | 0.055 |
| | ≥0.15 | 94 | 0.86 (0.63, 1.10) | 0.12 | 0.055 (0.006, 0.104) | 0.025 | 0.62 | 0.79 | 0.091 |
| **TERRA** | all | 682 | 0.97 (0.87, 1.08) | 0.05 | 0.032 (0.025, 0.039) | 0.004 | 0.58 | 0.76 | 0.057 |
| | <0.15 | 634 | 1.09 (0.94, 1.23) | 0.07 | 0.026 (0.017, 0.034) | 0.004 | 0.34 | 0.58 | 0.055 |
| | ≥0.15 | 48 | 0.93 (0.46, 1.40) | 0.24 | 0.036 (-0.060, 0.133) | 0.049 | 0.65 | 0.81 | 0.082 |
| **AQUA** | all | 645 | 0.96 (0.75, 1.17) | 0.11 | 0.030 (0.016, 0.045) | 0.007 | 0.57 | 0.76 | 0.059 |
| | <0.15 | 599 | 1.11 (0.95, 1.27) | 0.08 | 0.021 (0.011, 0.030) | 0.005 | 0.32 | 0.57 | 0.055 |
| | ≥0.15 | 46 | 0.81 (0.41, 1.22) | 0.21 | 0.070 (-0.011, 0.152) | 0.042 | 0.60 | 0.78 | 0.100 |
| | | | | | **3 KM Resolution** | | | | |
| **TERRA & AQUA** | all | 1678 | 1.01 (0.85, 1.08) | 0.03 | 0.033 (0.028, 0.037) | 0.002 | 0.59 | 0.77 | 0.065 |
| | <0.15 | 1559 | 1.06 (0.96, 1.15) | 0.05 | 0.030 (0.024, 0.035) | 0.003 | 0.28 | 0.53 | 0.061 |
| | ≥0.15 | 119 | 0.96 (0.87, 1.05) | 0.05 | 0.048 (0.022, 0.074) | 0.013 | 0.68 | 0.83 | 0.108 |
| **TERRA** | all | 871 | 1.02 (0.96, 1.08) | 0.03 | 0.035 (0.031, 0.040) | 0.002 | 0.63 | 0.79 | 0.067 |
| | <0.15 | 801 | 1.01 (0.87, 1.14) | 0.07 | 0.035 (0.027, 0.044) | 0.004 | 0.26 | 0.51 | 0.062 |
| | ≥0.15 | 70 | 0.98 (0.91, 1.05) | 0.04 | 0.049 (0.017, 0.081) | 0.016 | 0.74 | 0.86 | 0.106 |
| **AQUA** | all | 807 | 1.00 (0.85, 1.15) | 0.08 | 0.031 (0.021, 0.040) | 0.005 | 0.54 | 0.74 | 0.063 |
| | <0.15 | 758 | 1.11 (0.97, 1.25) | 0.07 | 0.024 (0.016, 0.032) | 0.004 | 0.31 | 0.55 | 0.059 |
| | ≥0.15 | 49 | 0.92 (0.69, 1.15) | 0.12 | 0.049 (0.003, 0.096) | 0.024 | 0.58 | 0.76 | 0.111 |

Table A-4. Fraction of data within, below, and above the error envelope (EE) and bias for the Barrow site.

| Satellite | $\tau_A$ | N | below EE | w/in EE | above EE | Median Bias | Mean Bias |
|---|---|---|---|---|---|---|---|
| **10 KM Resolution** | | | | | | | |
| **TERRA & AQUA** | all | 1327 | 4.1% | 71.6% | 24.2% | 0.018 | 0.029 |
| | <0.15 | 1233 | 3.2% | 72.5% | 24.2% | 0.018 | 0.029 |
| | ≥0.15 | 94 | 17.0% | 59.6% | 23.4% | 0.009 | 0.025 |
| **TERRA** | all | 682 | 4.4% | 70.1% | 25.4% | 0.019 | 0.030 |
| | <0.15 | 634 | 3.2% | 70.8% | 25.9% | 0.020 | 0.031 |
| | ≥0.15 | 48 | 20.8% | 60.4% | 18.8% | 0.007 | 0.021 |
| **AQUA** | all | 645 | 3.9% | 73.2% | 22.9% | 0.016 | 0.027 |
| | <0.15 | 599 | 3.2% | 74.3% | 22.5% | 0.017 | 0.027 |
| | ≥0.15 | 46 | 13.0% | 58.7% | 28.3% | 0.012 | 0.028 |
| **3 KM Resolution** | | | | | | | |
| **TERRA & AQUA** | all | 1678 | 1.1% | 70.7% | 28.1% | 0.022 | 0.034 |
| | <0.15 | 1559 | 0.7% | 71.3% | 28.0% | 0.022 | 0.033 |
| | ≥0.15 | 119 | 6.7% | 63.9% | 29.4% | 0.023 | 0.039 |
| **TERRA** | all | 871 | 1.4% | 67.3% | 31.3% | 0.024 | 0.037 |
| | <0.15 | 801 | 0.9% | 67.8% | 31.3% | 0.023 | 0.036 |
| | ≥0.15 | 70 | 7.1% | 61.4% | 31.4% | 0.026 | 0.045 |
| **AQUA** | all | 807 | 0.9% | 74.5% | 24.7% | 0.020 | 0.031 |
| | <0.15 | 758 | 0.5% | 74.9% | 24.5% | 0.020 | 0.031 |
| | ≥0.15 | 49 | 6.1% | 67.3% | 26.5% | 0.020 | 0.031 |

Appendix B

Chapter 3 Supplemental Data

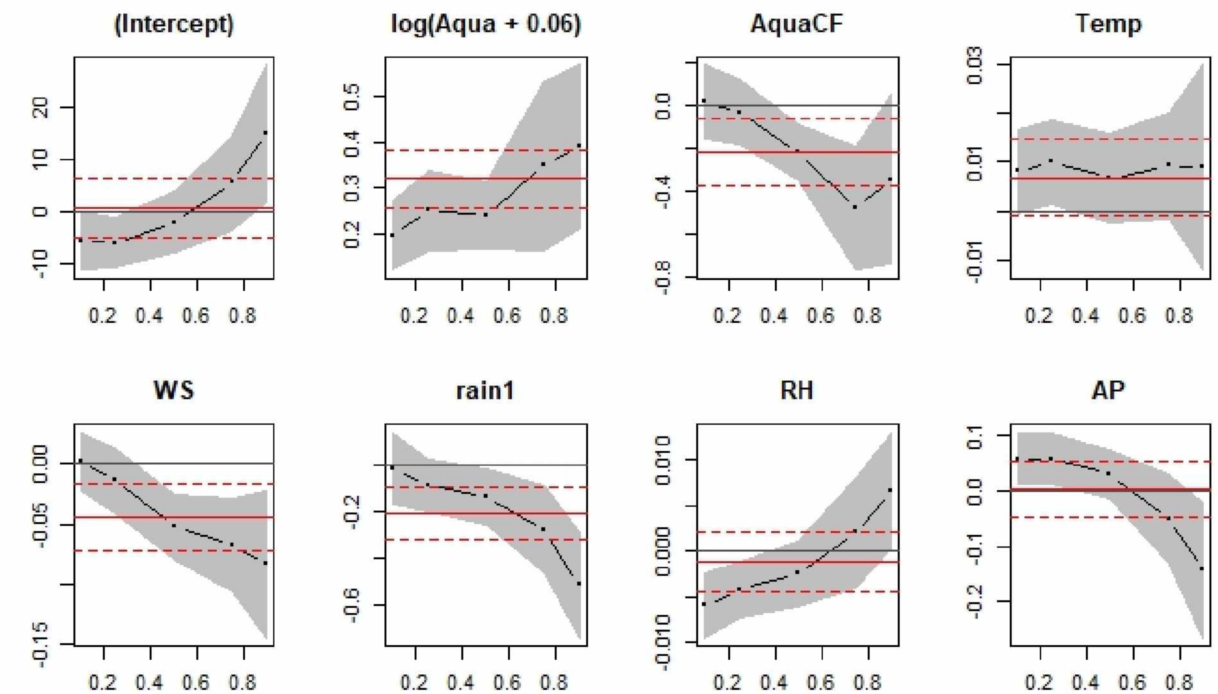


Figure B-1 Quantile regression for interior Alaska where log(PM2.5+5) is the response and log(Aqua+0.06), AquaCF (cloud fraction), Temp (temperature in K), WS (wind speed in m/s), rain, RH (relative humidity in percent), AP (air pressure in kPa) where Aqua is Aqua MODIS aerosol optical depth and PM2.5 is in µg/$m^3$. The solid black horizontal line is 0; the solid red line is the mean value from ordinary least squares regression; the dashed red line is the 95% confidence interval of the mean value from the ordinary least squares regression; the black dots are the quantile regression coefficient estimates; the gray shaded area is the 95% confidence interval.

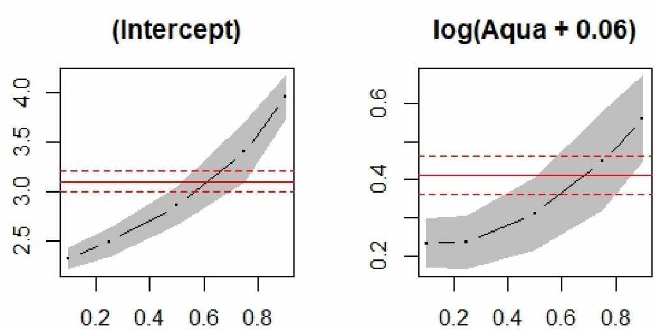


Figure B-2 Quantile regression for interior Alaska where log(PM2.5+5) is the response and log(Aqua+0.06) where Aqua is Aqua MODIS aerosol optical depth and PM2.5 is in µg/$m^3$. The solid black horizontal line is 0; the solid red line is the mean value from ordinary least squares regression; the dashed red line is the 95% confidence interval of the mean value from the ordinary least squares regression; the black dots are the quantile regression coefficient estimates; the gray shaded area is the 95% confidence interval.

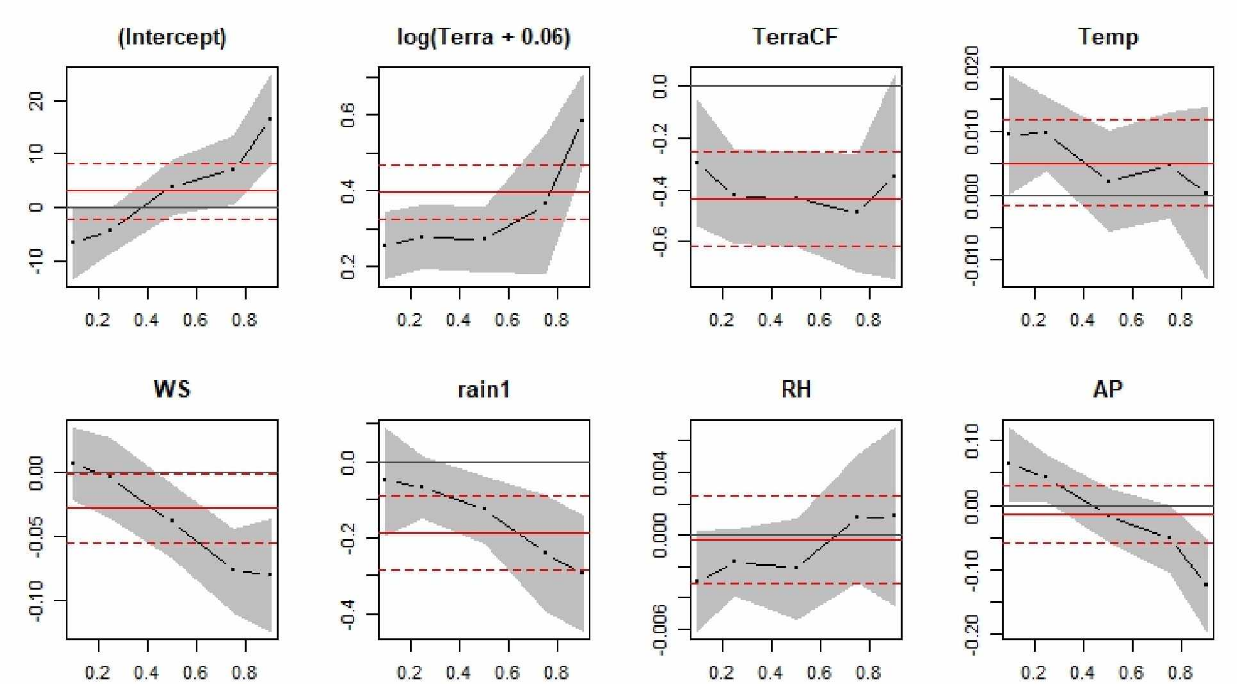


Figure B-3 Quantile regression for interior Alaska where log(PM2.5+5) is the response and log(Terra+0.06), TerraCF (cloud fraction), Temp (temperature in K), WS (wind speed in m/s), rain, RH (relative humidity in percent), AP (air pressure in kPa) where Terra is Terra MODIS aerosol optical depth and PM2.5 is in µg/m$^3$. The solid black horizontal line is 0; the solid red line is the mean value from ordinary least squares regression; the dashed red line is the 95% confidence interval of the mean value from the ordinary least squares regression; the black dots are the quantile regression coefficient estimates; the gray shaded area is the 95% confidence interval.

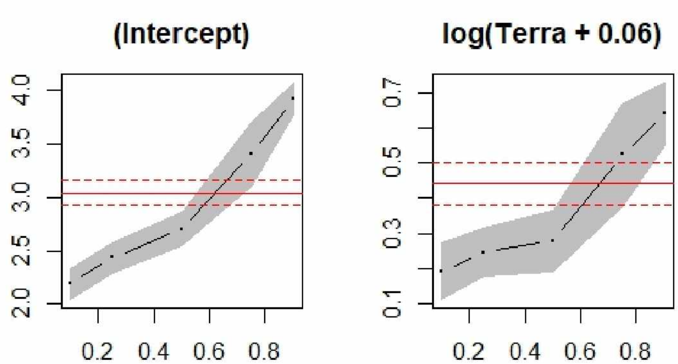


Figure B-4 Quantile regression for interior Alaska where log(PM2.5+5) is the response and log(Terra+0.06) where Terra is Terra MODIS aerosol optical depth and PM2.5 is in µg/m$^3$. The solid black horizontal line is 0; the solid red line is the mean value from ordinary least squares regression; the dashed red line is the 95% confidence interval of the mean value from the ordinary least squares regression; the black dots are the quantile regression coefficient estimates; the gray shaded area is the 95% confidence interval.

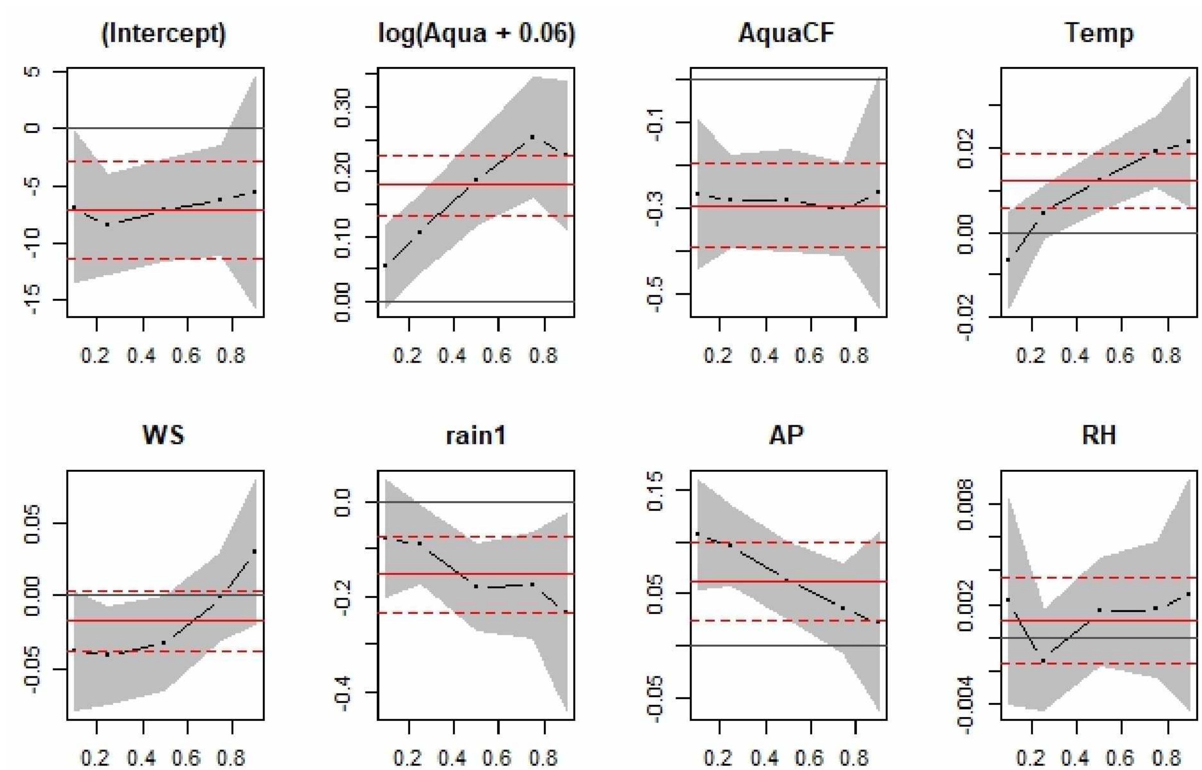


Figure B-5 Quantile regression for southcentral Alaska where log(PM2.5+5) is the response and log(Aqua+0.06), AquaCF (cloud fraction), Temp (temperature in K), WS (wind speed in m/s), rain, RH (relative humidity in percent), AP (air pressure in kPa) where Aqua is Aqua MODIS aerosol optical depth and PM2.5 is in μg/m$^3$. The solid black horizontal line is 0; the solid red line is the mean value from ordinary least squares regression; the dashed red line is the 95% confidence interval of the mean value from the ordinary least squares regression; the black dots are the quantile regression coefficient estimates; the gray shaded area is the 95% confidence interval.

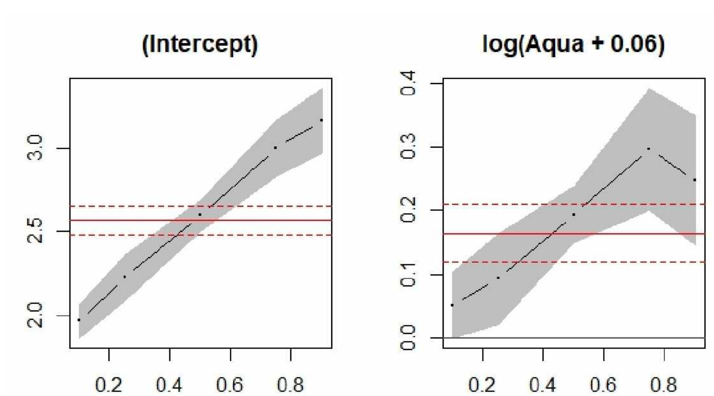


Figure B-6 Quantile regression for southcentral Alaska where log(PM2.5+5) is the response and log(Aqua+0.06 where Aqua is Aqua MODIS aerosol optical depth and PM2.5 is in μg/m$^3$. The solid black horizontal line is 0; the solid red line is the mean value from ordinary least squares regression; the dashed red line is the 95% confidence interval of the mean value from the ordinary least squares regression; the black dots are the quantile regression coefficient estimates; the gray shaded area is the 95% confidence interval.

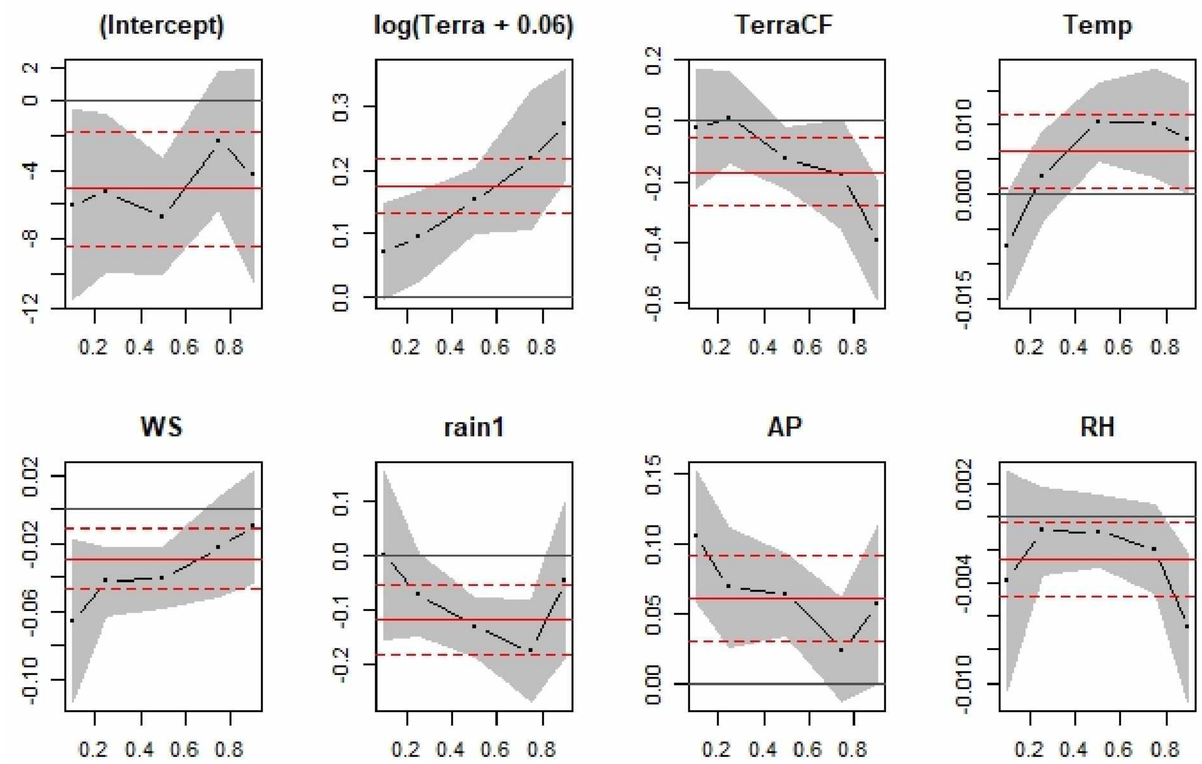


Figure B-7 Quantile regression for southcentral Alaska where log(PM2.5+5) is the response and log(Terra+0.06), TerraCF (cloud fraction), Temp (temperature in K), WS (wind speed in m/s), rain, RH (relative humidity in percent), AP (air pressure in kPa) where Terra is Terra MODIS aerosol optical depth and PM2.5 is in $\mu g/m^3$. The solid black horizontal line is 0; the solid red line is the mean value from ordinary least squares regression; the dashed red line is the 95% confidence interval of the mean value from the ordinary least squares regression; the black dots are the quantile regression coefficient estimates; the gray shaded area is the 95% confidence interval.

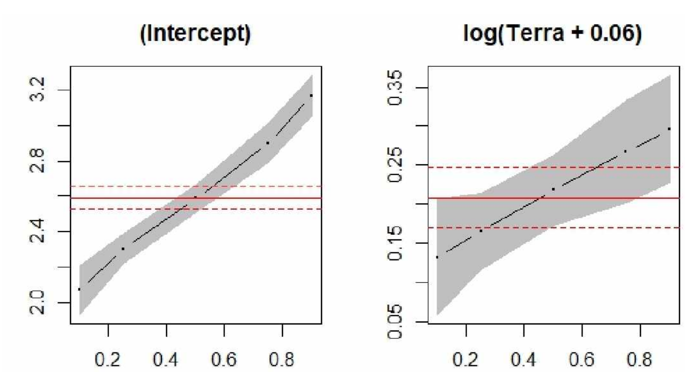


Figure B-8 Quantile regression for southcentral Alaska where log(PM2.5+5) is the response and log(Terra+0.06) where Terra is Terra MODIS aerosol optical depth and PM2.5 is in $\mu g/m^3$. The solid black horizontal line is 0; the solid red line is the mean value from ordinary least squares regression; the dashed red line is the 95% confidence interval of the mean value from the ordinary least squares regression; the black dots are the quantile regression coefficient estimates; the gray shaded area is the 95% confidence interval.

Table B-1. Cross-validated correlation coefficients (CV-R) of aerosol optical depth and PM2.5.

| Study | Study Area | Study Period | CV-R | Platform |
|---|---|---|---|---|
| [1] | Southeast U.S. | 2000-2003 | 0.579-0.661 | Terra |
| [2] | Sydney, Australia<br>Delhi, India<br>Hong Kong<br>New York City, U.S.<br>Switzerland | 2002 | 0.11-0.48<br>0.24-0.85<br>0.34-0.54<br>0.48-0.75<br>0.21-0.45 | Aqua and Terra |
| [3] | Southeast U.S. | 2000-2006 | 0.53 (annual)<br>0.38 (month) | Terra |
| [4] | Continental U.S. | 2005-2006 | 0.26-0.63<br>0.28-0.67 | Terra<br>Aqua |
| [5] | Beijing, China | 2013-2014 | 0.69 | Aqua |
| [6] | Israel | 2003-2013 | 0.85 | Aqua and Terra |
| [7] | Northeast U.S. | 2003-2005 | 0.88 | GOES |

[1] M. Z. Al-Hamdan *et al.*, "Methods for Characterizing Fine Particulate Matter Using Ground Observations and Remotely Sensed Data: Potential Use for Environmental Public Health Surveillance," *J. Air Waste Manage. Assoc.*, vol. 59, no. 7, pp. 865–881, 2009.

[2] P. Gupta, S. A. Christopher, J. Wang, R. Gehrig, Y. Lee, and N. Kumar, "Satellite remote sensing of particulate matter and air quality assessment over global cities," *Atmos. Environ.*, vol. 40, no. 30, pp. 5880–5892, 2006.

[3] P. Gupta and S. A. Christopher, "Seven year particulate matter air quality assessment from surface and satellite measurements," *Atmos. Chem. Phys. Atmos. Chem. Phys.*, vol. 8, pp. 3311–3324, 2008.

[4] H. Zhang, R. M. Hoff, and J. A. Engel-Cox, "The Relation between Moderate Resolution Imaging Spectroradiometer (MODIS) Aerosol Optical Depth and PM2.5 over the United States: A Geographical Comparison by U.S. Environmental Protection Agency Regions," *J. Air Waste Manag. Assoc.*, vol. 59, no. 11, pp. 1358–1369, 2009.

[5] Y. Xie, Y. Wang, K. Zhang, W. Dong, B. Lv, and Y. Bai, "Daily Estimation of Ground-Level PM2.5 Concentrations over Beijing Using 3 km Resolution MODIS AOD," *Environ. Sci. Technol.*, vol. 49, no. 20, pp. 12280–12288, 2015.

[6] I. Kloog *et al.*, "Estimating daily PM2.5and PM10across the complex geo-climate region of Israel using MAIAC satellite-based AOD data," *Atmos. Environ.*, vol. 122, pp. 409–416, Dec. 2015.

[7] Y. Liu, C. J. Paciorek, and P. Koutrakis, "Estimating regional spatial and temporal variability of PM2.5 concentrations using satellite data, meteorology, and land use information," *Environ. Health Perspect.*, vol. 117, no. 6, pp. 886–892, 2009.